Adsorption Behavior of Some Metal Ions on Titanium Dioxide Surface

Miki Kanna

Master of Science Thesis in Inorganic Chemistry

Prince of Songkla University
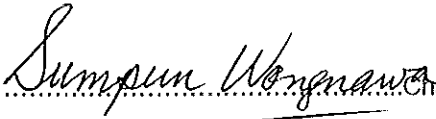
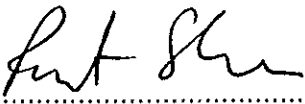2002

(1)

Thesis Title   Adsorption Behavior of Some Metal Ions on Titanium Dioxide Surface

Author   Miss Miki Kanna

Major Program   Inorganic Chemistry
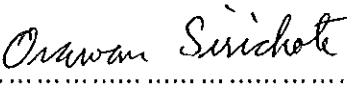

Advisory Committee

....Chairman
(Associate Professor Dr. Sumpun Wongnawa)

....Committee
(Assistant Professor Panit Sherdshoopongse)

Examining Committee
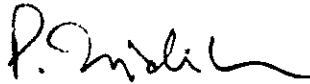
....Chairman
(Associate Professor Dr. Sumpun Wongnawa)

....Committee
(Assistant Professor Panit Sherdshoopongse)

....Committee
(Assistant Professor Dr. Orawan Sirichote)

....Committee
(Associate Professor Dr. Chakrit Tongurai)

The Graduate School, Prince of Songkla University, has approved this thesis as partial fulfillment of the requirement for the Master of Science degree in Inorganic Chemistry.

....
(Associate Professor Dr. Piti Trisdikoon)
Dean, Graduate School

(2)

ชื่อวิทยานิพนธ์	พฤติกรรมการดูดซับไอออนโลหะบางชนิดบนพื้นผิวไทเทเนียม-ไดออกไซด์
ผู้เขียน	นางสาวมิกิ กัณณะ
สาขาวิชา	เคมีอนินทรีย์
ปีการศึกษา	2545

บทคัดย่อ

ไทเทเนียมไดออกไซด์ที่ใช้ในงานวิจัยนี้ได้จากการทำปฏิกิริยาระหว่างไทเทเนียม
เตตระคลอไรด์กับสารละลายแอมโมเนียเจือจางที่อุณหภูมิต่ำ หลังจากนั้นศึกษาด้วย
เทคนิค XRD, EDXRF, TGA, DSC และ FT-IR พบว่าไทเทเนียมไดออกไซด์ที่ได้อยู่ใน
รูปของไทเทเนียมไดออกไซด์อสัณฐาน ซึ่งอยู่ในรูป $TiO_2 \cdot 1.6H_2O$ (ต่อไปจะแทนด้วย
สัญลักษณ์ $TiO_2(syn)$) $TiO_2(syn)$ มีพื้นที่ผิว (BET) ค่อนข้างมาก คือ 449 ตารางเมตร
ต่อกรัม จึงได้ศึกษาการดูดซับไอออนโลหะ Cu(II), Mn(II), Pb(II) และ Fe(III) บนพื้นผิว
ของ $TiO_2(syn)$ ที่สภาวะสมดุลด้วยการทดลองแบบไม่ต่อเนื่อง โดยศึกษาผลกระทบ
จากเวลาในการกวน ปริมาตรของสารละลายตัวอย่าง ความเข้มข้นของไอออนโลหะ
และ pH นอกจากนี้ยังศึกษาไอโซเทอร์มการดูดซับของไอออนโลหะโดยการศึกษาที่
pH 7 ซึ่งพบว่าการดูดซับไอออน Cu(II), Mn(II) และ Pb(II) บน $TiO_2(syn)$ สอดคล้อง
กับ ไอโซเทอร์มการดูดซับแบบ Langmuir ในขณะที่การดูดซับไอออน Fe(III) สอดคล้อง
ทั้งไอโซเทอร์มแบบ Langmuir และ Freundlich ตลอดงานวิจัยนี้ใช้เครื่องอะตอมมิก
แอบ-ซอร์บชั่นในการวิเคราะห์หาความเข้มข้นของสารละลายโลหะทุกครั้ง

Thesis Title	Adsorption Behavior of Some Metal Ions on Titanium Dioxide Surface
Author	Miss Miki Kanna
Major Program	Inorganic Chemistry
Academic Year	2002

Abstract

Titanium dioxide was prepared from the reaction titanium tetrachloride and diluted ammonia solution at low temperature. The oxide thus obtained was characterized by XRD, EDXRF, TGA, DSC, and FT-IR techniques to be in the form of hydrated amorphous titanium dioxide, $TiO_2 \cdot 1.6H_2O$, and will be referred to as TiO_2(syn) throughout this work. TiO_2(syn) exhibits high BET surface area at 449 m^2/g. Adsorptions of metal ions onto the TiO_2(syn) surface were investigated in the batch equilibrium experiments, using Cu(II), Mn(II), Pb(II), and Fe(III) solutions. The concentrations of metal ions were determined by atomic absorption spectrometer. Effect of stirring time, sample volume, concentration of metal ion, and pH were studied. The adsorption isotherms of all metal ions were also studied at pH 7. The adsorption of Cu(II), Mn(II), and Pb(II) on TiO_2(syn) conformed to the Langmuir isotherm while that of Fe(III) fit equally well to both Langmuir and Freundlich isotherms.

Acknowledgements

I would like to express my sincere thanks to my advisor, Associate Professor Dr. Sumpun Wongnawa, who suggested this research problem, for his numerous suggestions, encouragement and criticism without which I would have been unable to complete this work.

I am also indebted to Assistant Professor Panit Sherdshoopongse my co-advisor who gave his time in reviewing the text and suggested the improvement of the report. I am also grateful to Assistant Professor Dr. Orawan Sirichote and Associate Professor Dr. Chakrit Tongurai, the examining committee for their kind comments and correction of the report.

I am very grateful to thanks Assistant Professor Phadoong Boonsin for the valuable comments on my thesis. I am also indebted to Dr. Tawan Sooknoi, Department of Chemistry, Faculty of Science, King Mongkut's University of Technology Ladkrabang, Bangkok, for the measurement of the specific surface area.

I would like to thank the Department of Chemistry, Faculty of Science, Prince of Songkla University, for all necessary laboratory facilities used throughout this research.

I am grateful to the Postgraduate Education and Research Program in Chemistry (PERCH) and the Graduate School, Prince of Songkla University, for the financial supports of this research.

I also would like to thank all of my collaborators who helped creating an enjoyable atmosphere to be working in and for their many helpful in many countless ways throughout the years.

<div align="right">Miki Kanna</div>

Contents

Contents (continued)

List of Tables

List of Tables (continued)

List of Tables (continued)

List of Figures

List of Figures (continued)

List of Figures (continued)

Chapter 1

INTRODUCTION

1.1 Introduction

Titanium is a chemical element with symbol Ti, atomic number 22 and atomic weight 47.90. It belongs to the fourth group of the periodic table, and its chemistry shows similarities to that of silicon and zirconium. Titanium occurs in nature as ilmenite ($FeTiO_2$), rutile (tetragonal TiO_2), anatase (tetragonal TiO_2), brookite (rhombic TiO_2), perovskite ($CaTiO_3$), sphene ($CaTiSiO_5$), and geikielite ($MgTiO_3$) (Kirk and Othmer , 1985 : 1182).

Titanium is a silvery, ductile metal with important industrial possibilities because it is less dense than iron, much stronger than aluminium, and almost as corrosion-resistant as platinum. Although it is unlikely ever to be as steel, its rare combination of properties makes it ideal for a variety of uses, particularly in engines, aircraft frames, some marine equipment, in industrial plant and in laboratory equipment. Certain properties may be improved by alloying it with aluminium (Clark , 1968 : 4-5). Some properties of titanium are given in Table 1.

The most important industrial use of titanium is in the form of titanium dioxide (TiO_2) which is widely used as a pigment for paint, coating ink, paper, plastic, cosmetic products, catalyst supports, photoconductors, dielectric materials, and so on because of its very whiteness, outstanding hiding property and non-toxicity. Titanium dioxide exists in three types according to its crystal structure: anatase, rutile, and brookite.

1

The brookite type cannot be used in industries because of its instability at room temperature. The anatase type has the problems of poor light and heat resistance and of gradually decreasing whiteness due to the weather. The anatase type also has drawbacks for applications involving adsorption technology owing to its low surface energy. The rutile type has outdoor applicability because of its good light resistance and can be applied to surfaces by the use of adsorption technology without advanced skills or sophisticated equipment (Kim and Chung, 2001).

Table 1 Properties of titanium

Property	value
[a]Electronic structure	$3d^2 4s^2$
[b]Melting point, $^\circ$C	1668 ± 5
[b]Boiling point, $^\circ$C	3260
[b]Density, g/cm^3	
α phase at 20 $^\circ$C	4.507
β phase at 885 $^\circ$C	4.35
[b]Thermal conductivity at 25 $^\circ$C, W/(m·K)	21.9
[b]Electrical resistivity at 20 $^\circ$C, nΩ·m	420
[b]Magnetic susceptibility, mks	180×10^{-6}
[b]Modulus of elasticity,Gpa	
tension	ca. 101
compression	103
shear	44
[a]Metallic redius (Å)	1.47
[a]Entropy S$^\circ$ 298 (cal/deg/m)	7.33
[a]E$^\circ$ (M^{2+}/M) volts , 25 $^\circ$C	-1.63
[a]E$^\circ$ (M^{3+}/M^{2+}) volts , 25 $^\circ$C	-0.37
[a]Heat of atomisation (kal/g·atom)	112.6

a (Clark , 1968 : 6), b (Kirk and Othmer ,1985 : 1183)

In recent years, TiO_2 photocatalysis has been studied as a potential technique for the treatment of pollutants (both organic and inorganic) and microorganisms. In addition, there are many studies that used titanium dioxide for solid-phase extraction (SPE) because of its high chemical stability and high ion-exchange capacity (Poznyak, et al., 1999). Vassileva, et al., (1996) developed a system for column solid-phase extraction by using TiO_2 (anatase). Liang, et al., (2001) proposed a new method for using nanometer TiO_2 as solid-phase extractants for the simultaneous preconcentration of trace metals. However, the conversion of synthetic TiO_2 to anatase and another form requires high temperature. In general, TiO_2 is obtained either from minerals or from a solution of titanium salts or alkoxides. Freshly synthesized TiO_2 usually exists as an amorphous solid. Therefore, in this research TiO_2 (amorphous) is used to study the adsorption properties to see if it can replace the anatase in this respect.

1.2 Review of Literatures

Titanium dioxide has three crystal structures: anatase , brookite, and rutile as show in Figure 1. The crystallographic data on the three oxide modifications are summarised in Table 2. Both anatase and rutile are tetragonal, whereas brookite is orthorhombic. In all three forms, each titanium atom is coordinated to six almost equidistant oxygen atoms, and each oxygen atom to three titanium atoms (Clark, 1968 : 269). All three oxide modifications are birefringent ; anatase is uniaxial negative, brookite is biaxial positive and rutile is uniaxial positive. Further data are given in Table 3.

Table 2   X-ray data on TiO_2 modifications (Clark ,1968 : 268).

	Space group	Z	Cell parameters (Å)			Ti-O (Å)[b]
			A	B	C	
Anatase	$C_{4h}^{19} = C4/amc$	8	5.36		9.53	1.91(2)
						1.95(4)
Brookite	$D_{2h}^{15} = Pbca$	8	9.15	5.44	5.14	1.84-2.03
Rutile	$D_{4h}^{14} = P4_2/mnm$	2	4.954		2.959	1.944(4)
						1.988(2)
α - PbO_2 form	$D_{2h}^{14} = Pbcn$	4	4.515	5.497	4.939	1.91(4)
						2.05(2)

[b] The numbers in parentheses refer to the number of equivalent oxygen atoms at the stated distance from a titanium atom.

Table 3   Properties of the three modifications of titanium dioxide (Clark, 1968 : 270).

	Anatase	Brookite	Rutile
Density (g/cc)	3.90	4.13	4.27
Hardness (Mohs'scale)	5.5-6.0	5.5-6.0	6.0-6.5
Melting Point (^{o}C)	change to rutile	change to rutile	1840 ± 10
Entropy $S^o_{298.16}$ (cal/deg/m)	11.93	-	12.01
Refractive Index (25 ^{o}C) ($\lambda = 5893$ Å)	n_ω 2.5612 n_ε 2.4880	n_α 2.5831 n_β 2.5843 n_γ 2.7004	n_ω 2.6124 n_ε 2.8993
Dielectric Constant	$\varepsilon = 48$ (powder)	$\varepsilon = 78$	$\varepsilon_{av} = 110\text{-}117$ $\varepsilon_{\parallel} = 180$,at 3×10^5 c/s 25 ^{o}C $\varepsilon_{\perp} = 89$,at 3×10^5 c/s 25 ^{o}C

(a)   (b)   (c)
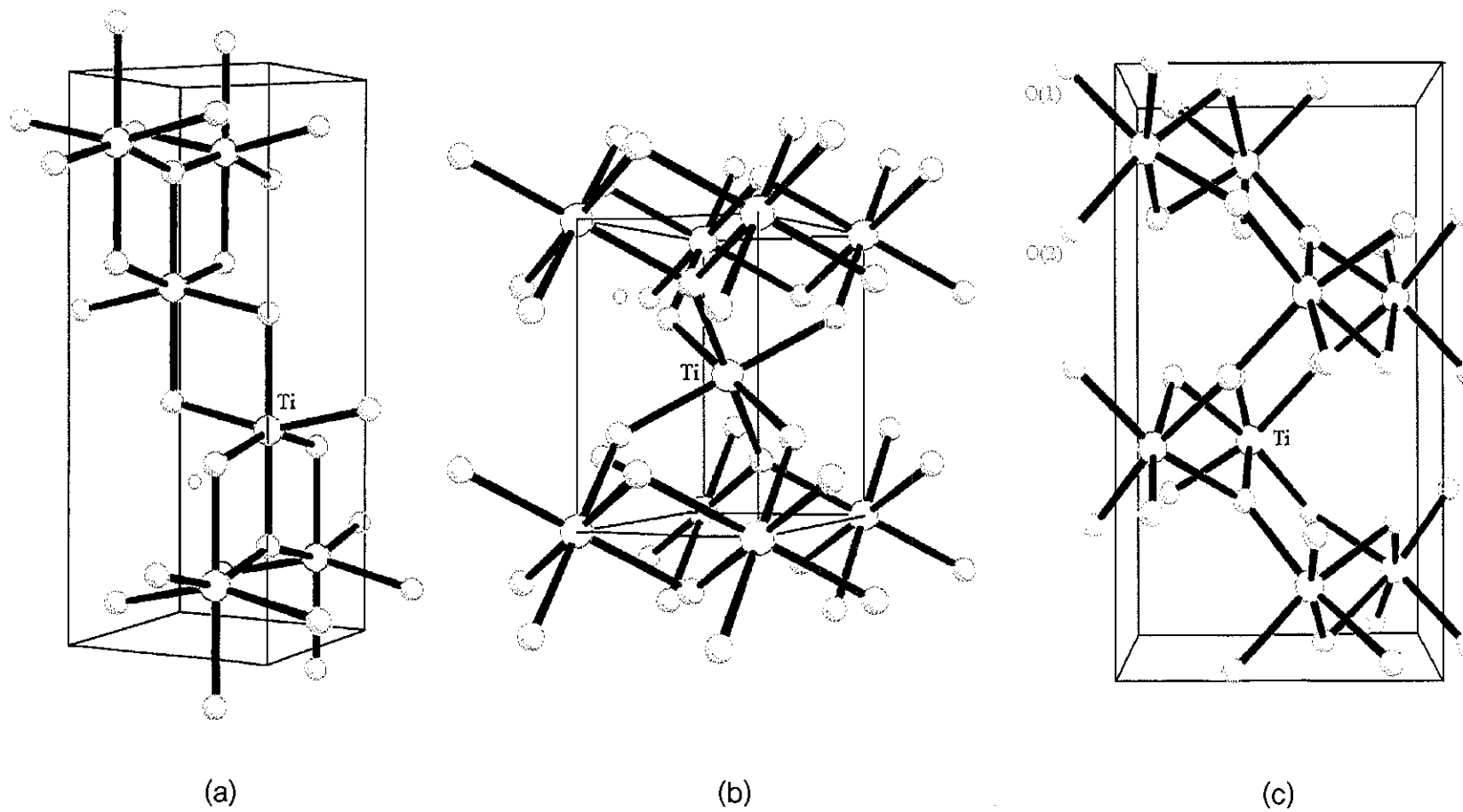
Figure 1 Crystal sturcture of TiO_2, (a) Anatase, (b) Rutile, (c) Brookite.

Generally, TiO$_2$ pigments are either manufactured using the older sulfate or newer chloride processes. The economics of the two processes are very much dependent upon the raw material available. The starting materials for TiO$_2$ production are ilmenite and titaniferous slag in the case of the sulfate process (Figure 2) and leucoxene, rutile, synthetic rutile, and in the future possibly also anatase for the chloride process (Figure 3) (Büchner, et al., 1989 : 523-525).
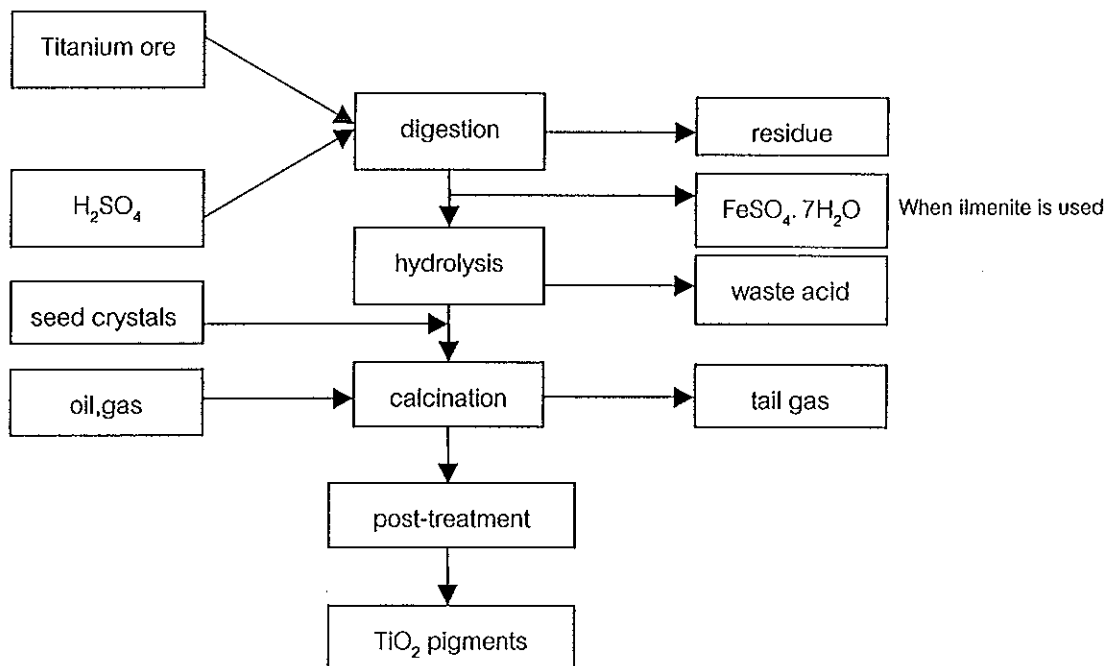
Figure 2 TiO$_2$ pigment manufactured by the sulfate process. (Büchner, et al., 1989 : 526)
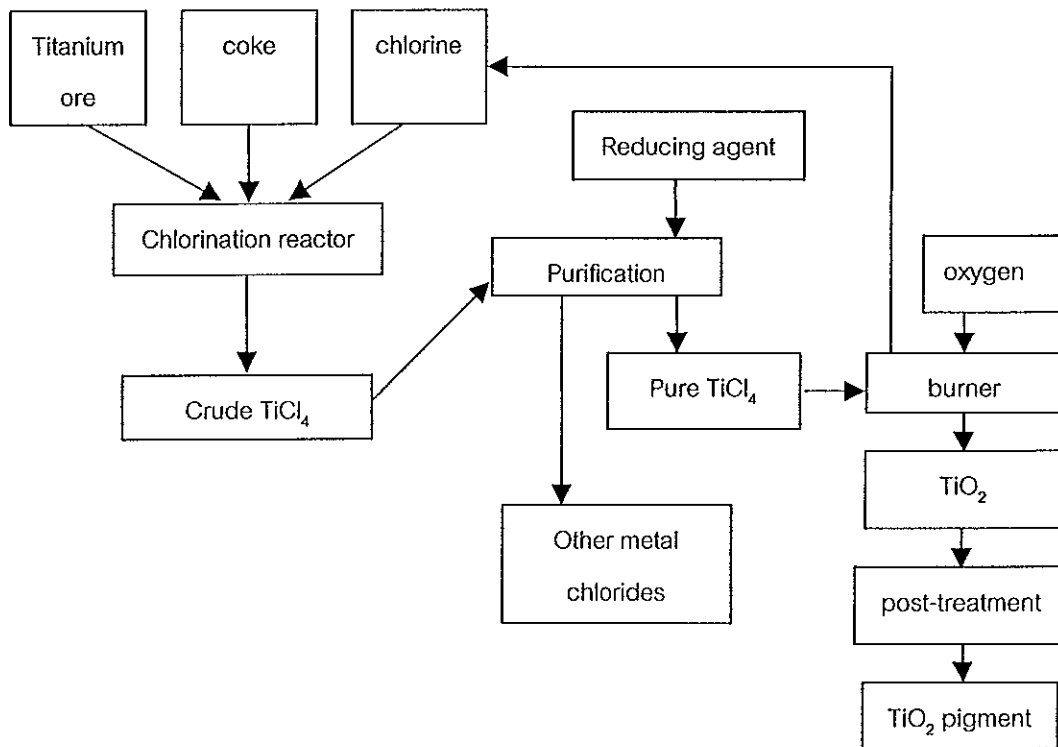
Figure 3 TiO$_2$ pigment manufactured by the chloride process. (Büchner, et al., 1989 : 528)

Titanium dioxide manufacturing is obtained from minerals by sulfate and chloride processes. Synthetic routes of TiO$_2$ production depend on the preparation route and experimental conditions. Many researches involving the preparation of TiO$_2$ can be summarized as follows.

Abe, et al., (1989) synthesized hydrated titanium dioxide (HTDO) by slowly adding water (150 mL) into TiCl$_4$ (50 mL) and a 2.8 M sodium hydroxide solution (800 mL) was added to the resulting solution. The precipitate that formed was washed with demineralised water and left for 2 days then filtered under suction. This procedure was repeated until the pH of the filtrate reached a constant value (about pH 12). The precipitate was then air-dried at room

temperature until it had been transformed into a semi-transparent glassy gel. This gel was immersed in de-mineralised water to break it down into fine particles. The product was ground and sieved to 100-200 mesh size. It was found that amorphous HTDO is a semi-transparent glassy gel. The composition of the gel can be written as $TiO_2 \cdot 1.6H_2O$.

Sclafani, et al., (1990) prepared TiO_2-hp (home prepared) by two different methods. The first one was obtained by reacting an aqueous solution of $TiCl_3$ (15 wt%, Carlo Erba) with an aqueous solution of ammonia (25 wt%, Merck), which was added dropwise at room temperature with vigorous stirring to avoid overheating due to the exothermicity of the reaction. After standing 24 h at room temperature, the solid was filtered and washed repeatedly with bidistilled water to remove residual Cl^- ions (tested as AgCl(s)). The resulting solid was dried in air at 393 K for 24 h and subsequently was devided into several portions; each portion underwent at different thermal treatment of 3, 24 or 192 h at 473, 523, 573, 623, 673, 723, 773, 823, 873, 923, 973, 1073 and 1273 K. These specimens were designated as TiO_2-hp-ex3. The second series of TiO_2-hp catalysts was obtained by reacting $TiCl_4$ (Carlo Erba) with pure water at about 278 K and adjusting to pH 4.5 with NaOH. The subsequent preparation procedure was the same as for TiO_2-hp-ex3. This second specimen is labeled as TiO_2-hp-ex4. Characterization by XRD, the TiO_2-hp-ex3 specimens was an anatase up to the firing temperature of 923 K. Rutile phase appears at this firing temperature, while the complete conversion to rutile was observed to occur at 1073 K. For TiO_2-hp-ex4 specimens the rutile phase appears at lower firing temperature. Rutile was detected even at 673 K.

The rutile content increased with the temperature and time of firing. The transformation to rutile occurred between 873 and 973 K.

Vassileva, et al., (1996) synthesized a high surface area titanium dioxide (anatase) from $TiCl_4$. A 100 mL of $TiCl_4$ was hydrolysed carefully in 1 L of water, then the solution was adjusted to pH 9 by dropwise addition of 12.5% ammonia solution. The precipitate produced was filtered, washed well with water and calcined for 2 h at 400 °C. The powder obtained was ground in an agate mortar, washed again to remove residual chloride ions and dried in air at 120 °C. This sample was anatase structure and the specific surface area was 84 m^2g^{-1}, higher than the titania commercial product from Fluka (31 m^2g^{-1}).

Khalil and Zaki (1997) synthesized titania (TiO_2) powders by calcination of the dried hydrolysis products of $Ti(OPr^i)_4$ at 400 °C for 3 h. Hydrolysis of $Ti(OPr^i)_4$ was affected by aqueous ammonia in isopropanol (or n-heptane) solvent. First, a 200 mL portion of 0.4 M solution of $Ti(OPr^i)_4$ in isopropanol (or n-heptane) was prepared. Then, the desired amount of ammonia (as a 25% aqueous solution) was added, while the solution was being stirred at 400 rpm at room temperature. The stirring was maintained for one minute for preparations carried out in isopropanol, and for 60 minutes for preparations carried out in n-heptane. The resulting suspensions were aged for three days and then filtered. The precipitates obtained, without washing, were allowed to dry overnight at room temperature in the open air, followed by heating at 60 °C for 24 h. In conclusions, whether in a polar (isopropanol) or a non-polar (n-heptane) solvent, the hydrolysis product of titanium (IV) isopropoxide on calcination at 400 °C for 3 h produced anatase TiO_2 powders. A controlled

addition of NH$_4$OH solution seems to catalyse the hydrolysis, leading eventually to a marked development in the specific surface area (up to 73 m^2/g) of the TiO$_2$.

Jalava, et al., (1998) studied the TiO$_2$ hydrated by x-ray diffraction, atomic force microscopy (AFM) and transmission electron microscopy (TEM). TiO$_2$ hydrated in this work were precipitated either by NH$_4$OH neutralization from an aqueous titanium tetrachloride solution at <30 °C (C samples) or by the sulfate process, which includes thermal hydrolysis from sulfuric acid solution containing titanium oxide sulfate (S sample). The neutralization of the C1 samples was carried out to pH 4.8. The material was then washed and aged at 25 °C for 15 (C1a) or 29 months (C1b). Neutralization of the C2 samples was carried out to pH 5.8. These samples were aged at the same temperature as C1 samples for 19 months. All C samples were dried at room temperature after the aging. The S sample was dried at 110 °C without aging. From the x-ray diffraction indicating that the C2 sample is in amorphous form. The crystalline structure of the C1a sample is a polymorphic mixture of anatase and brookite. The degree of crystallinity of the C1a sample was 70% and average crystalline size is 20 nm. The structure of the S sample was found to be totally microcrystalline anatase. The volume-average crystalline size is approximately 15 nm.

Dalai, et al., (1998) synthesized and characterized the sulfated titania solid acid catalysts, which were prepared by incorporation of sulfate ions in a dried titanic acid precipitate by impregnation with 0.5 M sulfuric acid. The dried titanic acid was prepared by precipitate from titanium tetrachloride using

aqueous ammonia as the precipitating agent. The titanic acid precipitate (T-D) was dried overnight at 60 $^{\circ}$C. Altogether, sulfated titania catalysts with five levels of sulfate loading were prepared. The sulfate loading were 5, 7.5, 10, 12.5, and 15 wt % and were obtained by impregnating the dried titanic acid powder (T-D) with appropriate amount of 0.5 M sulfuric acid. All the catalysts were calcined at 450 $^{\circ}$C for 4 h. These are referred to as 450ST5, 450ST7, 450ST10, 450ST12, and 450ST15. The dried sulfated titania catalyst treated with 15 wt% SO_4^{2-} was also calcined at 500, 550 and 650 $^{\circ}$C. These sulfated titania catalysts are referred to as 500ST15, 550ST15, and 650ST15, respectively. Characterization data of sulfated titania catalysts are shown in Table 4.

Table 4 BET surface area, average pore diameter, and total pore volume of various titania catalysts (Dalai, et al.,1998 : 3871).

Catalysts	Sulfur loading (wt %)	BET surface area (m^2/g)	av pore diam (Å)	tot. Pore vol (cm^3/g)
T-D	0.0	334±10	33±2	0.27±0.01
T-C	0.0	61±2	95±7	0.14±0.01
450ST5	0.36	84±2	87±6	0.18±0.01
450ST7	0.42	114±3	70±5	0.20±0.01
450ST10	1.2	154±4	52±4	0.20±0.01
450ST12	1.6	173±4	46±3	0.20±0.01
450ST15	1.75	135±3	53±4	0.18±0.01
500ST15	1.55	90±2	77±5	0.17±0.01
550ST15	1.3	97±2	85±6	0.21±0.01
650ST15	0.30	57±1	141±9	0.20±0.01

Xu, et al., (1999) prepared TiO_2 powder by slowly addition of predetermined amount of $Ti(OBu)_4$ (chemically pure) into a container that contained alcohol with continuous stirring. The pH value was then adjusted to 2.0 with nitric acid (chemically pure). Deionized water was then added to the mixture, and the composition (molar ratio) was controlled at 20:1:2.5 for alcohol: $Ti(OBu)_4$: H_2O. Stirring the mixture was continued for about 10 min, and the solution was maintained at room temperature for a few days until a gel could be obtained. Then the material was dried at 60~70 °C in a vacuum for 3 h and milled. The crystal structure of TiO_2 depends on the temperture of heat treatment. Amorphous-, anatase- and rutile-type TiO_2 could be obtained at 120, 500, and 900 °C, respectively. Their BET surface area listed in Table 5.

Table 5 BET surface areas of different TiO_2 powders at 25 °C (Xu, et al.,1999 : 375).

Particle size	Particle type	BET surface area (m^2/g)
49.0 µm	anatase	12.44
11.6 µm	anatase	19.70
6.1 µm	anatase	27.81
3.0 µm	anatase	76.72
2.4 µm	anatase	79.32
30 nm	anatase	94.17
12 nm	amorphous	127.14

Yanagisawa and Ovenstone (1999) studied crystallization of anatase from amorphous titania by using the hydrothermal technique. Amorphous titania in their work was prepared from different routes. (1) $TiCl_4$ (30 mL, 0.273 mol) was diluted with ice cold water (300 mL). A 1.5 M NH_3 solution was added dropwise to the clear $TiCl_4$ solution until the pH was raised from 0.5 to

3.0 (approx. 740 mL). The white precipitate formed was aged for 24 h before washing with water until the pH reached 7. The amorphous powder (A3) was dried for 24 h at room temperature. (2) $TiCl_4$ (20 mL, 0.182 mol) was diluted with ice-cold water (200 mL) and added dropwise to a 7.5 M ammonia solution. The pH fell from 12.5 to 10.9 as the white precipitate formed. Again the amorphous precipitate was aged for 24 h before washing until the pH reached 9.2. The amorphous powder (B3) was then dried for 24 h at room temperature. (3) $Ti(OC_2H_5)_4$ (25 g) was added to 550 ml of dry ethanol and mixed thoroughly before being added to a 0.6 M solution of water in ethanol [5.94 ml (0.33 mol) water in 550 mL ethanol]. After aging for 25 min, the reaction mixture was centrifuged and washed twice with ethanol before drying in a vacuum desiccator. The results clearly showed the presence of the anatase phase short-range order in the A3 powder but not in the B3 or C3 powder. This implies that the anatase nuclei were already present in the starting powder for A3, but that B3 and C3 were truly amorphous. The specific surface areas (measured by BET) for all three starting materials were high at over 350 m^2g^{-1}.

Youn, et al., (1999) and Ha, et al., (2000) studied the effects of alcohol rinsing on the crystallization behavior and the anatase–rutile transition behavior of titanium oxide precipitates. Titania powders in their work were prepared by controlled precipitation at room temperature. A 2 M solution of titanium chloride was added to 5 N NH_4OH solution under vigorous stirring. The titanium-ion concentration of the mixed solution was adjusted to 0.2 M so that the precipitation was carried out at a pH of 10.3. The white precipitate was aged in the mother solution for 2 h under stirring and then filtered.

Deionized water was used for the filtration and washing, which were repeated until no chloride ions were found by $AgNO_3$ solution test. Prepared powders were then subjected to two different treatments. The other was rinsed in ethanol and then butanol and dried at 110 °C for 24 h. Powder obtained using this method was designed PB powder. From the results, it was observed the ethanol/butanol rinsing of hydrated titania powder precipitated from titanium chloride solution retarded its crystallization to anatase (crystallization temperatures of 390 °C and 467 °C for PW and PB, respectively) but accelerated the phase transition from anatase to rutile lowered the onset transition temperature about 250 °C (from 800 °C for water-washed powder to 550 °C for alcohol-rinsed powder).

Zhang, et al., (1999) prepared and characterized nanosized TiO_2 powders. Titania powder was prepared by dissolving $TiCl_4$ in distilled water in an ice-water bath. The concentration of titanium was adjusted to 3 M. This aqueous solution was then mixed with pure distilled water or $(NH_4)_2SO_4$ solution in a glass bottle and placed in a temperature-controlled bath. Temperatures were varies in the 20 - 95 °C range. The mixture was stirred at high speed while the amount of $TiCl_4$ solution necessary for the desired $[H_2O]:[Ti]$ molar ratio was added dropwise. Maintaining at the same temperature for 1 h, the mixed solution were treated with 2.5 M diluted NH_4OH until the pH value was 7. Subsequently, the precipitated titanium hydroxide/hydrous titanium oxide ($TiO_2 \bullet nH_2O$) was separated from the solution by filtration and repeatedly washed with distilled water and dilute NH_4OH solution to make $TiO_2 \bullet nH_2O$ that was free of chloride ions. The hydrous oxide was dried at room temperature (~30 °C) under vacuum and

ground to fine powder. A summary of the x-ray diffraction and BET surface area results of nanocrystalline powders prepared under various hydrolysis conditions are shown in Table 6.

Table 6 Comparison of powders prepared under various hydrolysis conditions.

(Zhang, et al.,1999 : 1296)

Sample	$[Ti]/[SO_4^{2-}]$	Hydrolysis T/°C	Dried at RT Particle size*/nm	Calcined at 400 °C		Weight fraction of rutile(χ)
				Particle size*/ nm	BET surface area/ $m^2.g^{-1}$	
1	1:2	95	4.0	6.8	189	0
2	20:1	70	3.5	9.5	138	0
3	1:0	70	4.4(R)	10.7(A)	73	0.63(RT) 0.58(400 °C)
			6.0(R)	14.2(R)		0.72(400 °C)
4	1:0	RT	Amorphous	10.1	131	0
5	20:1	RT	Amorphous	9.5	136	0

* Calculated by XRD, A denoted anatase and R denotes rutile.

The addition of a small amount of $(NH_4)_2SO_4$ promotes occurrence of anatase phase and inhibits the anatase-rutile transformation such that the powder is completely anatase after calcining at 650 °C for 2 h and rutile occurs at around 700 °C. Otherwise, in the absence of SO_4^{2-} ions, the powders had both rutile and anatase phase, when they were calcined at 600 °C, anatase starts to transform to rutile. The transformation temperature of anatase to rutile is approximate to those of alkoxide-derived process. The concentration of SO_4^{2-} ions has some effects on the primary particle size : as the ratio of Ti to sulfate is equivalent to 1:2, finer titania crystallite can be prepared, smaller than 7 nm,

and BET surface area of this powder is as high as 189 m^2/g even calcined at 400 °C for 2 h.

Zhang, et al., (2002) studied nanocrystalline TiO_2 films by optical, XRD, and FT-IR spectroscopy. The TiO_2 films were grown on RCA cleaned silicon wafer and silica glass substrates by ultraviolet-assisted injection liquid source chemical vapor deposition (UVILS-CVD) using a KrCl excimer lamp emitting 222 nm radiation. The reactant used was 10% cyclohexane solution of titanium tetraisopropoxide $(Ti(OC_3H_7)_4)$ precursor, which was injected pulsewise at a rate of 1 Hz into the reactor, while nitrous oxide (N_2O) was used as an oxidising agent. In summary, they have successfully demonstrated the feasibility of depositing titanium oxide films at high growth rates and very low temperatures by the new UVILS-CVD technique which combines excimer UV sources with a novel injection liquids source method. The absense of absorption peaks for CH_2, CH_3, and OH groups on the FT-IR spectra indicates that no impurities such as carbon, OH, and organic compounds etc. were contained in the films. AFM and XRD analysis revealed that nanocrystalline TiO_2 layers with the anatase phase could be grown at low deposition temperatures between 210 and 350 °C. A uniform structure down to a nanostructure scale with particle sizes of 20-30 nm was observed at temperature between 250 and 350 °C.

Zhang, et al., (2002) prepared mesoporous nanocrystalline titanium dioxide by adding 2 g of butadiol in a beaker containing 3 g tetrapropyl titanate at room temperature. The mixture was aged at ambient temperature for 1-8 weeks. During these aging, the fluid became progressively viscous

and eventually resulted in a dry-gel. After the aging, the dry-gel was heated at 300- 800 °C in air. The mesoporous nanophase TiO_2 solid was obtained by annealing this dry-gel between 380 and 480°C for 2 h. By using the sample calcinated at 400 °C for 2 h, they conducted the thermal stability study by reheating it at 350, 400 and 500 °C, labeled as RT1, RT2, and RT3, respectively. From the result, it indicated that, in all cases the products obtained at lower calcination temperature (300 °C) were amorphous, while after heating at higher temperature, the broad anatase peaks appeared. With the increasing of the calcination temperature, the intensity of the anatase peaks became stronger and well-resolved, indicating that larger size particles are formed. When the calcination temperature continues to be increased, small rutile peaks were found, showing the beginning of the transformation of anatase to rutile. Finally, the anatase peaks disappeared, a sign indicating the end of phase transformation from anatase to rutile in the nanophase TiO_2. The effects of aging time on the phase transition are shown in Table 7. Surface area analysis and pore size analysis are shown in Table 8.

Table 7 The influence of aging time to the phase transition of nanocrystalline
titanium dioxide (Zhang, et al., 2002 : 376).

Aging time (week)	The beginning of amorphous to anatase (°C)	The beginning of anatase to rutile (°C)	The end of anatase to rutile (°C)
1	345	630	740
4	330	600	700
8	315	500	685

Table 8 Surface area analysis and pore sized analysis from mesoporous nanophase titania and reheated samples at different temperature (Zhang, et al., 2002:377).

Reheating temperature ($^{\circ}$C)	Surface area (m^2/g)	Average pore diameter (nm)	Time (h)
400[a]	97	3.7	2
350	97	3.7	1
400	92	3.8	1
500	12	3.9	1

a Calcination temperature

Adsorption

The adsorption is a process where molecules from the gas phase or from solution bind in a condensed layer on a solid or liquid surface. The molecules that bind to the surface are called *the adsorbate* while the substance that holds the adsorbate is called *the adsorbent*. The process when the molecules bind is called *adsorption*. Removal of the molecules from the surface is called *desorption*. There are two different types of adsorption: (1) chemisorption (or chemical adsorption), where there is a direct chemical bond between the adsorbate and the surface, and (2) physisorption (or physical adsorption), where the adsorbates were held by physical (i.e., Van der Waals) forces.

Chemisorption and physical adsorption are usually distinguishable from each other without any great difficulty. Table 9 summarizes the main criteria.

Table 9 Criteria for distinguishing between chemisorption and physical adsorption.
(Bond, 1987 :13)

Criteria	Chemisorption	Physisorption
Enthalpy of adsorption, $-\Delta H_{ads}$	40-800 kJ mol^{-1}	8-20 kJ mol^{-1}
Activation energy, E_a	Usually small	Zero
Temperature of occurrence	Depends on E_a but usually low	Depends on boiling point, but usually low
Number of layers adsorbed	Not more than 1	More than one possible

The adsorption characteristics between the adsorbent and adsorbate were explained by the adsorption isotherm in general. The Langmuir and Freundlich models are widely used since they are simple and can describe experimental results over a wide range of concentrations. They can easily be transformed into linear forms to obtain adjustable parameters by graphical means or linear regression analysis (Kim and Chung, 2001).

The Langmuir isotherm is commonly used on the assumption that the adsorbed surface state is homogeneous and the adsorption layer is a monolayer (Kim and Chung, 2001). The Langmuir isotherm is given by :

$$q_e = \frac{Q^0 b C_e}{1 + b C_e} \qquad (1)$$

where q_e is metal uptake per unit weight of adsorbent

Q^0 is adsorption capacity

b is the energy of adsorption

C_e is the equilibrium adsorbate concentration in the bulk fluid phase

Equation (1) is usually linearlized by inversion to obtain the following form.

$$\frac{1}{q_e} = \frac{1}{Q^0} + \frac{1}{bQ^0}\frac{1}{C_e} \qquad (2)$$

Equation (2) is usually used to analyse batch equilibrium data by plotting $1/q_e$ versus $1/C_e$, which yields a linear if data conform to the Langmuir isotherm.

The Freundlich isotherm is the most widely used non-linear sorption model. It is given by the general form:

$$q_e = K_F \bullet C_e^n \qquad (3)$$

Where K_F is related to sorption capacity and n to sorption intensity.
The logarithmic form of equation (3) given below is usually used to fit data from batch equilibrium studies:

$$\log q_e = \log K_F + n\log C_e \qquad (4)$$

Equation (2) and (4) are usually used for the analysis of equilibrium batch experimental data assuming Langmuir and Freundlich isotherms, respectively (Gharaibeh, et al., 1998).

There were many investigations dealing with the adsorption of metal ions on oxide surface. This interest is due both to the importance of the process in ,for example, analytical chemistry, colloid chemistry, flotation and water chemistry, and also to the possibilities of synthesis the new

ion-exchange type catalysts (Hadjiivanov, et al., 1991). Many researches studied the adsorption of metal cations on many types of TiO_2 such as:

Malati and Smith (1979) studied the adsorption isotherms of Ca^{2+}, Sr^{2+} and Ba^{2+} ions on anatase at pH 7 and at 10, 25 and 45 $^\circ$C by using 2.0 g of the powder shaken with 50 cm^3 of the cation solution in a Grant shaking thermostat. After filtration through GF/C or GF/F paper, the cation concentration was determined by complexometric titration. The result, indicated that the initial rate of adsorption increased in the series: $Ba^{2+} < Sr^{2+} < Ca^{2+}$. This sequence reversed with that observed when quartz, silica, γ-MnO_2 and δ-MnO_2 were used as adsorbents. It is tempting to assume that the cations become dehydrated prior to adsorption on titanium dioxide. A similar trend was found for the adsorption of these cations on rutile at pH 7 and 25 $^\circ$C. However, Bérubé and de Bruyn explained the sequence $Cs^+ < Na^+ < Li^+$ of the adsorption of the alkali ions on rutile by postulating the presence of an oriented layer of water molecules hydrogen-bonded to the hydroxylated rutile surface, and suggesting that hydrated ions least likely to destroy the water structure would be preferentially adsorbed. This suggestion would also explain the sequence: $Ba^{2+} < Sr^{2+} < Ca^{2+}$ observed in the present work (Malati and Smith) for rutile. The adsorption isotherms of three cations on anatase at 10 $^\circ$C had a Langmuir shape and the results approximately fitted the linear form of the Langmuir equation. The adsorption of the three cations on anatase was found to be exothermic. The adsorption density on rutile was higher than the adsorption density on anatase in the case of Ba^{2+} ion but not for Ca^{2+} and Sr^{2+} ions. The results are discussed in terms of the hydration of the surface and of the cations.

Ottaviani, et al., (1985) studied the interaction between hydrated Mn^{2+} or Cu^{2+} and the surface of porous TiO_2. The TiO_2 sample used in these experiments was an amorphous, anatase-oriented material obtained by the Blumenfeld-type thermal hydrolysis of titanyl sulfate solutions. The electron spin resonance (ESR) technique was used to study in conjunction with classical colloid chemistry. $[Mn(H_2O)_6]_2^+$ is specifically adsorbed at the surface. It shows a strong dependence on the surface potential. The interacting Mn^{2+} amount sharply increases at a pH higher than the isoelectric point (i.e.p.); on the contrary, noninteracting Mn^{2+} is only found at pH< i.e.p. Mn^{2+} shows a weak specific interaction with the surface sites which is stronger than simple counterion binding, yet without loss of water from the inner hydration shell. In contrast, divalent copper interacts strongly with the surface –OH groups, with loss of primary hydration water. Adsorption of Cu^{2+} has been recorded even on positive TiO_2 surfaces shown to be chemisorbed at the surface –OH groups.

Abe, et al., (1989) reported the adsorption and desorption behavior of a number of heavy metal ions on amorphous HTDO (Am-HTDO) at different pH and in different media. Their selectivities and the applicability of some chromatographic separations of these heavy metal ions are discussed. The ion-exchange selectivity of a number of divalent metal ions was studied as a function of pH in nitrate and chloride media. Separations of mixtures of metal ions were carried out on a column (5 × 0.5 cm i.d.) of Am-HTDO in the hydrogen ion form. A mixed solution containing 1 µmol of each metal ion was loaded on the top to the column and then eluted with different eluents. The order of selectivity was $Pb^{2+} > Hg^{2+} > Cd^{2+} > Mg^{2+}$ in nitrate solution and

$Pb^{2+} > Cd^{2+} > Ca^{2+} > Mg^{2+} > Hg^{2+}$ in chloride solution. A good linear relationship between the logarithm of the distribution coefficient of the heavy metal ions and their effective ionic radius was found. On the basis of the K_d values, the separation of a mixture of Cd^{2+}, Hg^{2+} , and Pb^{2+} and the group separation of Hg^{2+} and Pb^{2+} from several common metal ions were achieved on an ion-exchange column containing amorphous hydrated titanium dioxide.

Vassileva, et al., (1996) studied the adsorption of heavy metal cations on two TiO_2 (anatase) samples. The first sample (T1) was synthesized by hydrolysis of $TiCl_4$, whereas the second (T2) was a commercial product. To study metal ion sorption under static conditions, samples of 0.1 g of TiO_2 were each suspended in solutions containing 0.02-1.0 μg mL^{-1} of the analytes and both phases were kept in contact for 5 min. To study the sorption of metal ions under dynamic conditions, a glass microcolumn was utilized. The column contained a homogeneous mixture of 0.5 g of TiO_2 and 0.5 g of glass beads and was connected to a peristaltic pump. Sorption was performed using 10-1000 ml of solution, containing 10-20 μg mL^{-1} of the analyte ions and adjusted to pH 8 with 0.1 mol/L ammonia solution. This solution was passed through the column at a flow rate of 3 mL min^{-1}. The sorbed metal ions were eluted with 1.0 mol/L HNO_3 and/or 1.0 mol/L EDTA. The adsorption kinetics, pH curves, adsorption isotherms and adsorption capacities were studied. Sample T1 possesses a significant capacity towards sorption of heavy metal cations (approximately 5000 $\mu g/g$), which is much higher than the adsorption capacity of the commercial sample T2 and, in most instances, higher than the capacity of silica. The adsorption capacity of titania depends strongly on the preparation technique (sample morphology). Quantitative and fast sorption of

various heavy metal in trace concentrations on T1 occurs, but in different pH ranges for each element. At pH 8 quantitative sorption was detected for Bi, Cd, Co, Cr, Cu, Fe, Ge In, Mn, Ni, Pb, Sb, Sn, Te, Tl, V, and Zn. On the basis of the results obtained, optimum conditions for the joint and quantitative solid-phase extraction of the most common heavy metal ions are proposed. Column solid-phase extraction using a high surface area anatase is proposed as an efficient preconcentration technique allowing a high concentration factor.

Vohra and Davis (1997) investigated the adsorption behavior of Pb(II) and NTA, both as individual species and as complex species onto titanium dioxide (Degussa P25). Nitrilotriacetic acid (NTA) is extensively used in different industries because of its excellent chelating properties. The method for the adsorption was studied at concentration of 5×10^{-6} to 10^{-3} M for Pb(II), NTA, and Pb(II)-NTA onto 2 g/L TiO_2. The pH of these TiO_2 suspension samples was adjusted from 2 to 10 and kept shaking overnight at normal room temperature. Pb(II) shows a typical cationic type of adsorption behavior, whereas NTA demonstrates an anionic type of adsorption trend. Model fits were obtained using the geochemical speciation software MINTEQA2 employing a diffuse layer surface complexation model. Experimental and model results from ternary systems suggest adsorption of free Pb(II) and NTA, as well as ternary Ti-NTA-Pb(II) and $Ti-O-Pb(II)-NTA^{2-}$ species. The cationic-type complexation, i.e., $Ti-O-Pb(II)-NTA^{2-}$, was essential for the successful NTA adsorption modeling, especially at higher pH and for Pb > NTA systems. Hence results from the present study show that aqueous transport modeling of metal-ligand complexes will require consideration of cationic-type surface

complexes in addition to the conventional ligand-type surface species to correctly predict the movement of such pollutants in the subsurface environment.

Esumi, et al., (1998) studied the adsorption of Cu^{2+} and 2-naphthol from aqueous solutions by anionic surfactant (sodium dodecyl sulfate, SDS) adsorbed on titanium dioxide. Two types of titanium dioxide were used; one was untreated and the other was hydrophobic with dodecyl chain groups. For this study, aqueous solutions of desired concentrations of SDS in the presence of fixed concentrations of 2-naphthol of $CuCl_2$ were prepared. These solutions were added into vials containing titanium dioxide. The pH of aqueous suspensions was adjusted by adding HCl. Then, the vials (0.2g of TiO_2/20mL solution) were shaken to attain adsorption equilibrium at 25 °C for 24 h. When anionic surfactants are adsorbed on positively charged metal oxides, the adsorption occurs predominantly by electrostatic attraction below their i.e.p. (isoelectric point). The i.e.p. of titanium dioxide was ca 6.5. At pH 3, 4 and 5, the adsorption of Cu^{2+} increased with increasing SDS concentration and then decreased slightly on untreated titanium dioxide; the adsorption of Cu^{2+} decreased in a following order, pH5 > pH4 > pH3. The adsorption behavior of Cu^{2+} by SDS adsorbed on hydrophobic titanium dioxide was similar to that on untreated titanium dioxide, although the amount of SDS adsorbed on the former was half as that on the latter. This difference derives from different adsorption states of SDS.

Lehmann, et al., (1999) studied the removal of chromate anions and zinc cations from dilute aqueous solutions by sorption. The experiments was

investigated by the addition of sorbents at constant temperature (25 °C) and agitated in a reciprocal shaker (150 rpm) for 24 h. Sorbent concentrations of 1 g/L were applied throughout. Seven inorganic materials have been examined as sorbents. Four of the sorbents were applied in powdered form (magnesite mineral – consisting mainly from $MgCO_3$, titanium dioxide, hydrotalcite ($Mg_6Al_2(OH)_{16}.CO_3.4H_2O$), and goethite ($\alpha$-FeOOH)), while the other three were applied in granulated form (activated carbon, ferric hydroxide (β-Fe(OH)$_3$), and goethite, which was granulated by freezing/crystallization). Main examined parameters were the pH value of metal solutions and their initial concentrations. These material were of varying specific surface area and they were existed either in powdered and/or granulated form, depending upon their origin or preparation technique. The type of sorbents used ranged from specifically prepared materials, where manufacturing costs are high, such as activated carbon, to relatively cheap, naturally occurring materials such as magnesite mineral fine particles. Among them, "crystallized" goethite was found to be best suited for the removal of both metal forms (cations and anions), when a fixed bed operation mode would be selected, which were found to fit the Langmuir isotherm equation.

Poznyak, et al., (1999) studied the adsorption processes at nanostructured TiO_2 contacting aqueous Cu(II) ion solutions. The state of the adsorbed copper species, and the electronic interactions in the adsorbed copper-TiO_2 systems by using electrochemical methods in combination with electroreflection, ESR, and XPS spectroscopies are applied as a tool. Adsorption of Cu^{2+} ions on TiO_2 nanocrystalline electrodes was carried out by immersing the electrodes into $Cu(ClO_4)_2$ solutions at a constant ionic strength

(0.1 M) and corrected periodically in the course of the adsorption. After 24 h of equilibration at the temperature of 20 ± 1 °C, the electrodes were removed from solution and then immersed in distilled water for 10 min to remove unbound Cu^{2+} ions. Analysis of the voltammograms in combination with ESR data has allowed us at least four types of copper species formed on the TiO_2 surface after the adsorption of aqueous Cu^{2+} ions. These are monovalent copper ions, magnetically isolated Cu(II) ions, Cu(II) ions forming specific areas ("associates") with a high local concentration and strong interaction between the ions, and formally diamagnetic copper hydroxide species. The appearance of them can be associated with the partial reduction of adsorbed Cu^{2+} ions by electrons of the TiO_2 matrix. The Cu(II) ions bound to the TiO_2 surface give rise to the electroactive surface states within the band gap of the oxide.

Liang, et al., (2001) studied the adsorption characteristics of some metal ions on nanometer TiO_2 under dynamic condition, optimized the conditions for the simultaneous preconcentration of trace elements and proposed a new method using a microcolumn packed with nanometer TiO_2 coupled with ICP-AES for simultaneous determination of trace elements in biological sample and water. A new method using a PTFE microcolumn packed with nanometer TiO_2 as solid-phase extractants has been developed for the simultaneous preconcentration of trace amounts of Cu, Mn, Cr and Ni. Aliquots of 20 mL solutions of metal ions containing 10 µg Cu^{2+}, Mn^{2+}, 20 µg Cr^{3+} and 50 µg Ni^{2+} were prepared and the solution was passed through the column by using a peristaltic pump adjusted to the desired flow rate. Afterwards, the retained metal ions were eluted with 1.0 mL of 2.0 mol/L HCl

solution. Effect of pH, sample flow rate and volume, elution solution and interfering ions on the recovery of the analytes have been investigated. The pH values plays an important role with respect to the adsorption of different ions on oxide surfaces. It can be seen that all the metal ions were adsorbed poorly at pH < 6. A quantitative recovery (>90%) was found for Cr^{3+} and Cu^{2+} at the pH range of 6-9. For Mn^{2+} and Ni^{2+}, the highest recovery was obtained in the pH range of 8-9. The adsorption capacity of nanometer TiO_2 was found as 0.108, 0.14, 0.039 and 0.034 mmol/g for Cu, Cr, Mn and Ni, respectively.

1.3 Objectives

1.3.1 To synthesize and characterize the titanium dioxide.

1.3.2 To study the adsorption properties of metal ions, Cu(II), Mn(II), Pb (II) and Fe(III), on the synthesized titanium dioxide.

Chapter 2
METHOD OF STUDY

2.1 Materials

2.1.1 Ammonium hydroxide (Ammonia solution) 28.0 - 30.0%, NH_4OH; A.R., code no. 9721-03, J.T. Baker.

2.1.2 Silver nitrate, $AgNO_3$; A.R., code no. 102333J, BDH, England.

2.1.3 Sodium hydroxide, $NaOH$; A.R., code no. 102525P, BDH, England.

2.1.4 Titanium tetrachloride, $TiCl_4$; A.R., code no. 488407, Carlo Erba.

2.1.5 Titanium dioxide (Anatase), TiO_2; A.R.,code no. 488257, Carlo Erba.

2.1.6 Titanium dioxide P25; code no. D-60287, Degussa AG, Frankfurt, Germany.

2.1.7 Nitric acid, HNO_3; A.R., code no. 9601-06, J.T Baker.

2.1.8 Copper standard solution 1000 mg/L ; $Cu(NO_3)_2$ in HNO_3 0.5 mol/L, code 1.19786.0500, Merck, Germany.

2.1.9 Iron standard solution 1000 mg/L ; $Fe(NO_3)_3$ in HNO_3 0.5 mol/L, code 1.19781.0500, Merck, Germany.

2.1.10 Manganese standard solution 1000 mg/L ; $Mn(NO_3)_2$ in HNO_3 0.5 mol/L, code 1.19789.0500, Merck, Germany.

2.1.11 Lead standard solution 1000 mg/L ; $Pb(NO_3)_2$ in HNO_3 0.5 mol/L, code 1.19776.0500, Merck, Germany.

2.1.12 Filter papers No.1 ; Qualitative, Whatman, England.

2.1.13 Ultra pure water 18.2 MΩ ; maxima, ELGA, England.

2.1.14 Universal indicator ; full range pH 1 – 14, Whatman, England.

2.2 Instruments

2.2.1 Chemistry Department, PSU

1. Analytical balances ; AE 200S, SNR M10802, Mettler Toledo A.G., Switzerland.

2. Atomic absorption spectrometer, AAS ; AAnalyst 300, perkin Elmer, Norwalk, CT, U.S.A.

3. Centrifuge ; EBA 20, Hettich, Germany.

4. Energy dispersive x-ray fluorescence, EDXRF; Spectrace 5000, Spectrace Instruments,Inc., Mountainview, California, U.S.A.

5. Magnetic stirrer ; Jenway 1000, JENWAY, UK.

6. Oven ; National, Heinicke Company, U.S.A.

7. pH meter ; model 8519, HANNA Instruments, U.S.A.

8. pH electrode ; model 300731.1 with wetting cap removed, Denver Instrument company.

9. Photovolt ; model 577,Seradyn,Inc., Indiapolis, U.S.A.

10. Precision variable volume pipette, L200 (20-200 µL) and L1000(100-1000 µL), LABMATE, Poland.

11. U.S. Standard sieve series A.S.T.M. E-11, Sieve no.200, DUAL Manufacturing Co, Chicago, U.S.A.

2.2.2 Scientific Equipment Center, PSU

1. Differential scanning calorimeter, DSC ; DSC7, Perkin Elmer, Singapore.

2. Fourier-transformed infrared spectrophotometer, FT-IR ; EQUINOX 55, Bruker, Germany.

3. Thermogravimetric analyzer, TGA; TGA7, Perkin Elmer,
   Singapore.

2.2.3   Central Equipment Unit, Faculty of Science, PSU

1. X-ray diffractrometer, XRD ; PW 3710 mpd control,
   Ni-filtered Cu Kα radiation, Philips.

2.2.4   Chemical Engineering Department, PSU

1. Surface area / pore size ; SA 3100, Coulter, U.S.A.

2.2.5   Chemistry Department, KMUTL

1. Surface area by BET methods ; Autosorb-1-C, Quantachrome,
   U.S.A.

2.3 Methods

This work can be devided into 2 parts; (1) synthesis and characterization of titanium dioxide, and (2) studies of the adsorption of metal ions Cu(II), Mn(II), Pb(II), and Fe(III) on the synthesized titanium dioxide. Equipment such as XRD, BET, EDXRF, FT-IR, TGA, and DSC were used for the first part while AAS was the main equipment for the second part.

2.3.1 Synthesis and characterization of titanium dioxide

2.3.1.1 Synthesis of titanium dioxide

Titanium dioxide was prepared from two different routes.

(A) NH_3 solution (5.87 M) was added slowly to titanium tetrachloride ($TiCl_4$) in 2-necked round bottom flask while stirring simultaneously until the white precipitate was obtained. The precipitate was filtered gravimetrically with Whatman no.1 filter paper and subsequently washed several times with distilled water until the filtrates did not show any cloudiness of AgCl with silver nitrate solution test nor ammonium ions were found by the NaOH solution test. The white solid was dried at 105 °C and ground to fine powder.

(B) NH_3 solution (2.93 M, approx. 240mL) was added slowly to $TiCl_4$ (30 mL, 0.267 mol) in 2-necked round bottom flask which placed in an ice-water bath and stirring simultaneously until the white precipitate was obtained. The precipitate was filtered gravimetrically with Whatman no.1 filter paper and subsequently washed with distilled water until free of chloride and ammonium ions. The product obtained was dried at 105° C, ground and sieved to –200 mesh size (75 Microns).

2.3.1.2 Characterization of titanium dioxide

2.3.1.2.1 X-ray powder diffraction patterns (XRD)

The XRD spectra were obtained through the Equipment Division of the Faculty of Science, Prince of Songkla Universety, Hat Yai, Songkla using an x-ray diffractrometer, PW 3710 mpd control, Ni-filtered Cu Kα radiation, Philips.

2.3.1.2.2 Surface area / Pore size

The specific surface area was measured by the BET method (Autosorb-1-C, Quantachrome). All data were measured by Dr. Tawan Sooknoi, Department of Chemistry, Faculty of Science, King Mongkut's University of Technology Ladkrabang, Bangkok. The pore size distribution were acquired by the Department of Chemical Engineering, Faculty of Engineering, Prince of Songkla Universety, Hat Yai, Songkla (Coulter, model SA3100, U.S.A).

2.3.1.2.3 Energy dispersive x-ray fluorescence (EDXRF)

The element composition was checked by EDXRF. The energy dispersive x-ray fluorescence (EDXRF) spectrometer (Spectrace 5000, Spectrace Instruments, Inc., Mountainview, California) is of the tube type. The excitation x-ray is generated from a tube using a Rh target. The detector is Si(Li) with resolution of 164 eV for the Mn Kα line. This spectrometer is fully computerized and controlled by the software EDXRF version 1.35.

2.3.1.2.4 Fourier-transformed infrared spectrophotometer
(FT-IR)

The functional groups were checked by FT-IR in diffuse reflectance mode at 4000-400 cm^{-1} with KBr as blank (EQUINOX 55, BRUKER, Germany). The spectrum was acquired by the Scientific Equipment Center, Prince of Songkla University, Hat Yai, Songkla.

2.3.1.2.5 Thermogravimetric analysis (TGA)

Mass change with temperature was studied in the range 50-500 $^\circ$C under nitrogen atmosphere with heating rate of 10 $^\circ$C per minute (TGA7, Perkin Elmer, U.S.A). All data were acquired by the Scientific Equipment Center, Prince of Songkla University, Hat Yai, Songkla.

2.3.1.2.6 Differential scanning calorimetric (DSC)

The change of energy with temperature was studied in the temperature range of 50-500 $^\circ$C under nitrogen atmosphere with heating rate of 10 $^\circ$C per minute (DSC7, Perkin Elmer, U.S.A). All data were acquired by the Scientific Equipment Center, Prince of Songkla University, Hat Yai , Songkla.

2.3.1.2.7 Whiteness

The whiteness of TiO_2 samples were measured on a Photovolt ; model 577, Seradyn, Inc., Indiapolis, U.S.A.

2.3.2 Adsorption of metal ions by TiO_2(syn)

The adsorptions of metal ions : Cu(II), Mn(II), Pb(II), and Fe(III) on the synthesized titanium dioxide [TiO_2(syn)], which was obtained from method B were studied.

2.3.2.1 Analytical methods

Atomic absorption spectrometer (AAnalyst 300, Perkin Elmer, Norwalk, CT, U.S.A.) was used for the determinations of metal ions

studied. The linear calibration curve of each metal ions was used for the analyte. The working conditions are given in Table 10.

Table 10 Instrumental working conditions

Element	Wavelength/nm	Slit/nm	Flame gases	Lamp current/mA
Cu	324.8	0.7	A-Ac*	15
Fe	247.7	0.2	A-Ac*	30
Mn	279.8	0.2	A-Ac*	20
Pb	283.3	0.7	A-Ac*	10

*A-Ac = air - acetylene

2.3.2.1.1 Preparation of calibration standards

Four calibration standards for each elements (Cu, Mn, Pb, and Fe) were used for linear curve plots. All of calibration standard solutions were prepared daily by dilution 1000 mg/L of the atomic absorption standards (Merck) with ultra pure water (18.2 MΩ). The concentration of standards solutions were 1, 2, 3, and 4 mg/L for Cu, Mn, and Fe. For Pb were 5, 10, 15, and 20 mg/L

2.3.2.1.2 Preparation of the sample solutions

The sample solutions were prepared daily by dilution 1000 mg/L of the atomic absorption solution standards (Merck) with ultra pure water (18.2 MΩ).

2.3.2.2 The optimum condition for the adsorption

The optimum conditions for the adsorptions of metal ions, Cu(II), Mn(II), Pb(II), and Fe(III), were determined by studying the effect of stirring time, sample volume, concentration of metal ions, and pH.

2.3.2.2.1 Stirring time

The effect of stirring time on the adsorption on TiO_2(syn), was investigated by using single solution [7.0 mg/L for Pb(II) and 3.5 mg/L for Cu(II), Mn(II) and Fe(III)] . In each case, the pipetted 20 mL of metal ions solutions was added into a beaker (0.05 g TiO_2(syn)) at room temperature and stirred for 5, 10, 15, 30, and 60 minutes using the magnetic stirrer. The aqueous phase was then separated from TiO_2(syn) by centrifugation and the concentration of the metal ions in the aqueous phase (C_e, mg/L) were determined by AAS.

2.3.2.2.2 Sample volume

The effect of sample volume on the adsorption on TiO_2(syn) was investigated by using single solution [7.0 mg/L for Pb(II) and 3.5 mg/L for Cu(II), Mn(II), and Fe(III)]. In each case, the pipetted 10, 20, 25, 30, 40, 50, 75, and 100 mL for (Cu, Mn and Fe) and 10, 20, 25, 30, 40, 50, 75, 100, and 150 mL for Pb of sample solutions was added into a beaker containing 0.05 g of TiO_2(syn) at room temperature and stirred for 10 minutes for Cu and Mn and 15 minutes for Fe and Pb. After equilibration the TiO_2(syn) were separated by centrifugation and the concentration of metal ions in the supernatants were determined with AAS.

2.3.2.2.3 Concentration of metal ions

The effect of concentration of metal ions was investigated by using single solution of Cu(II), Mn(II), Pb(II), and Fe(III). The concentration of metal ions were 2, 4, 5, 6, 7, and 8 mg/L for Cu(II), 2, 3, 4, 5, and 6 mg/L for Mn(II), 2, 4, 6, 8, 15, 20, 25, 30, 40 and 50 mg/L for Pb(II), and 2, 4, 5, 6, 10, and 15 mg/L for Fe(III). In each case, pipetted sample solutions (25 mL for Cu, 30 mL for Mn, and 50 mL for Pb and Fe) into a beaker (0.05 g of TiO_2(syn) for Cu, Mn, and Fe and 0.025 g for Pb) at room temperature and stirred for 10 minutes for Cu and Mn, and 15 minutes for Pb and Fe. The solutions were centrifuged in order to separate the two phases. The concentrations of the unsorbed ions in the liquid phase were determined directly by AAS.

2.3.2.2.4 pH

The effect of pH was investigated by using single solution (6, 5, 25, and 8 mg/L for Cu(II), Mn(II), Pb(II), and Fe(III), respectively). In each case, the pH of sample solutions was adjusted to the desired value (3, 5, 7, 9, and 11) with HNO_3 and NH_3 solution. A 25 mL for Cu(II), 30 mL for Mn(II), and 50 mL for Pb(II) and Fe(III) of the sample solution was added into a beaker (0.05 g of TiO_2(syn) for Cu, Mn and Fe and 0.025 g for Pb) at room temperature and stirred for 10 minutes for Cu and Mn and 15 minutes for Pb and Fe. The residual concentration of metal ions was then separated from TiO_2(syn) by centrifugation. The analytes in the aqueous phase was determined by AAS.

2.3.2.3 Adsorption isotherm

The adsorption isotherms between TiO_2(syn) and metal ions [Cu(II), Mn(II), Pb(II), and Fe(III)] were investigated by using single solution. In each case, various concentrations of sample solutions [25, 35, 50, 75, 100, 150, 200, 250, and 300 mg/L for Cu(II), 5, 15, 20, 25, 50, 75, 100, 150, and 200 mg/L for Mn(II), 5, 10, 15, 20, 25, 50, 75, 100, 200, 300, and 400 mg/L for Pb(II), and 2, 4, 5, 10, 12, 15, and 25 mg/L for Fe(III)] were used. Pipetted 25 mL for Cu(II), 30 mL for Mn(II), and 50 mL for Pb(II) and Fe(III) of the sample solution into a beaker (0.05 g of TiO_2(syn) for Cu, Mn and Fe and 0.025 g for Pb) at room temperature and stirred for 10 minutes for Cu and Mn, and 15 minutes for Pb and Fe. After centrifugation, the concentration of the metal ions in the liquid phase (C_e, mg/L) were determined by AAS.

Langmuir and Freundlich equations were used to analyse data by plotting the reciprocal of Q_e (metal ions adsorbed, mg/g) versus the reciprocal of C_e and the logarithm of Q_e versus the logarithm of C_e, respectively.

2.3.2.4 Comparison of the adsorption capacities between TiO_2(syn) and the commercial TiO_2

The comparison of the adsorption capacities between TiO_2(syn) and the commercial TiO_2 (anatase: Carlo Erba, P25: Degussa and rutile: TOA Co, Thailand) was investigated by using single solution [200 mg/L for Cu(II), 75 mg/L for Mn(II), 400 mg/L for Pb(II) and 15 mg/L for Fe(III)]. The pH was adjusted to the desired pH 7 with small amount of HNO_3 and NH_3 solution. In each case, a 25 mL for Cu(II), 30 mL for Mn(II), and 50 mL for Pb(II) and Fe(III) was added into a beaker (0.05 g of TiO_2 for Cu, Mn and Fe

and 0.025 g for Pb) at room temperature and stirred for 10 minutes for Cu and Mn, and 15 minutes for Pb and Fe. Following sorption, the TiO_2(syn) was separated by using a centrifuge and the concentration of metal ions (C_e, mg/L) in the supernatants were determined with AAS.

Chapter 3

RESULTS

3.1 Synthesis and characterization of titanium dioxide

3.1.1 Synthesis of titanium dioxide

Titanium dioxide powders were prepared by two different routes (method A and B). In both methods, when NH_3 solution was added to $TiCl_4$ in the hood, it gave off a large amount of white smoke and the reaction was vigorous. Then a yellow precipitate was obtained when adding NH_3 solution at first time which eventually changed to the white precipitate. After that it was dried at 105°C and ground to fine white powder. The product is shown in Figure 4.
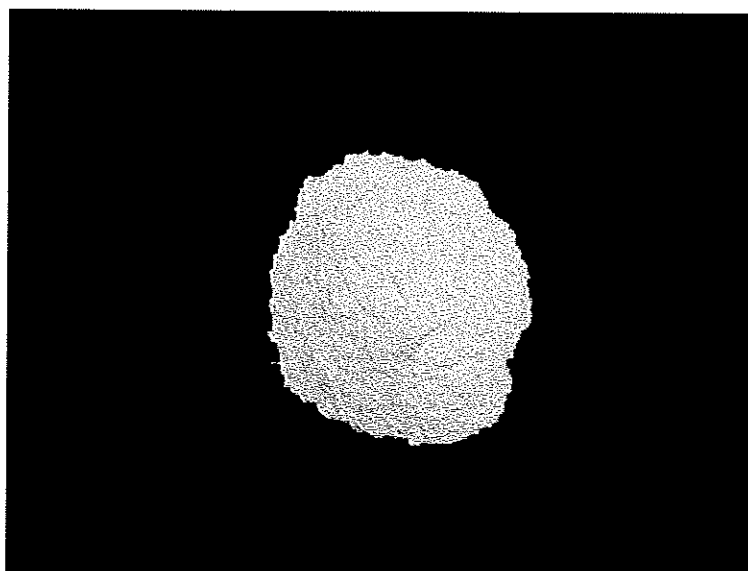
Figure 4 $TiO_2(syn)$

3.1.2 Characterization of titanium dioxide

3.1.2.1 X-ray powder diffraction patterns (XRD)

The x-ray powder diffraction method is unique in that it is the only analytical method that is capable of providing qualitative and quantitative information about the compounds present in a solid sample. The identification of a species from its powder diffraction pattern is based upon the position of the lines (in terms of θ or 2θ) and their relative intensities (Skoog and Leary, 1992). The XRD pattern of TiO_2(syn) (from method A) in Figure 5(a) shows broad weak peaks at (2θ) 25.4, 38, 48, 53, and 55 which correspond to 101, 004, 200, 105, and 211 reflections of anatase (Park, et al.,1999). In Figure 5(b) shows XRD pattern of TiO_2(syn) (from method B) which has only flat base line indicating non-crystalline, amorphous, phase.
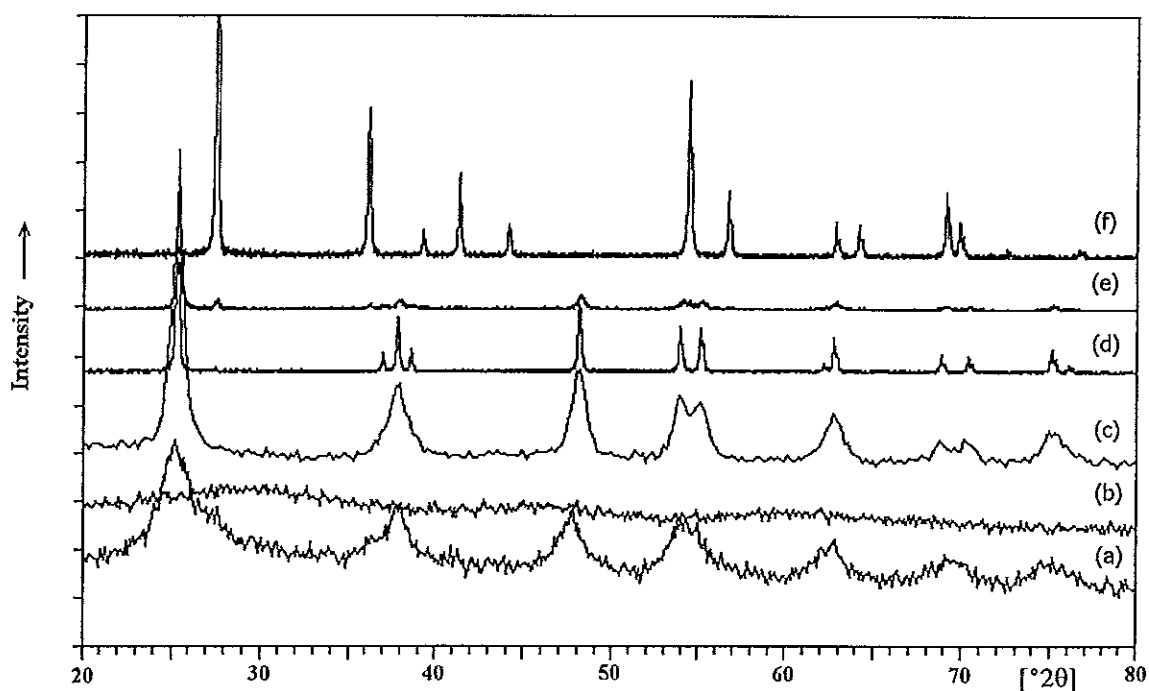
Figure 5 XRD patterns of (a) TiO_2(syn) by method A, (b) TiO_2(syn) by method B,

(c) calcination TiO_2(syn) from method B at 426 °C, (d) anatase: Carlo Erba,

(e) P25: Degussa, and (f) rutile: TOA Co, Thailand.

Figure 5(d) shows XRD pattern of TiO_2 (anatase), the commercial product from Carlo Elba, at (2θ) 25.4, 38, 48, 53, and 55 that correspond to 101, 004, 200, 105, and 211 reflections of anatase (Park, et al.,1999). XRD pattern of TiO_2 (rutile : TOA Co, Thailand) in Figure 5(f) shows peaks at (2θ) 27.5, 36, 41, and 56 that correspond to 110, 101, 111, and 220 reflections of rutile (Park, et al.,1999). Figure 5(e) shows XRD pattern of Degussa P25 at (2θ) 25.4, 38, 48, 53, and 55 that correspond to 101, 004, 200, 105, and 211 reflections of anatase and (2θ) at 27.5, 36, 41, and 56 that correspond to 110, 101, 111, and 220 reflections of rutile (Park, et al.,1999).

3.1.2.2 Surface area / pore size

The surface area is an average measurement of the external surface of a large number of particles and expressed in terms of the area per unit mass (m^2/g). There are two main analysis techniques for measuring surface area; gas adsorption and gas permeability. In this work gas adsorption surface area analysis was used.

The gas adsorption approach starts with a clean surface achieved through vaccum or inert gas bakeout. The clean powder surface is exposed to varying partial pressures of known adsorbing vapors. A measurement is made of the amount of gas adsorbed on the powder surface versus the partial pressure. The measurement is often referred to as the BET specific surface area after Brunauer, Emmett and Teller who developed the concept in 1938.

Under equilibrium, the rate of adsorption equals the rate of evaporation. Letting P equal the partial pressure of adsorbate, P_0 equal the saturation pressure of adsorbate (which depends on the gas and

temperature), X equal the amount of gas adsorbed at a pressure P, X_m equal the monolayer capacity of the powder (the amount of gas necessary to form a uniform surface coating one atomic layer thick), and C equal a constant relating to the adsorption enthalpy, gives

$$\frac{P}{X(P_0 - P)} = \frac{1}{X_m C} + \frac{C-1}{X_m C} \frac{P}{P_0} \qquad (5)$$

Note the linear relation between the term on the left of the equal sign and the partial pressure ratio P/P_0. This is the BET equation, and is generally valid for powders in the range P/P_0 from 0.05 to 0.30. Equation (5) can be rewritten in a general form as,

$$\frac{P}{X(P_0 - P)} = B + A \frac{P}{P_0} \qquad (6)$$

where

$$X_m = \frac{1}{A+B} \qquad (7)$$

giving A as the slope and B as the intercept of the linear equation. Finally, the surface area is calculated as

$$S = X_m N_0 A_0 / (wM) \qquad (8)$$

using M as the molecular weight of adsorbate, A_0 as the average occupational areas of an adsorbate molecule, N_0 as Avogadro's number, and w as the sample weight (German, 1984).

Surface area and porosity of titanium dioxide are shown in Table 11 and Table 12, respectively. The data were compared between TiO_2(syn) (from method B) and commercial product.

Table 11 Surface area of titanium dioxide.

Titanium dioxide samples	Surface area[a] (m^2/g)	Surface area[b] (m^2/g)
TiO_2(syn)-method B	260-332[c]	-
TiO_2(syn)-method B (-200 mesh)	-	449
Anatase (Carlo Erba)	10.72	9.65
Rutile (TOA)	16.08	13.08
P25 (Degussa)	54.50	51.41

a Data were determined by using Autosorb-1-C, Quantachrome.

b Data were determined by using SA3100, Coulter.

c Surface area was measured from 5 samples, 260, 290, 298, 308 and 332 m^2/g.

Table 12 Porosity of titanium dioxide

sample	Pore volume (%) for pore diameter[a] :								Porosity[a] (ml/g)	Micropore[b] surface area (m^2/g)
	<6	6-8	8-10	10-12	12-16	16-20	20-80	>80(nm)		
TiO_2(syn)-method B (-200mesh)	51	12	7	5	5	4	11	5	0.098	107
Anatase (Carlo Erba)	2	1	1	1	1	1	15	78	0.019	0
Rutile (TOA)	7	5	4	4	6	6	34	34	0.049	0
P25 (Degussa)	5	3	2	2	3	4	38	43	0.235	0

a Data were determined by using SA3100, Coulter.

b Micropore have diameter < 2 nm (Sclafani, et al.,1990).

3.1.2.3 Energy dispersive x-ray fluorescence (EDXRF)

X-ray fluorescence (XRF) is one of the most widely used of all analytical methods for the qualitative identification of elements having atomic numbers greater than oxygen (>8) ; in addition, it is often employed for semiquantitative or quantitative elemental analyses as well (Skoog and Leary, 1992). The EDXRF spectra of TiO_2(syn) (from method B) in Figure 6 shows only peaks from K-lines of titanium (Ti).
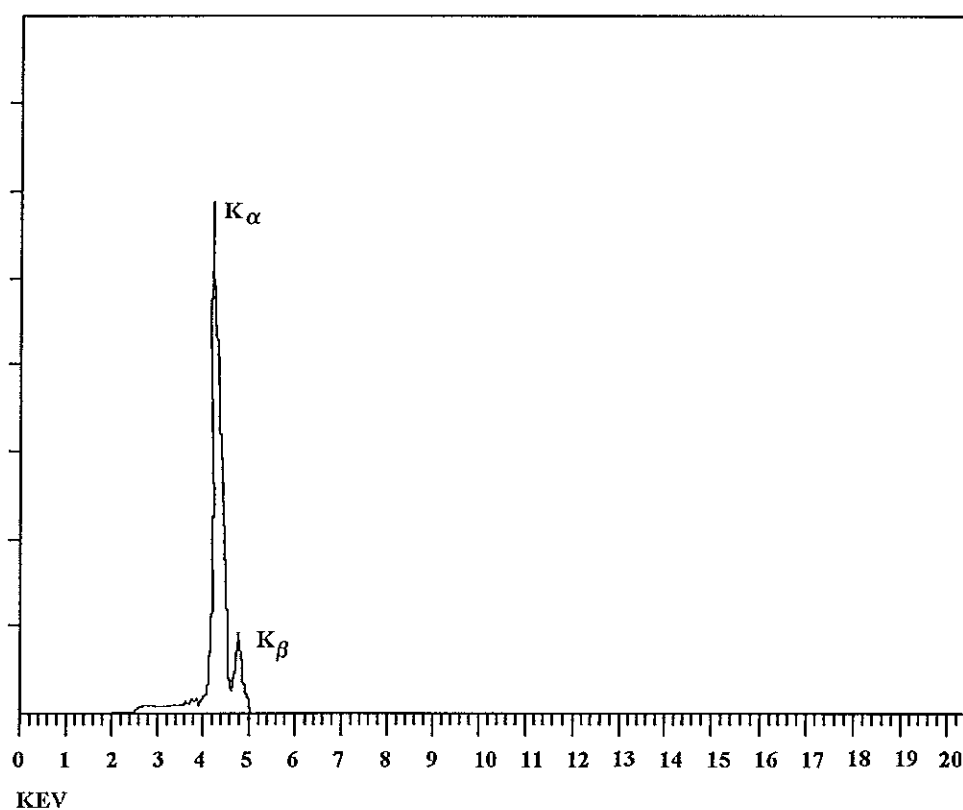
Figure 6 EDXRF spectrum of TiO_2(syn).

3.1.2.4 Fourier-transformed infrared spectrophotometer (FT-IR)

IR is a technique for determining the functional groups within the compounds. The spectral range of greatest use in the mid-infrared

region, which covers the frequency from 200 cm^{-1} to 4000 cm^{-1} (50-25 μm). In Figure 7 shows the FT-IR spectrum of TiO_2(syn) (from method B) and Table 13 lists the assigned modes of functional groups that are responsible for the vibration bands shown in Figure 7.
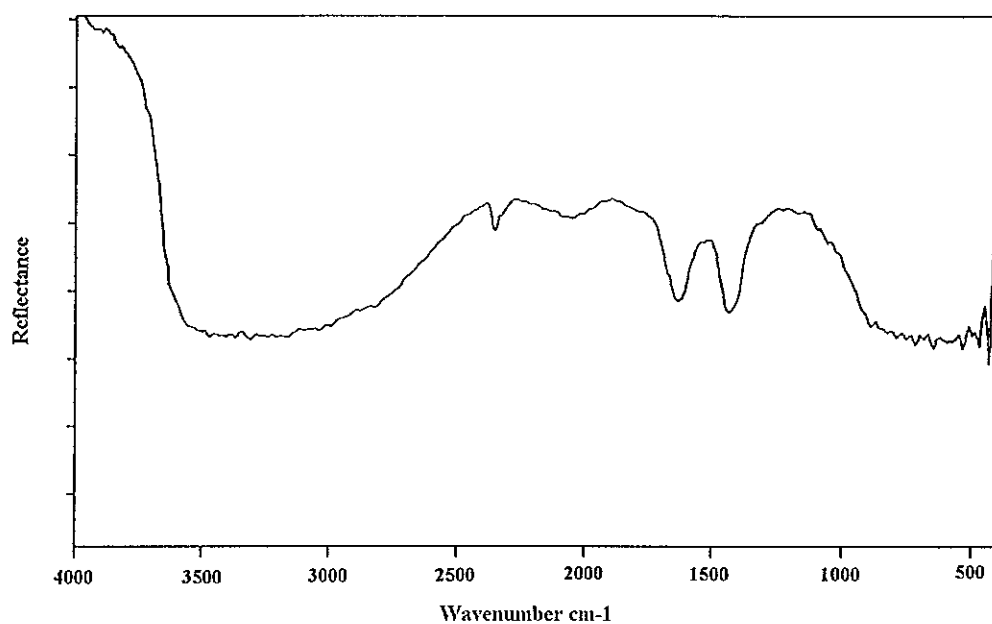
Figure 7 FT-IR spectrum (reflectance mode) of TiO_2(syn).

Table 13 Assignment of the FT-IR bands (from Figure 7).

Wave Number	Assignment	Functional groups / molecule
3500-3100	O-H or N-H stretching	OH group or NH_4^+
1638	HOH bending	H_2O
1432	N-H bending	NH_4^+ (composite)
442	Ti-O	TiO_2

3.1.2.5 Thermogravimetric analysis (TGA)

Thermogravimetric analysis provides the analyst with a quantitative measurement of any weight change associated with a transition. For example, TGA can directly record the loss in weight with time or temperature due to dehydration or decomposition (Willard, et al., 1974). Figure 8 displays TG curve obtained for TiO_2(syn) (from method B). The curve shows a gradual weight loss commencing near 50 °C and coming to completion near 450 °C. The initial weight loss in the range 50-150 °C occurs at higher rate than that taking place at higher temperatures. The total weight loss of the product was 25.98% (averaged from 2 samples, 27.74 % and 24.22 %).
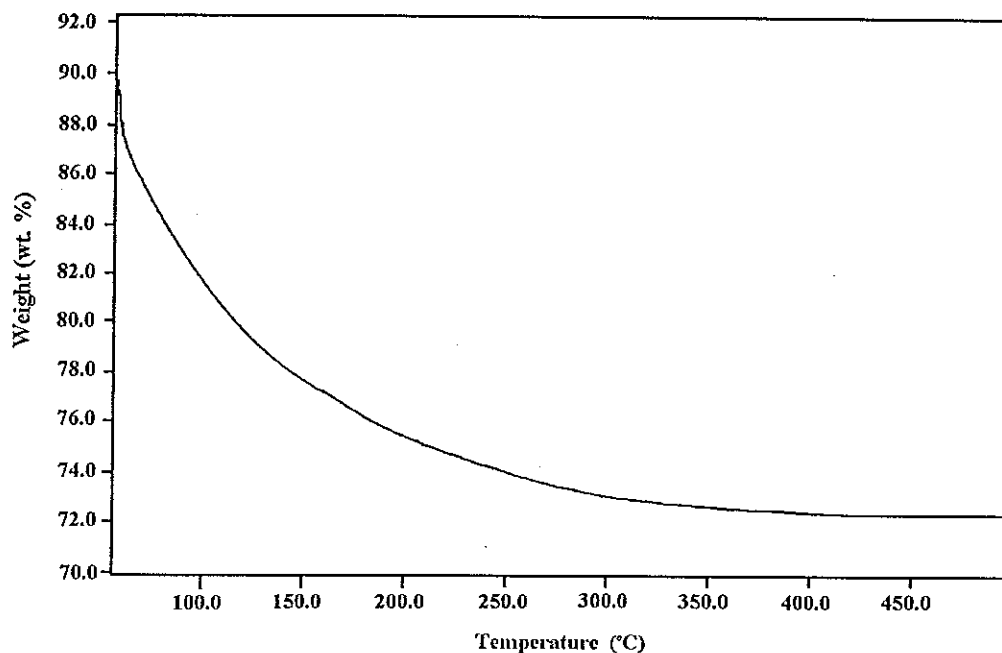
Figure 8   TGA curve of TiO_2(syn).

3.1.2.6 Differential scanning calorimetry (DSC)

DSC is a thermal technique in which differences in heat flow into a substance and a reference are measured as a function of sample temperature while the two are subjected to a controlled temperature program (Skoog and Leary, 1992). In Figure 9 shows a DSC curve for TiO_2(syn) (from method B), which has exothermic and endothermic peaks at 426 $^{\circ}C$ and 109 $^{\circ}C$, respectively.
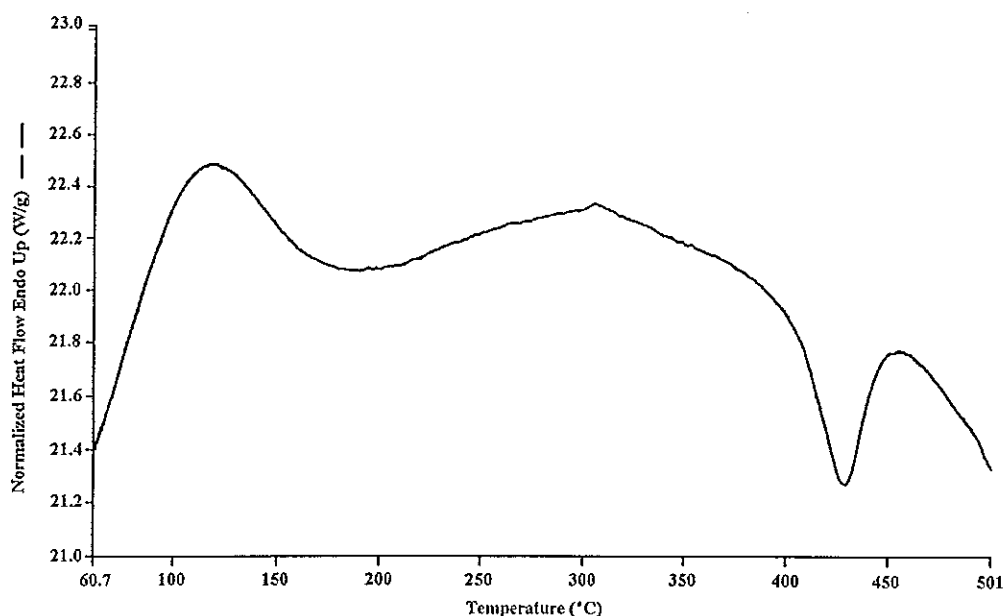
Figure 9 DSC spectra of TiO_2(syn).

3.1.2.7 Whiteness

The measured whiteness (%reflection) of all the titanium dioxide samples (synthesis and commercial product) are shown in Table 14.

Table 14 The whiteness of various titanium dioxides.

Titanium dioxide	Whiteness (%reflection)
TiO_2(syn)	94.7
TiO_2 anatase (Carlo Erba)	96.6
TiO_2 rutile (TOA)	95.5
TiO_2 P25 (Degussa)	98.7

3.2 Adsorption of metal ions by TiO_2(syn)

3.2.1 Analytical methods

In this work, all samples were analysed by AAS (AAnalyst 300, Perkin Elmer). The detection limits, expressed as three times the standard deviation of the blank (3σ), and the sensitivity of each element in this measurement technique are reported in Table 15. The accuracy and precision for the AAS determination of each element in sample are shown in Table 16 (see the calculation in Appendix B).

Table 15 Detection limits and sensitivity of element.

Metal ions	Detection limits (mg/L)	Sensitivity (mg/L)
Cu(II)	0.006	0.0752
Mn(II)	0.024	0.0700
Pb(II)	0.057	0.4489
Fe(III)	0.015	0.1133

Table 16 Accuracy and precision for the AAS determination of element.

Metal ions	Amount sample (mg/L)	Added (mg/L)	Found* (mg/L)	% Recovery
Cu(II)	1.0	1.0	1.980 ± 0.012	96.3
Mn(II)	1.0	0.5	1.549 ± 0.004	100.4
Pb(II)	10.0	10.0	19.62 ± 0.078	94.4
Fe(III)	1.0	1.0	2.163 ± 0.014	106.1

* n = 10

The linear calibration curve for each elements (Cu, Mn, Pb, and Fe) are shown in Figures 10-13.
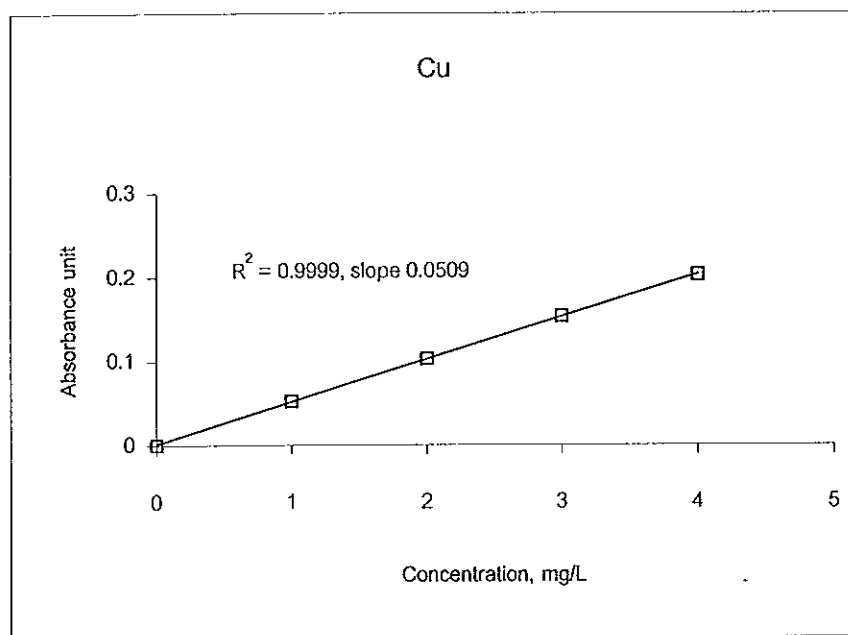
Figure 10 Linear calibration curve for Cu.
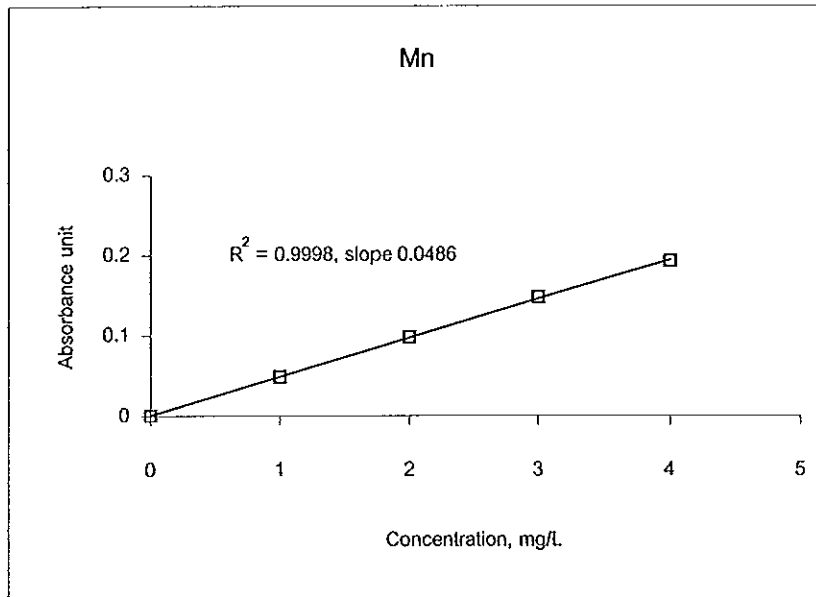
Figure 11 Linear calibration curve for Mn.
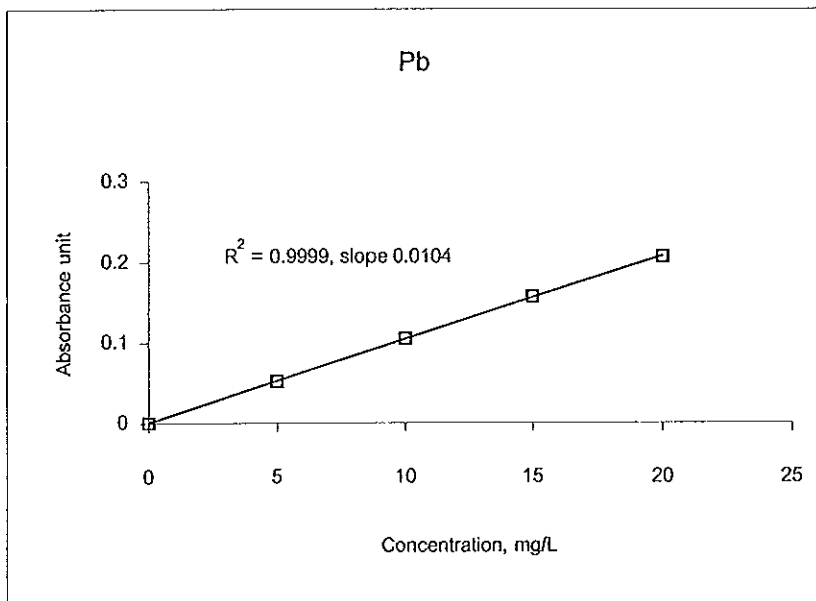
Figure 12 Linear calibration curve for Pb.
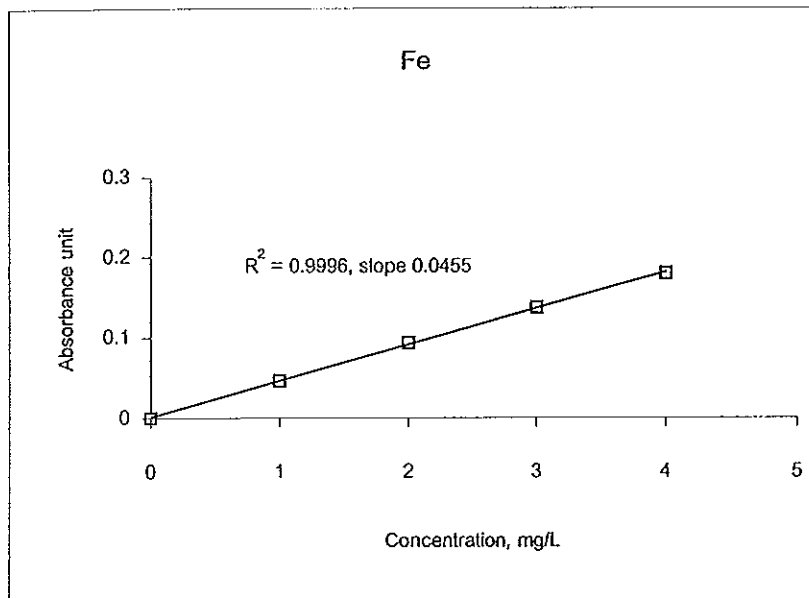
Figure 13 Linear calibration curve for Fe.

3.2.2 The optimum conditions for adsorption

Optimum conditions for the adsorption of metal ions in this work were determined by studying the effect of stirring time, sample volume, concentration of metal ions, and pH. The metal ions adsorbed per unit mass of TiO_2 (mg metal ions / g TiO_2) and % adsorption were determined.

The metal ions adsorbed (Q_e, mg/g) and % adsorption were calculated by

$$Q_e = \frac{\left[(C_0 - C_e) \times V\right]}{(m \times 1000)}$$

and

$$\% \, Adsorption = \frac{C_0 - C_e}{C_0} \times 100$$

where C_0 is the initial concentration of metal ions in aqueous phase (mg/L), C_e is the residual equilibrium concentration of metal ions in aqueous phase (mg/L), V is the volume of the aqueous phase (mL) and m is the amount of TiO_2 used (g).

3.2.2.1 Stirring time

The effect of stirring time for the adsorption of metal ions on the TiO_2(syn) was investigated by varying time of stirring. The initial concentration of the sample solution were 3.5 mg/L for Cu, Mn and Fe and 7.0 mg/L for Pb. After equilibrium, metal ions adsorbed per unit mass of TiO_2 (mg metal ions / g TiO_2) and % adsorption (Table 17 and Table 18), were calculated.

Table 17 Metal ions adsorbed per unit mass of TiO_2 and stirring time.

Time	Metal ions adsorbed per unit mass of TiO_2 (mg metal ions / g TiO_2)			
(minute)	Cu(II)	Mn(II)	Pb(II)	Fe(III)
5	1.3626	1.2950	2.9747	1.2657
10	1.3657	1.4526	2.9813	1.2598
15	1.3608	1.4389	3.0046	1.2851
30	1.3691	1.4654	2.9823	1.2787
60	1.3775	1.4803	2.9947	1.2901

Table 18 % Adsorption and stirring time.

Time	% Adsorption			
(minute)	Cu(II)	Mn(II)	Pb(II)	Fe(III)
5	99.50	97.78	98.60	98.14
10	99.68	98.58	98.89	99.02
15	99.64	97.32	98.70	99.29
30	99.58	99.24	98.66	99.51
60	99.72	99.43	99.27	99.60

3.2.2.2 Sample volume

The effect of sample volume of the adsorption of metal ions on the TiO_2(syn) was investigated by varying volume of sample. After equilibration the metal ions adsorbed per unit mass of TiO_2 (mg metal ions / g TiO_2) and % adsorption were calculated. The data are shown in Table 19 and Table 20, respectively.

Table 19 Metal ions adsorbed per unit mass of TiO_2 and sample volume.

Sample volume	Metal ions adsorbed per unit mass of TiO_2 (mg metal ions / g TiO_2)			
(mL)	Cu(II)	Mn(II)	Pb(II)	Fe(III)
10	0.7071	0.6891	1.2978	0.6831
20	1.3601	1.3723	3.0047	1.3048
25	1.8202	1.7861	3.3026	1.7013
30	1.4296	1.8995	4.3156	2.0510
40	1.0797	0.8006	5.5282	2.7505
50	0.7793	0.2820	6.2752	3.0819

Table 19 (continued)

Sample volume	Metal ions adsorbed per unit mass of TiO_2 (mg metal ions / g TiO_2)			
(mL)	Cu(II)	Mn(II)	Pb(II)	Fe(III)
75	0.4874	0.2429	7.2195	3.0994
100	0.4560	0.2311	8.4060	3.0147
150	-	-	8.6191	-

Table 20 % Adsorption and sample volume.

Sample volume	% Adsorption			
(mL)	Cu(II)	Mn(II)	Pb(II)	Fe(III)
10	99.54	99.32	96.27	99.32
20	99.67	98.97	98.70	99.10
25	99.58	98.48	98.87	99.42
30	64.32	86.00	97.12	98.86
40	36.62	27.74	93.76	99.36
50	21.61	8.45	88.25	90.31
75	9.05	4.34	65.72	59.87
100	6.20	3.33	60.96	43.30
150	-	-	40.16	-

3.2.2.3 Concentration of metal ions

The effect of concentration of metal ions for the adsorption of metal ions on the TiO_2(syn) was investigated by varying concentration of metal ions. After equilibrium, metal ions adsorbed per unit mass of TiO_2 (mg metal ions / g TiO_2) and % adsorption, are shown in Tables 21-24, were calculated.

Table 21 Metal ions adsorbed per unit mass of TiO_2, % adsorption and concentration of Cu(II).

Concentrations (mg/L)	Metal ions adsorbed per unit mass of TiO_2 (mg metal ions / g TiO_2)	% Adsorption
2	1.0290	99.44
4	2.0365	99.64
5	2.4682	97.92
6	1.6985	56.80
7	1.4042	40.38
8	1.0707	27.06
10	0.6224	12.19

Table 22 Metal ions adsorbed per unit mass of TiO_2, % adsorption and concentration of Mn(II).

Concentrations (mg/L)	Metal ions adsorbed per unit mass of TiO_2 (mg metal ions / g TiO_2)	% Adsorption
2	1.2528	99.29
3	1.8129	98.12
4	2.1531	88.97
5	0.8701	28.14
6	0.2639	7.11

Table 23 Metal ions adsorbed per unit mass of TiO_2, % adsorption and
concentration of Pb(II).

Concentrations (mg/L)	Metal ions adsorbed per unit mass of TiO_2 (mg metal ions / g TiO_2)	% Adsorption
2	4.1886	98.00
4	8.1586	95.93
6	11.0537	87.35
8	12.5925	75.64
10	14.1835	67.62
15	14.3659	48.80
20	14.8097	37.12
25	15.6258	31.42
30	12.3439	20.52
40	11.2748	13.35
50	10.1421	10.51

Table 24 Metal ions adsorbed per unit mass of TiO_2, % adsorption and
concentration of Fe(III).

Concentrations (mg/L)	Metal ions adsorbed per unit mass of TiO_2 (mg metal ions / g TiO_2)	% Adsorption
2	2.1708	98.51
4	3.6666	88.82
5	3.9565	74.57
6	4.1250	64.64
8	4.3592	52.39
10	4.0002	37.70
15	3.4757	23.83

3.2.2.4 pH

The effect of pH for the adsorption of metal ions on the TiO$_2$(syn) was investigated by varying pH of sample solution. The metal ions adsorbed per unit mass of TiO$_2$ (mg metal ions / g TiO$_2$) and % adsorption after equilibrium were calculated. The data are shown in Table 25 and Table 26, respectively.

Table 25 Metal ions adsorbed per unit mass of TiO$_2$ and pH.

pH	Metal ions adsorbed per unit mass of TiO$_2$ (mg metal ions / g TiO$_2$)			
	Cu(II)	Mn(II)	Pb(II)	Fe(III)
3	2.9414	2.9634	49.3027	3.4346
5	2.9738	2.9994	50.1720	7.6703
7	2.9104	3.0702	49.8029	7.7015
9	2.9120	2.8832	49.3096	7.7036
11	2.6224	2.7659	41.7992	7.2968

Table 26 % Adsorption and pH.

pH	% Adsorption			
	Cu(II)	Mn(II)	Pb(II)	Fe(III)
3	100	96.01	99.20	44.34
5	99.59	97.47	99.17	99.73
7	98.22	98.16	98.96	98.53
9	98.01	91.87	99.01	98.56
11	98.03	92.85	93.90	96.90

3.2.3 Adsorption isotherms

Adsorption characteristics between the adsorbent and adsorbate can be described by adsorption isotherms. In this work, the Langmuir and Freundlich isotherm plots were used for studying the adsorption data. These isotherms relate metal per unit weight of adsorbent (Q_e, mg/g) to the residual equilibrium concentration of metals (C_e, mg/L). The Langmuir is usually used to analyse data by studying the relation between $1/Q_e$ and $1/C_e$. Whereas, the Freundlich is usually used to analyse data by studying the relation between log Q_e and log C_e. The data are shown in Tables 27-30.

Table 27 Data of the Langmuir and Freundlich for the adsorption of Cu(II).

Residual conc. C_e (mg/L)	Metal ions adsorbed Q_e (mg /g TiO_2)	Langmuir		Freundlich	
		$1/C_e$	$1/Q_e$	log C_e	log Q_e
0.04	12.3997	25.0000	0.0806	-1.3979	1.0934
0.08	16.9638	12.5000	0.0589	-1.0969	1.2295
0.09	24.2899	11.1111	0.0412	-1.0458	1.3854
0.22	35.8378	4.5455	0.0279	-0.6576	1.5543
0.50	44.9037	2.0000	0.0223	-0.3010	1.6523
1.87	72.7757	0.5348	0.0137	0.2718	1.8620
5.28	96.8207	0.1894	0.0103	0.7226	1.9860
53.59	99.1068	0.0187	0.0101	1.7291	1.9961
87.60	101.8775	0.0114	0.0098	1.9425	2.0081

Table 28 Data of the Langmuir and Freundlich for the adsorption of Mn(II).

Residual conc. C_e (mg/L)	Metal ions adsorbed Q_e (mg /g TiO_2)	Langmuir		Freundlich	
		$1/C_e$	$1/Q_e$	$\log C_e$	$\log Q_e$
0.10	3.0702	10.0000	0.3257	-1.0000	0.4872
0.39	8.7794	2.5641	0.1139	-0.4089	0.9435
0.64	11.3224	1.5625	0.0883	-0.1938	1.0539
0.88	13.9390	1.3164	0.0717	-0.0555	1.1442
10.65	21.6861	0.0939	0.0461	1.0273	1.3362
31.01	25.2148	0.0322	0.0397	1.4915	1.4017
66.45	22.5892	0.0150	0.0443	1.8225	1.3539
104.10	25.5446	0.0096	0.0391	2.0175	1.4073
151.5	28.3764	0.0066	0.0352	2.1804	1.4530

Table 29 Data of the Langmuir and Freundlich for the adsorption of Pb(II).

Residual conc. C_e (mg/L)	Metal ions adsorbed Q_e (mg /g TiO_2)	Langmuir		Freundlich	
		$1/C_e$	$1/Q_e$	$\log C_e$	$\log Q_e$
0.04	10.2580	28.5714	0.0975	-1.4559	1.0111
0.07	19.8690	15.1515	0.0503	-1.1805	1.2982
0.09	29.1245	11.3636	0.0343	-1.0555	1.4643
0.10	39.1409	9.9010	0.0255	-0.9957	1.5926
0.30	49.8028	3.3333	0.0201	-0.5229	1.6973
0.57	106.6216	1.7452	0.0094	-0.2418	2.0278
0.71	158.4522	1.4144	0.0063	-0.1506	2.1999
1.98	204.7168	0.5038	0.0049	0.2978	2.3112
4.69	271.5289	0.2132	0.0037	0.6712	2.4338
12.67	394.4592	0.0789	0.0025	1.1027	2.5960

Table 29 (continued)

Residual conc.	Metal ions adsorbed	Langmuir		Freundlich	
C_e (mg/L)	Q_e (mg /g TiO_2)	$1/C_e$	$1/Q_e$	log C_e	log Q_e
78.29	474.5257	0.0128	0.0021	1.8937	2.6763
101.18	625.6299	0.0099	0.0016	2.0050	2.7963
390.40	621.7132	0.0026	0.0016	2.5915	2.7936

Table 30 Data of the Langmuir and Freundlich for the adsorption of Fe(III).

Residual conc.	Metal ions adsorbed	Langmuir		Freundlich	
C_e (mg/L)	Q_e (mg /g TiO_2)	$1/C_e$	$1/Q_e$	log C_e	log Q_e
0.01	2.0301	68.9655	0.4926	-1.8386	0.3075
0.02	3.9085	44.4444	0.2559	-1.6478	0.5920
0.04	5.2802	24.3902	0.1894	-1.3872	0.7226
0.07	10.3683	14.2857	0.0964	-1.1549	1.0157
0.09	12.1997	11.5607	0.0820	-1.0630	1.0863
0.11	14.8320	8.6957	0.0674	-0.9393	1.1712
0.27	25.1130	3.6364	0.0398	-0.5607	1.3999

3.2.4 Comparison of the adsorption capacities between TiO_2(syn) and

the commercial TiO_2.

The comparison of the metal ions adsorbed per unit mass of TiO_2 (mg metal ions / g TiO_2) between the TiO_2(syn) and the other titanium dioxides. The data are shown in Table 31. This experimental was studied at pH 7 (room temperature). The stirring time were 10 minutes for Cu(II) and Mn(II) and 15 minutes for Pb(II) and Fe(III). The volume of sample solution were 25 mL and 30 mL for Cu and Mn, respectively and 50 mL for Pb and Fe.

Table 31 Metal ions (Cu(II), Mn(II), Pb(II) and Fe(III)) adsorbed per unit mass of TiO_2

(syn, anatase, P25, and rutile).

Sample	Metal ions adsorbed per unit mass of TiO_2 (mg metal ions / g TiO_2)			
	Cu(II)	Mn(II)	Pb(II)	Fe(III)
TiO_2 (syn)	84.79	24.92	618.79	14.85
Anatase (syn)[a]	67.40	-	308.98	14.90
Anatase	71.15	-	194.28	14.90
P25	63.60	-	219.41	14.95
Rutile	68.84	-	187.99	15.02

a synthesized according to Vassileva, et al., 1996.   Surface area was 127.57 m^2/g,

determined by SA3100, Coulter.

Chapter 4

DISCUSSION

4.1 Synthesis and characterization of titanium dioxide

4.1.1 Synthesis of titanium dioxide

The reaction between $TiCl_4$ and NH_3 solution by method A and method B (dilute NH_3 solution) produced the white precipitate and large amount of white smoke due to formation of HCl (method A gave off a large amount of smoke and the reaction was more vigorous than method B). The white precipitate was filtered and the filtrates was tested for Cl^- and NH_4^+ with $AgNO_3$ and the indicator paper, respectively. Then the white precipitate was washed several times until the filtrates did not show any cloudiness and the indicator paper did not change to blue. The synthesis can be described by the following chemical reaction.

$$TiCl_4 + 4NH_4OH \rightarrow TiO_2 + 4NH_4Cl + 2H_2O$$

4.1.2 Characterization of titanium dioxide

4.1.2.1 X-ray diffraction (XRD)

The XRD spectrum of TiO_2 (syn) by method A (Figure 5(a), page 41) shows broad weak peaks at (2θ) 25.4, 38, 48, 53 and 55 which correspond to 101, 004, 200, 105 and 211 reflections of TiO_2 in the form of anatase (Park, et al., 1999). The broad appearance of the peaks indicated that the TiO_2(syn) from method A is mainly the amorphous form of TiO_2 with small amount of anatase mixed in. The small amount of anatase as prepared by method A was determined to be *ca.* 5% by XRD method (Chamnan

Randorn, 2001, unpublished). On the other hand, the XRD spectrum of $TiO_2(syn)$ from method B (Figure 5(b), page 41) showed only a clean baseline indicating that the product is purely an amorphous titanium dioxide.

4.1.2.2 Surface area / pore size

The specific surface areas of $TiO_2(syn)$ from method B was shown in Table 11 (page 44). In order to ascertain this high value, other samples of TiO_2 were also subjected to the same measurement under the same conditions, such as the commercially available anatase from Carlo Erba, rutile from a paint factory (TOA, Co., Thailand), and the Degussa P25. From the results in Table 12 (page 44) showed that $TiO_2(syn)$ has micropores while all other TiO_2's measured simultaneously under same conditions, are non-porous. Wang and Adesina (1997) also reported P25 as non-porous. The values of surface area of all these commercial TiO_2 came out similar to those given in literatures. Data in Table 32 are examples of such literature values.

Table 32 Specific surface areas of titanium dioxide

TiO_2	company	Specific surface area (m^2/g)	Reference
Anatase	Aldrich	9.45	Tanaka, et al., 1991
	Aldrich	10	Rekoske and Barteau, 1999
	Bayer PK5585/1	90	Ludwig and Schindler, 1995
	BDH	10.50	Sclafani, et al., 1990
	Carlo Erba	5.90	Sclafani, et al., 1990
	Fluka	31	Vassileva, et al., 1996
	Fujititan TP-2	17.30	Tanaka, et al., 1991
	Ishihara A-100	10.10	Tanaka, et al., 1991

Table 32 (continued)

TiO$_2$	company	Specific surface area (m^2/g)	Refferance
Anatase	Merck	10.00	Augugligro, et al., 1999
	Merck	10.50	Sclafani, et al., 1990
	Tioxide 1601/1	14.00	Sclafani, et al., 1990
Rutile	Aldrich rutile	2.75	Tanaka, et al., 1991
	Alfa-Aesar	2	Rekoske and Barteau, 1999
	Dupont	105 ±15	Kim and Chung, 2001
	Fujititan TM-1	6.10	Tanaka, et al., 1991
	Fujititan TP-3	4.40	Tanaka, et al., 1991
	Katayama	2.80	Tanaka, et al., 1991
	NCLA 600	8.40	Tanaka, et al., 1991
	Teikoku-kako	9.18	Suda, et al., 1987
	Tioxide 1601/2	20	Sclafani, et al., 1990
	Waka	6.85	Tanaka, et al., 1991
P25	Degussa	~50	Chuang, et al., 1999
	Degussa	52	Mpadou and siffert, 1984
	Degussa	55	Vohar and Davis, 1997
Amorphous	Idemitsu	107.70	Tanaka, et al., 1991
	Idemitsu(UF-IT-S)	115.00	Ohtani, et al., 1997

4.1.2.3 Energy dispersive x-ray fluorescence (EDXRF)

The EDXRF spectrum of TiO$_2$(syn) showed only one peaks from K-lines of Ti indicating no contamination from other impurity. This technique will not able to detect oxygen (O in H$_2$O) and nitrogen (N in NH$_4^+$) atoms due to their too low characteristic energies.

### 4.1.2.4 Fourier-transformed infrared spectrophotometer (FT-IR)

The FT-IR spectrum of TiO_2(syn) showed large broad band at 3500-3100 cm^{-1} and rather narrow bands at 1638 and 1432 cm^{-1}, together with one weak absorption at 442 cm^{-1}. The broad one at 3500-3100 cm^{-1} can be assigned to both stretching mode of O-H and N-H while at 1638 and 1432 cm^{-1} can be assigned to the bending of O-H and N-H, respectively. The absorption at 442 cm^{-1} can be assigned to stretching mode of Ti-O bond. According to Youn, et al., (1999) their FT-IR spectra showed the presence of OH^- and H_2O absorption bands because of 4 absorption at 3400, 3100, 1624 and 1402 cm^{-1}. Khalil and Zaki (1997) reported 4 absorption peaks at 3380, 3220, 1630 and 1400 cm^{-1} due to vO-H (H-boned), vNH_4^+, δO-H and δNH_4^+ vibrations, respectively. Zhang, et al., (2002) reported TiO_2 has the Ti-O stretching vibration at 438 cm^{-1}. Therefore, the FT-IR spectra of the TiO_2(syn) powders shown in Figure 7 (page 46) confirmed the presence of impurities such as NH_4^+ and H_2O at the surface of TiO_2(syn). The amount of NH_4^+ was, however , very small at 1.3 - 1.8% by elemental analysis for nitrogen contents. This small amount of nitrogen also rendered it undetectable by SEM/EDX and WDXRF. Their spectra were shown in Appendix A, Figure A1 and A2, respectively.

4.1.2.5 Thermogravimetric analysis (TGA)

From section 4.1.2.4 above TiO_2(syn) can be written as $TiO_2 \cdot nH_2O$ where n can be identified by TGA. Accordingly, a total weight loss of this product was 25.98% and would correspond to the decomposition of the product $TiO_2 \cdot 1.6H_2O$ into TiO_2 (see the calculation in Appendix C). Hence, n is equal to 1.6. A similar result was reported for the hydrolysis product of

$Ti(OPr^i)_4$ by Khalil and Zaki (1997). They suggested that a total weight loss of about 31% would be due to the decomposition of the hydrolysis products $TiO_2 \cdot 2H_2O$ into TiO_2.

Therefore, in this work the reaction of the synthesized TiO_2 can be expressed by

$$TiCl_4 + 4NH_4OH \rightarrow TiO_2 \cdot 1.6H_2O + 4NH_4Cl + 0.4H_2O$$
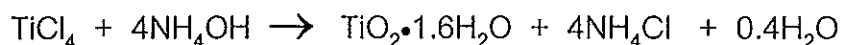
4.1.2.6 Differential scanning calorimetric (DSC)

Data from DSC pattern of TiO_2 sample in Figure 9 (page 48) showed an endothermic peak at ca.109 °C which could be attributted to liberation or decomposition of water. A characteristic exothermic peak was also observed at ca. 426 °C attributable to crystallization of amorphous phase to anatase. In Figure 5(c) showed the XRD pattern of TiO_2(syn) from method B calcined at 426 °C yielding an anatase form. A similar result was reported for the crystallization temperatures by Youn, et al., (1999). Their DSC and XRD results revealed crystallization temperatures (anatase) of 390 and 467 °C for nonrinsed (water-washed only) and ethanol/butanol-rinsed powders, respectively. Ha, et al., (2000) reported the crystallization temperatures for the titanium dioxide powders (referred to PW powders) at 440 °C.

4.1.2.7 Whiteness

From the results data (Table 14, page 49), it was found that TiO_2(syn), anatase (Carlo Erba), P25 (Degussa) and rutile (TOA Co., Thailand) had the whiteness values (%reflection) 94.7, 96.6, 98.7 and 95.5, respectively. The lower value of whiteness of TiO_2(syn) as compared to other

commercial titanium dioxides was probably from the effect of NH_4^+ ion coming from NH_3 which used in large amount during the hydrolysis stage and was not washed out completely at the washing stage.

4.2 Adsorption of metal ions by TiO_2(syn)

4.2.1 The optimum condition for adsorption

4.2.1.1 Stirring time

From the results (Table 17, page 53), it was found that adsorption of Cu(II) and Mn(II) ions reached equilibrium in 10 minutes and 15 minutes for Pb(II) and Fe(III) (as shown in Figure 14). In a similar experiment, Vassileva, et al.,(1996) also studied the adsorption of metal ions under static conditions where sample of titanium dioxide (anatase) was each suspended in solutions and both phases were kept in contact for 5 minutes to equilibrium. They concluded the titania (anatase) adsorbs rapidly. Similarly, Anderson and Rubin (1981) concluded the adsorption of cations by hydrous metal oxides is frequently found to be extremely rapid, most of the exchange occurring within a matter of minutes. The rapid adsorption reflects the fact that the adsorption is a surface phenomenon and that the surfaces are readily accessible to the ions in solution.
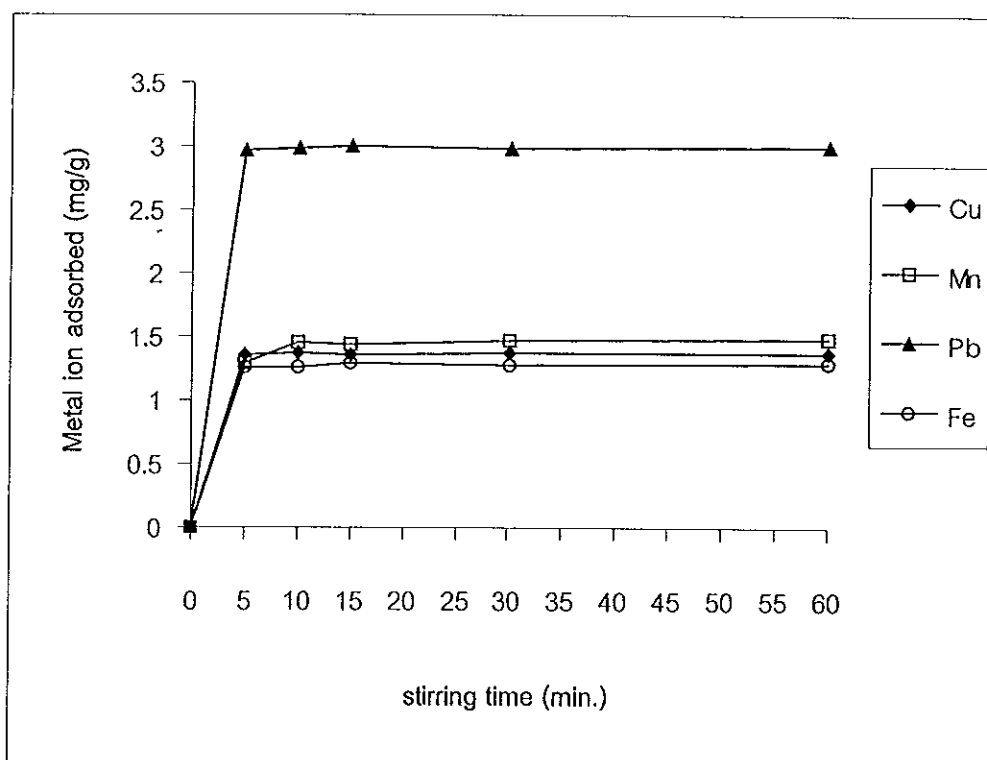
Figure 14 Effect of stirring time on the adsorption of Cu(II), Mn(II), Pb(II) and

Fe(III) on TiO_2(syn).

4.2.1.2 Sample volume

In order to explore the possibility of enriching low concentrations of analytes from large volumes, the effect of sample volume on the retention of metal ions was also investigated. For this purpose, 10, 20, 25, 30, 40, 50, 75, and 100 mL for (Cu, Mn and Fe) and 10, 20, 25, 30, 40, 50, 75, 100, and 150 mL for Pb, were studied with optimum of stirring time. As shown in Figure 15, quantitative adsorption (>85%) were obtained for sample volumes of $\leq$ 25 mL for Cu(II), $\leq$ 30 mL for Mn(II), and $\leq$ 50 mL for Pb(II) and Fe(III).
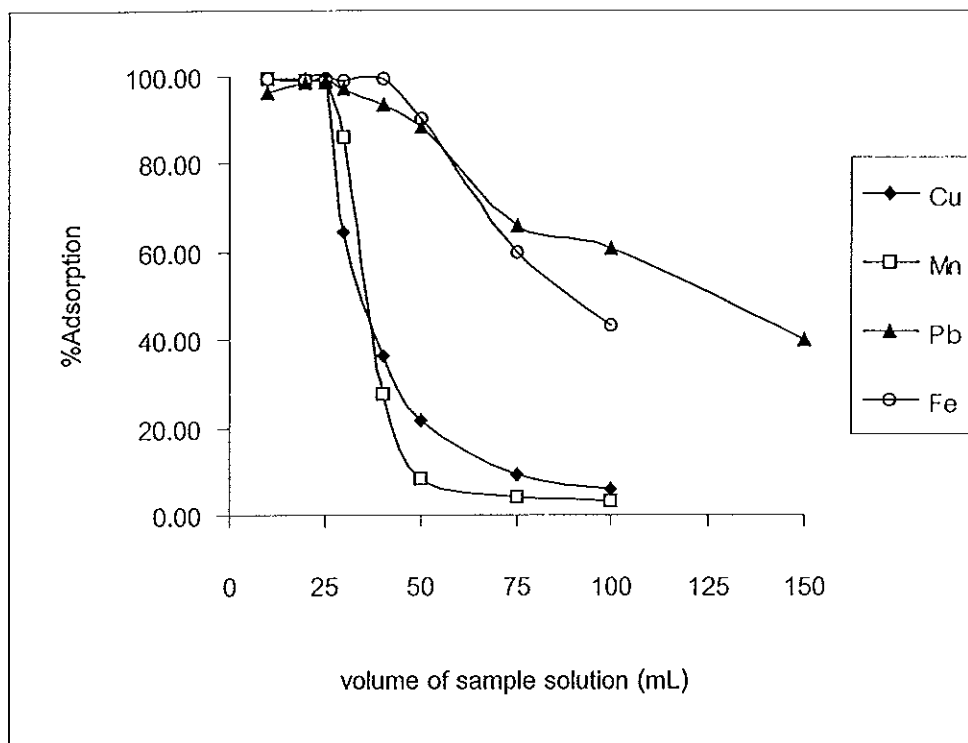
Figure 15 Effect of the volume of sample solution on the adsorption of Cu(II),

Mn(II), Pb(II) and Fe(III) on TiO_2(syn).

From the above results[1], the adsorption of metal ions (Cu, Mn, Pb and Fe) on TiO_2(syn) can be calculated for the optimum ratio of TiO_2(syn) used per metal ions solutions (g/L) and these values are shown in Table 33. From these data, the ratio (g/L) was used to studied in this work.

---

[1] This results fit for the finding optimum condition by using the column method. Liang, et al., (2001) studied the effect of the sample volume by using the microcolumn.

Table 33 The ratio of $TiO_2(syn)$ per volume of sample solution.

Metal ion	Mass of $TiO_2(syn)$ (g)	Volume of sample solution (mL)	Ratio (g/L)
Cu(II)	0.05	25	2
Mn(II)	0.05	30	1.67
Pb(II)	0.05	100*	0.5
Fe(III)	0.05	50	1

* Data was selected from the plateau values of metal ion adsorbed (mg/g)

(Table 19, page 54).

4.2.1.3 Concentration of metal ion

From the results in Tables 21-24 (pages 56-57), it was found that the amount of metal ions adsorbed depended on the concentrations of metal ions as shown in Figures 16-19. As seen here, the adsorption of each metal ions first increased with increasing the concentration, and reached maximum adsorption, after that it gradually decreased. The maximum adsorption of Cu(II), Mn(II), Pb(II) and Fe(III) were 5, 4, 25 and 8 ppm, respectively. The low adsorption at high metal ion concentrations can be described as a result from competition between H^+ and metal ion increases the pH of the solution decreases, hence, higher concentraion of H^+ ions in the solution. The competition between metal ion and the higher concentration of H^+ ions for sorption sites is in favor of H^+, and as a result less adsorption was observed(Manju, et al., 2002).
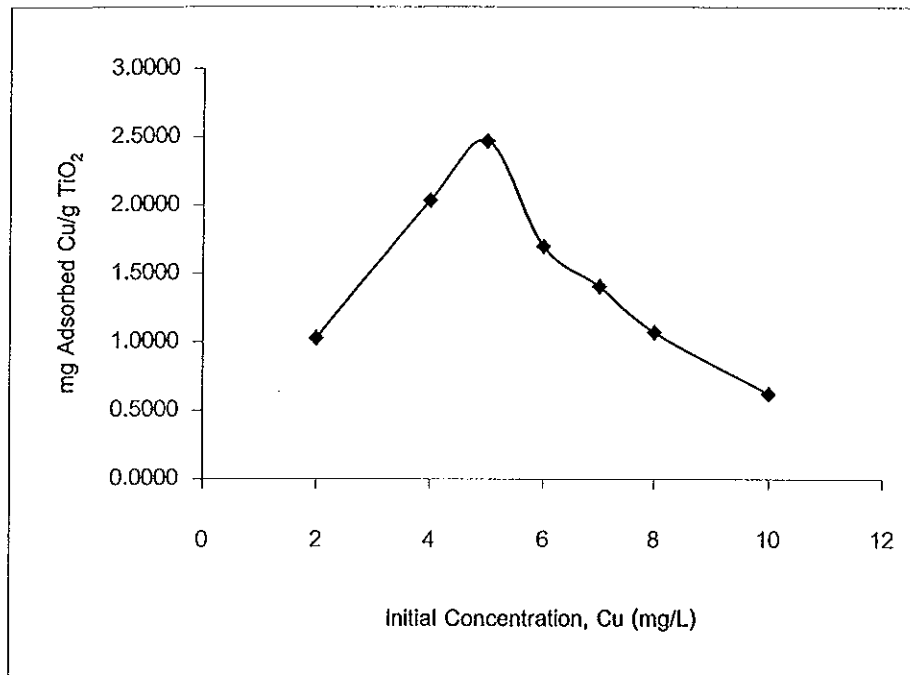
Figure 16 Effect of the concentration of metal ion on the adsorption of Cu(II) by TiO_2(syn).
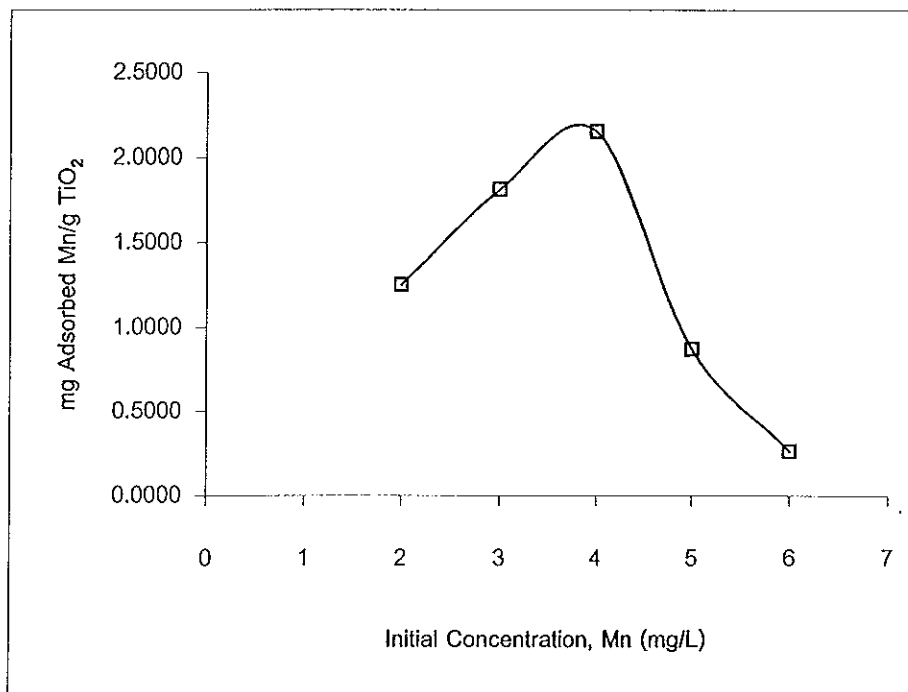

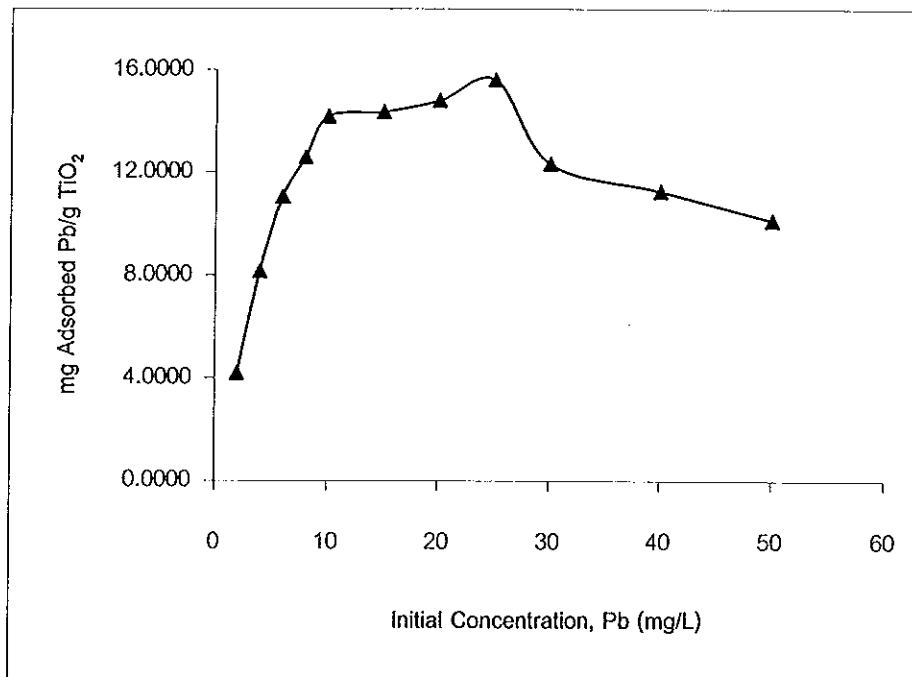Figure 17 Effect of the concentration of metal ion on the adsorption of Mn(II) by TiO_2(syn).

Figure 18 Effect of the concentration of metal ion on the adsorption of Pb(II)
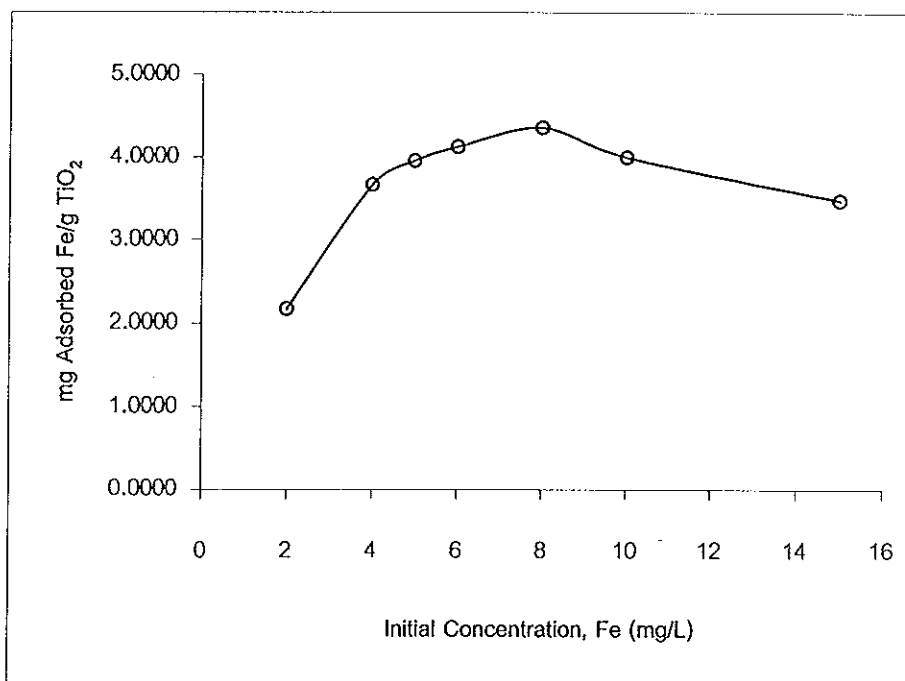by TiO_2(syn).

Figure 19 Effect of the concentration of metal ion on the adsorption of Fe(III)
by TiO_2(syn).

4.2.1.4 pH

The pH value plays a determining role with respect to the sorption of different ions on oxide surface. The pH of solution influences the distribution of active sites on the surface of TiO_2, and the $-OH$ on the surface provides the ability of the binding cation. The results of the effect of pH in this work are shown in Figures 20-23. It can be seen that quantitative sorption of Cu(II) and Pb(II) occurs in the pH range 3-9, Mn(II) occurs in the pH range 3-7, and Fe(III) occurs in the pH range 5-9. From these data, pH 7 was selected as the most common to all the metal ions studied in this work. The results of effect of pH in the literatures are shown in Table 34. To compare the results data in this work and literatures, it was found that for all metal ions studied in this work the adsorption took place at lower pH than those reported in the literatures. It can ascribed to the specific adsorption[2] of metal ions on TiO_2(syn). Accordingly, Malati, et al., (1982) reported the adsorption of cations at pH values equal to or less than the PZC (see PZC values in Table 38, page 86) is ascribed to specific adsorption.[2]

Table 34 Effect of pH (literatures).

TiO_2 sample	Metal	pH range	Reference
Nanometer TiO_2	Cu^{2+}	6-9	Liang, et al., 2001
Nanometer TiO_2	Mn^{2+}	8-9	Liang, et al., 2001
TiO_2 (anatase)	Cu, Mn, Pb, Fe	7-10	Vassileva, et al., 1996

[2] The term " specific adsorption" is used for all adsorption than cannot be accounted for solely by electrostatic force (Anderson and Rubin, 1981 :52).
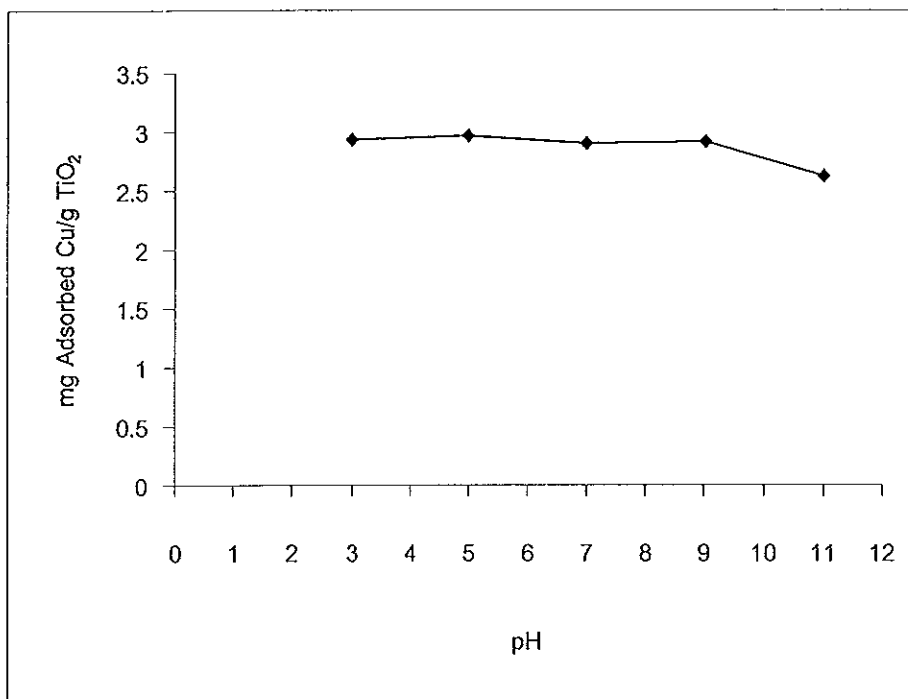
Figure 20 Influence of pH on the adsorption of Cu(II) on TiO_2 (syn).
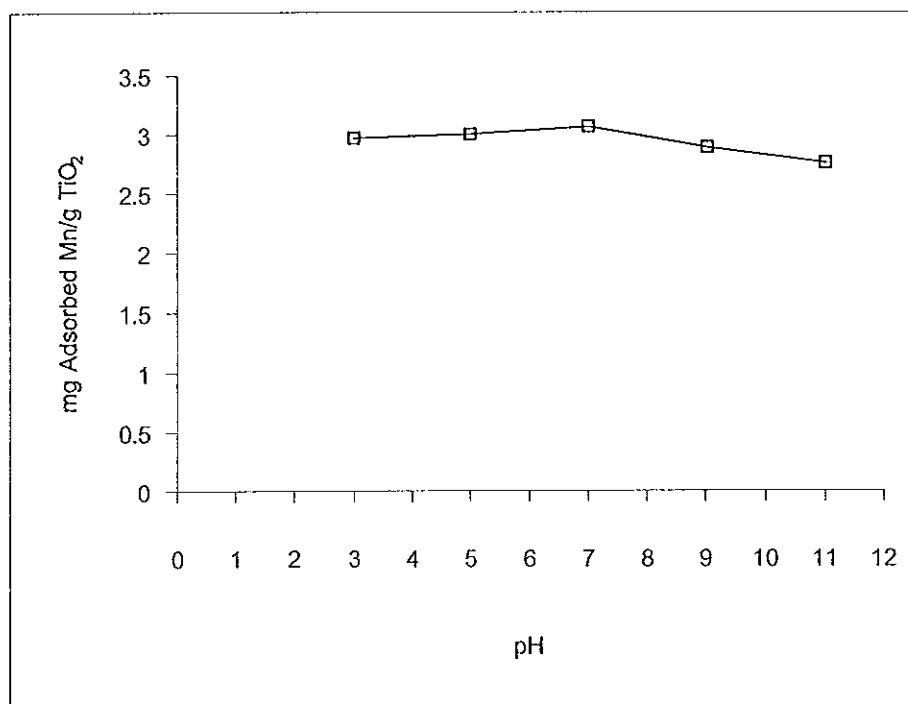

Figure 21 Influence of pH on the adsorption of Mn(II) on TiO_2 (syn).
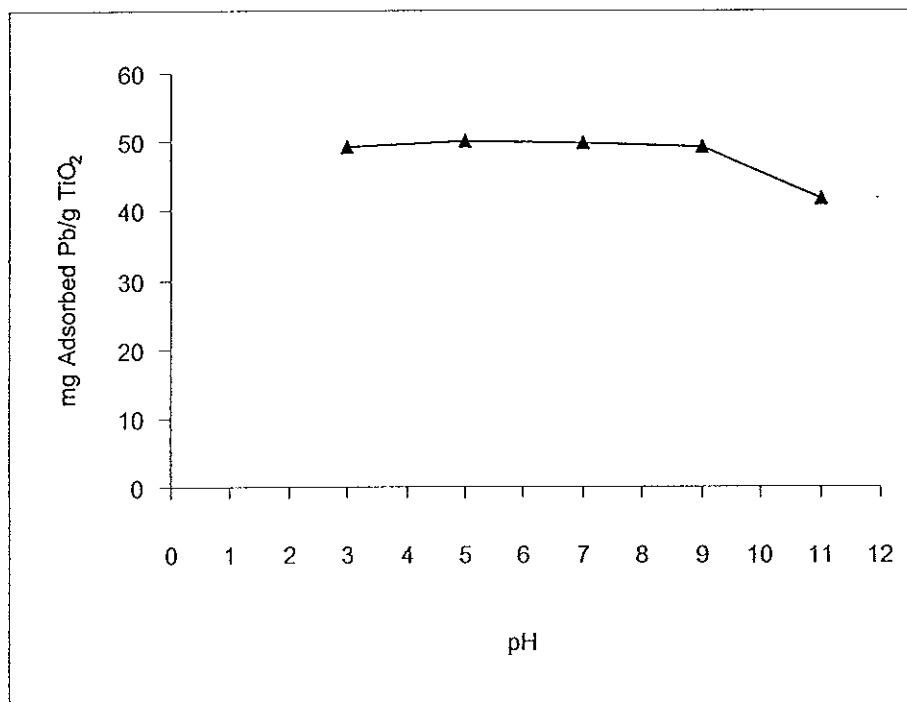
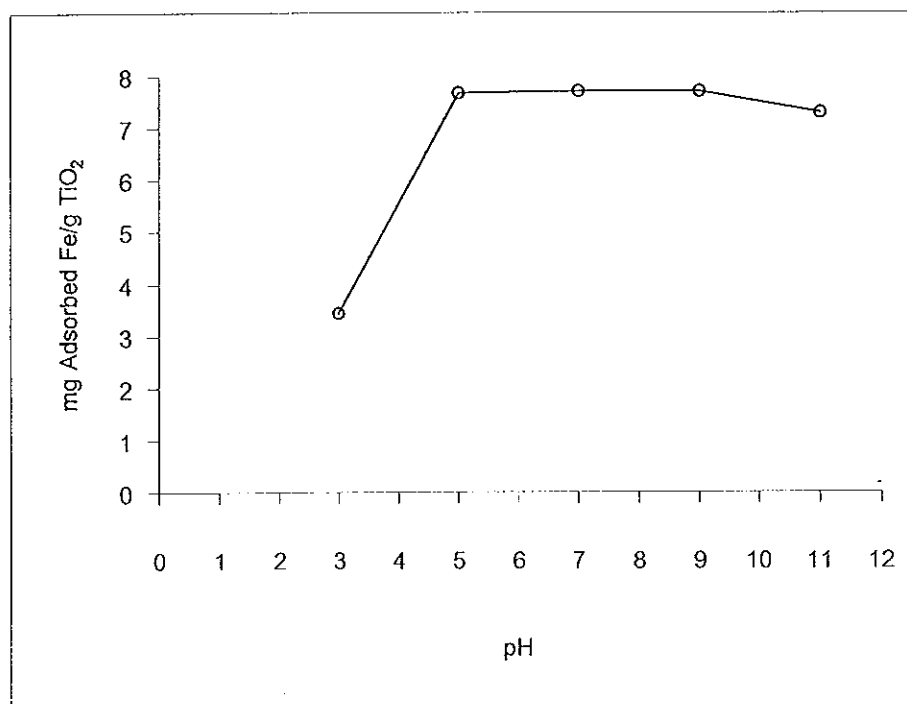Figure 22 Influence of pH on the adsorption of Pb(II) on TiO_2 (syn).

Figure 23 Influence of pH on the adsorption of Fe(III) on TiO_2 (syn).

4.2.2 Adsorption isotherms

The experiments were carried out at pH 7 on the basis of the results on the pH effect. From the results data in Tables 27-30 (pages 59-61), the fit to either isotherm (Langmuir or Freundlich) for the adsorption of metal ions (Cu(II), Mn(II), Pb(II), and Fe(III)) onto TiO_2(syn) can be obtained by comparing the correlation coefficient (R^2) of the data plots. The Langmuir isotherms were obtained by plotting $1/C_e$ (X axis) vs. $1/Q_e$ (Y axis), while the Freundlich isotherm was obtained by plotting log C_e (X axis) vs. log Q_e (Y axis). These isotherms were shown in Figures 24-31. To compare the reliability of these adsorption isotherms, the correlation coefficient (R^2) for each adsorption isotherm was calculated and shown in Table 35.

Table 35 The correlation coefficient (R^2) for adsorption isotherms of Cu(II), Mn(II), Pb(II) and Fe(III) on TiO_2(syn).

	Cu(II)	Mn(II)	Pb(II)	Fe(III)
Langmuir isotherm	0.9659	0.999	0.9828	0.9775
Freundlich isotherm	0.8556	0.8234	0.8956	0.9768

Based on the values of the correlation coefficient (R^2) for the different isotherm plots, the Langmuir isotherm gives the best fit for the adsorption of Cu(II), Mn(II) and Pb(II). Whereas the adsorption of Fe(III) seems to fit both Langmuir and Freundlich isotherms. In the case of Cu(II), Vassileva, et al., (1996) showed the adsorption isotherm of Cu^{2+} on TiO_2 (anatase) at pH 8 was Langmuir type. The correlation coefficient (R^2) is a good criteria and means that the difference between experimental data and theoretical values is small when the value of the coefficient approaches 1 (Kim and Chung, 2001).

Figure 24 Langmuir isotherm plot of Cu(II) adsorption on TiO_2 (syn).

Figure 25 Freundlich isotherm plot of Cu(II) adsorption on TiO_2 (syn).

Figure 26 Langmuir isotherm plot of Mn(II) adsorption on TiO_2 (syn).

Figure 27 Freundlich isotherm plot of Mn(II) adsorption on TiO_2 (syn).
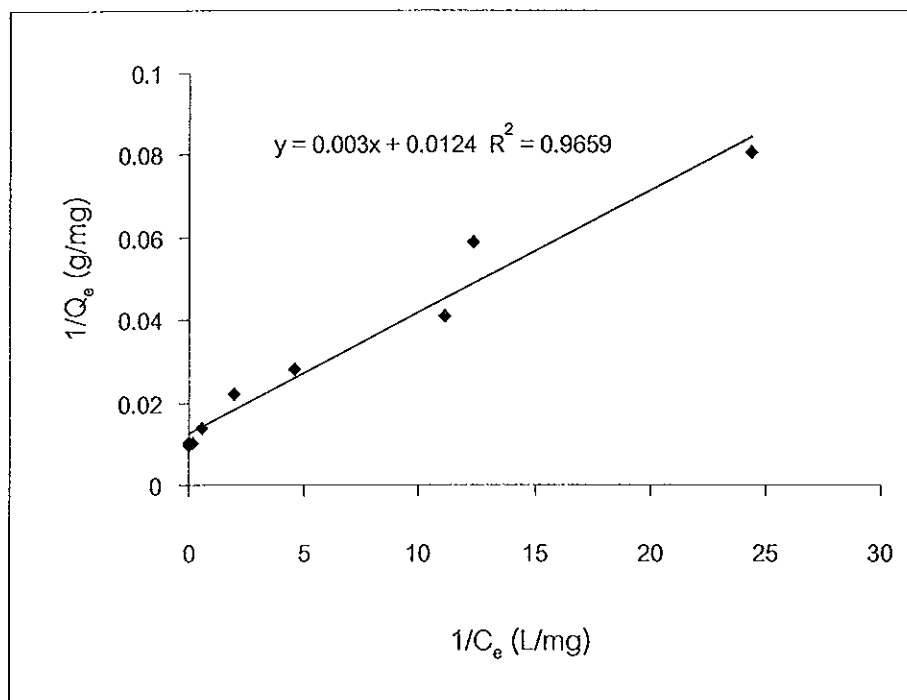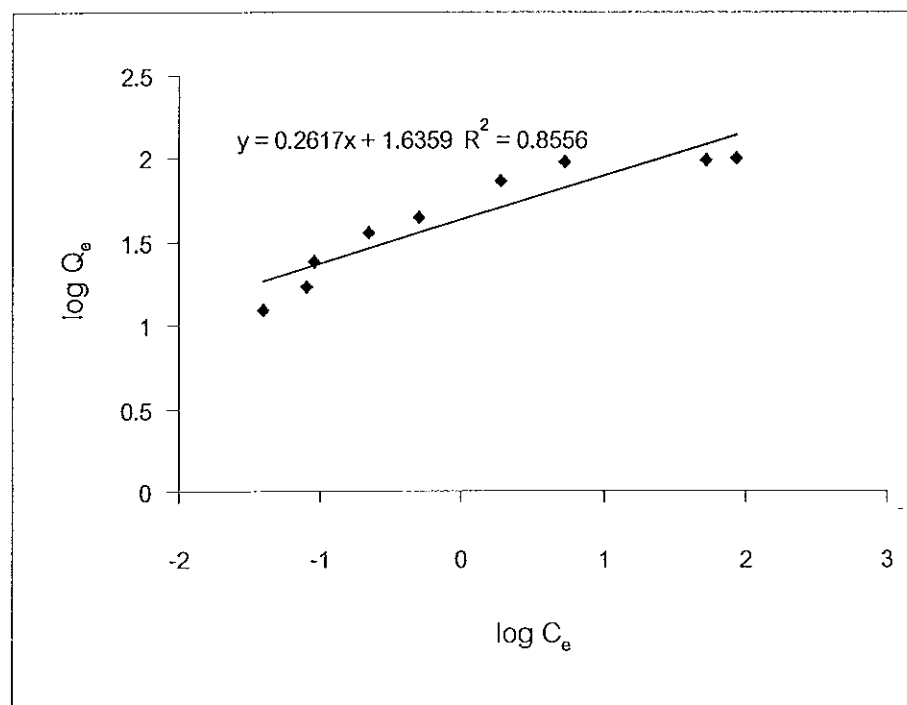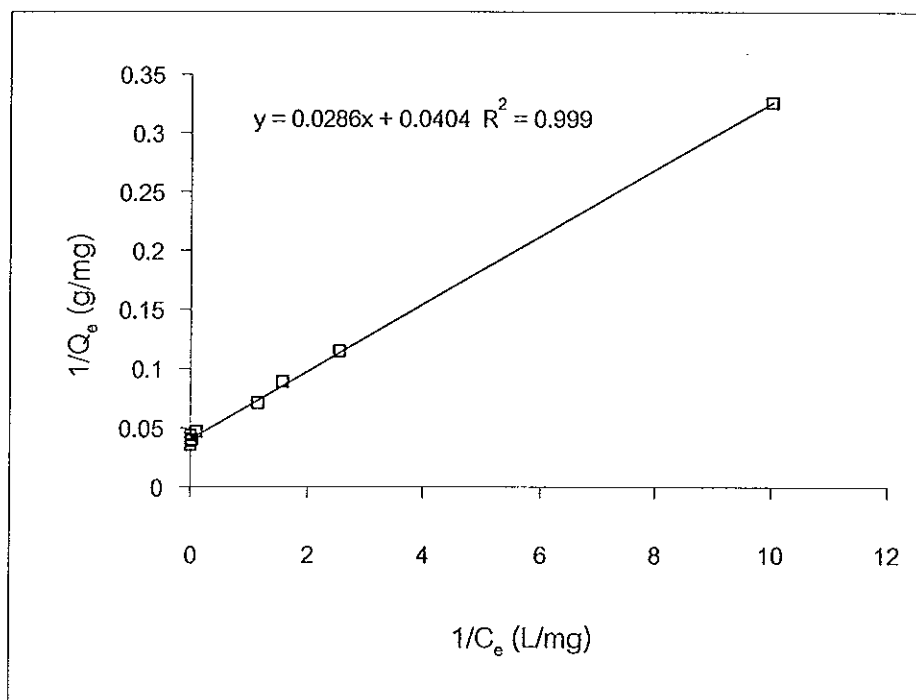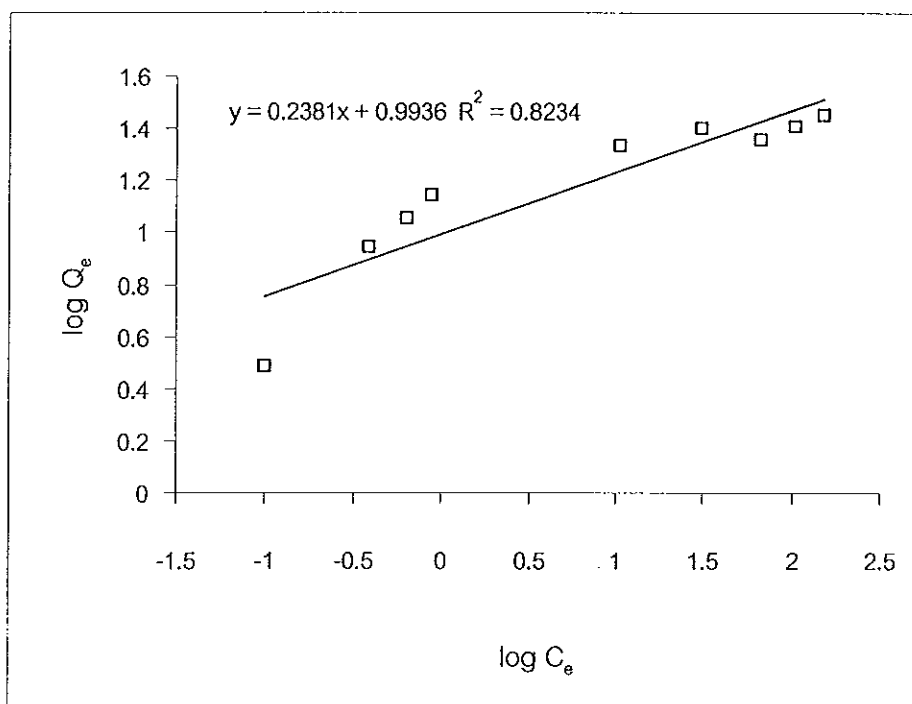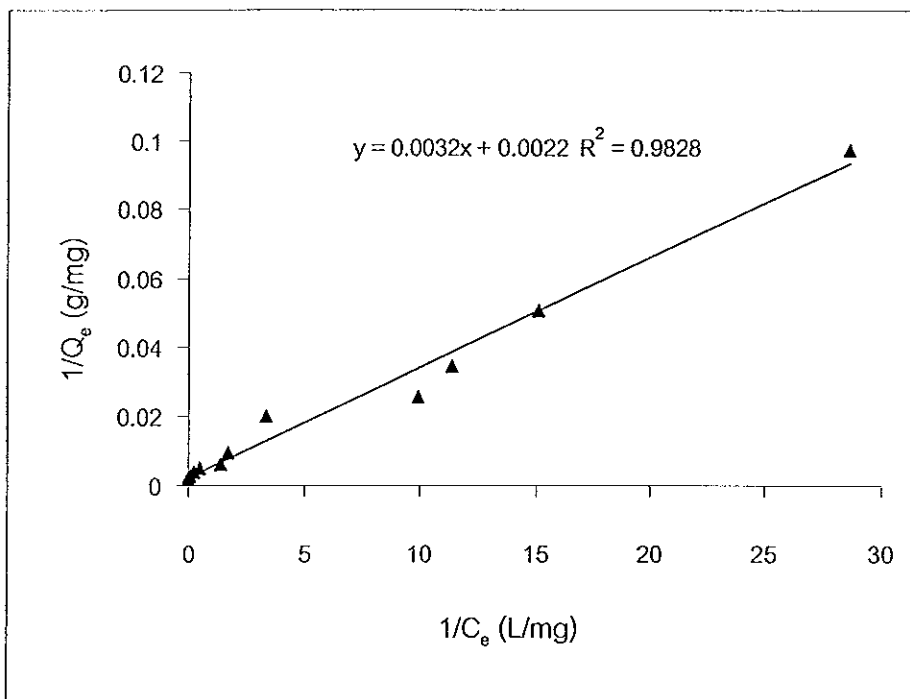
Figure 28 Langmuir isotherm plot of Pb(II) adsorption on TiO_2 (syn).
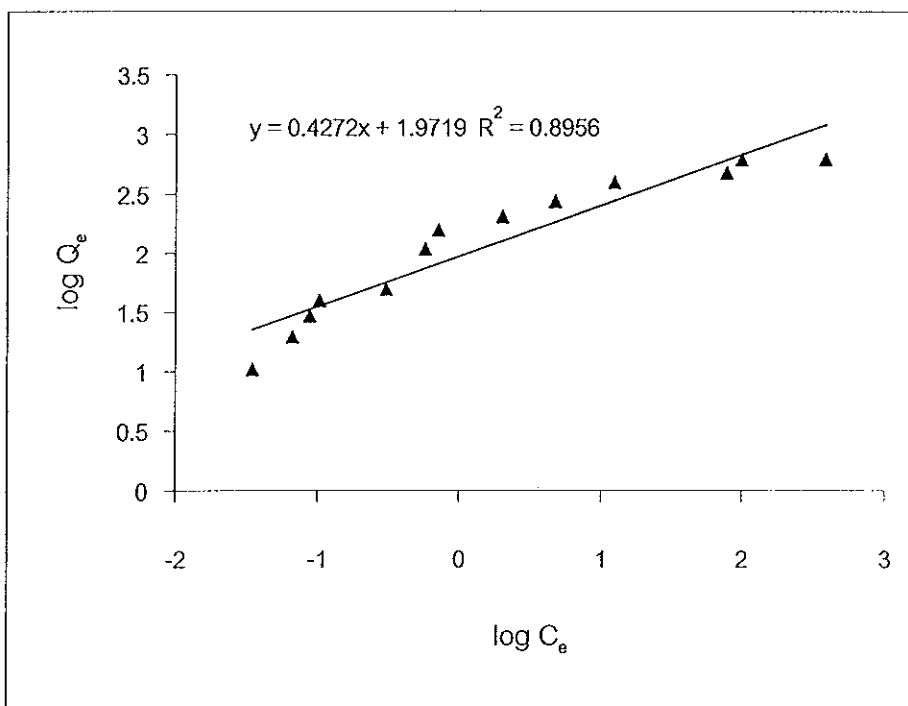
Figure 29 Freundlich isotherm plot of Pb(II) adsorption on TiO_2 (syn).
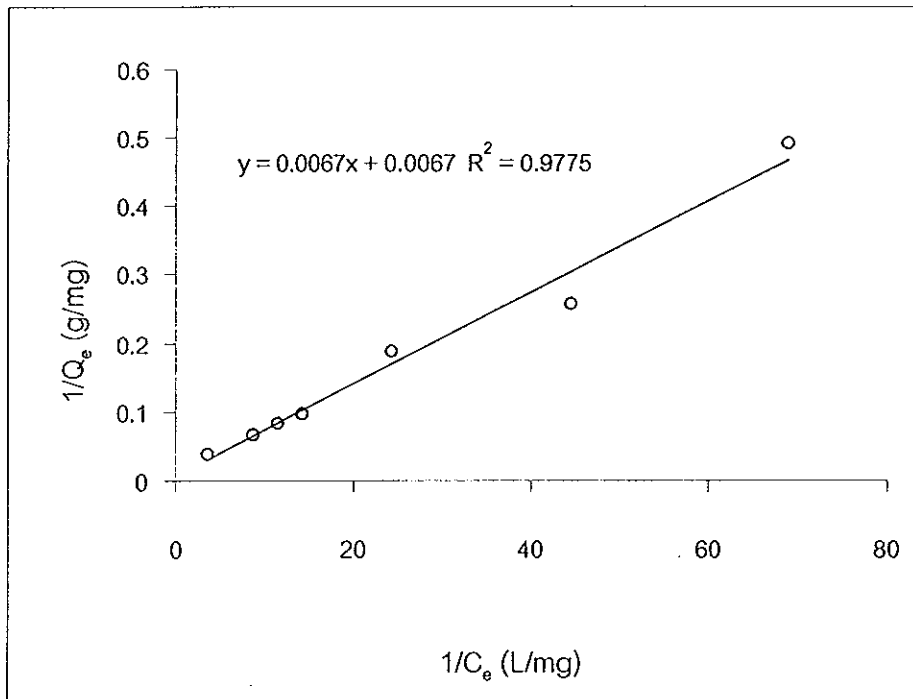
Figure 30 Langmuir isotherm plot of Fe(III) adsorption on TiO_2 (syn).
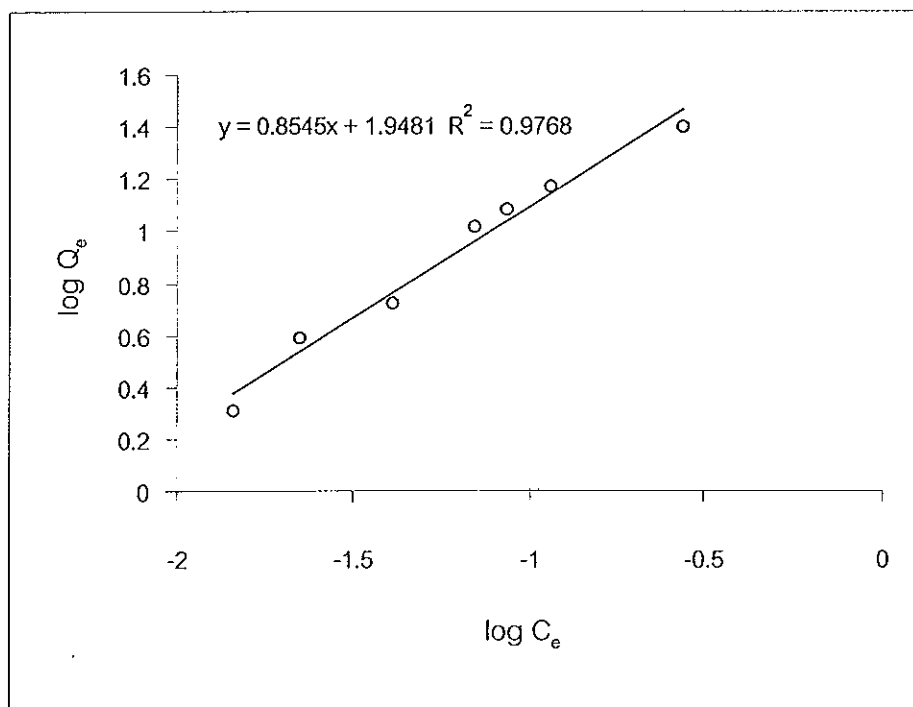
Figure 31 Freundlich isotherm plot of Fe(III) adsorption on TiO_2 (syn).

The adsorption capacities (Q^0) of the adsorption of Cu(II), Mn(II), Pb(II) and Fe(III) on the TiO_2(syn) were calculated from the Langmuir isotherm equation (eq. 2) and given in Table 36. Figures 32-35 showed the relation between the adsorption capacity (Y axis) and the residual concentration of metal ion (X axis) from the experimental data, Tables 27-30. For comparison, the adsorption capacity as calculated from the Langmuir isotherms equation and the experimental data are shown in Table 36.

Table 36 The adsorption capacity from the experimental data and the calculated values

Metal ions	Adsorption capacity (Q^0), mg/g	
	Calculated values	Experimental data (in Fig. 32-35)
Cu(II)	80.64	~90
Mn(II)	24.75	~25
Pb(II)	454.55	~600
Fe(III)	149.25[a], 88.74[b]	~[c]

a calculated from the Langmuir equation (eq.2) in page 20.

b calculated from the Freundlich equation (eq.4) in page 20.

c no data obtained because at the initial concentration of sample solution > 25 ppm, Fe(III) began to precipitate as $Fe(OH)_3$.
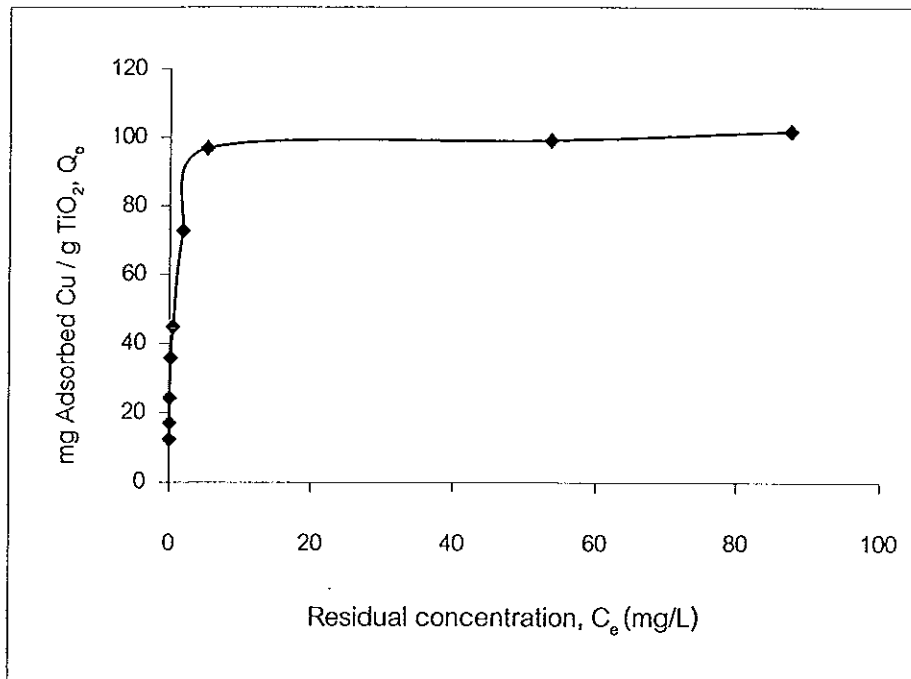
Figure 32 The relation between the adsorption capacity for the adsorption of Cu(II)

on TiO_2 (syn) and the residual concentration.
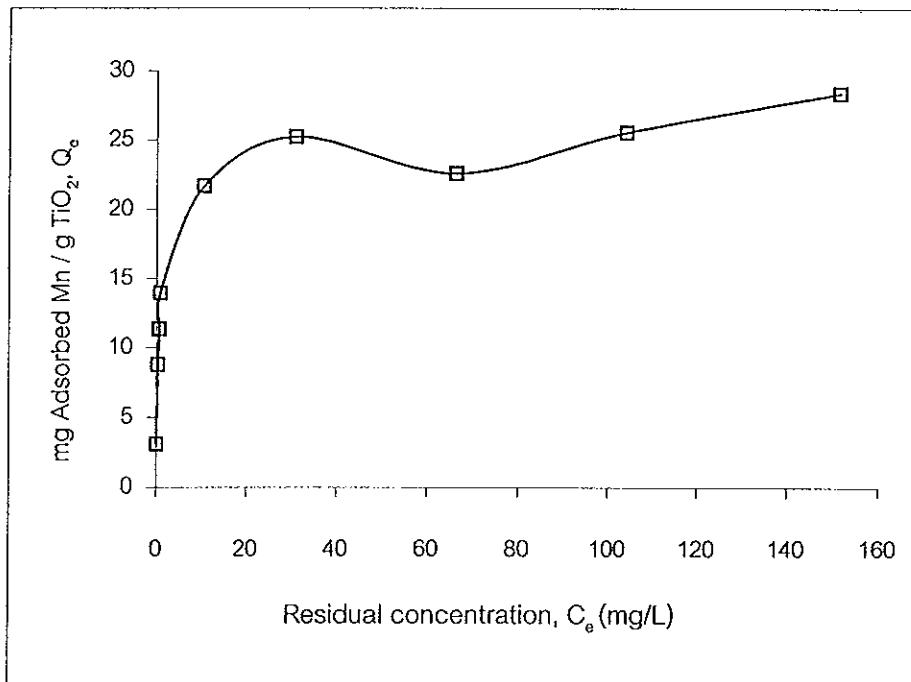
Figure 33 The relation between the adsorption capacity for the adsorption of Mn(II)

on TiO_2 (syn) and the residual concentration.
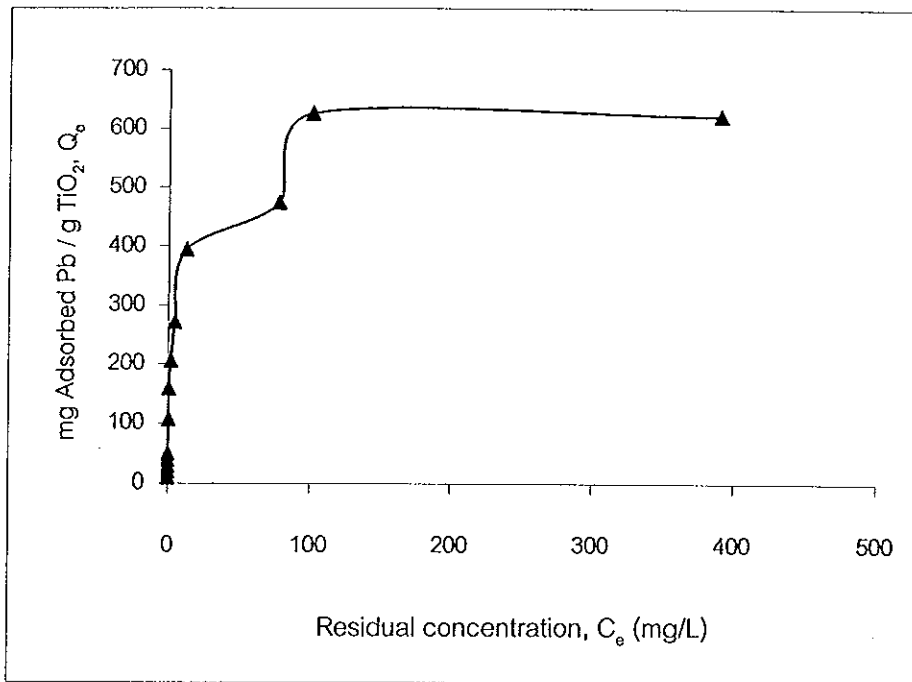
Figure 34 The relation between the adsorption capacity for the adsorption of Pb(II)

on TiO_2 (syn) and the residual concentration.
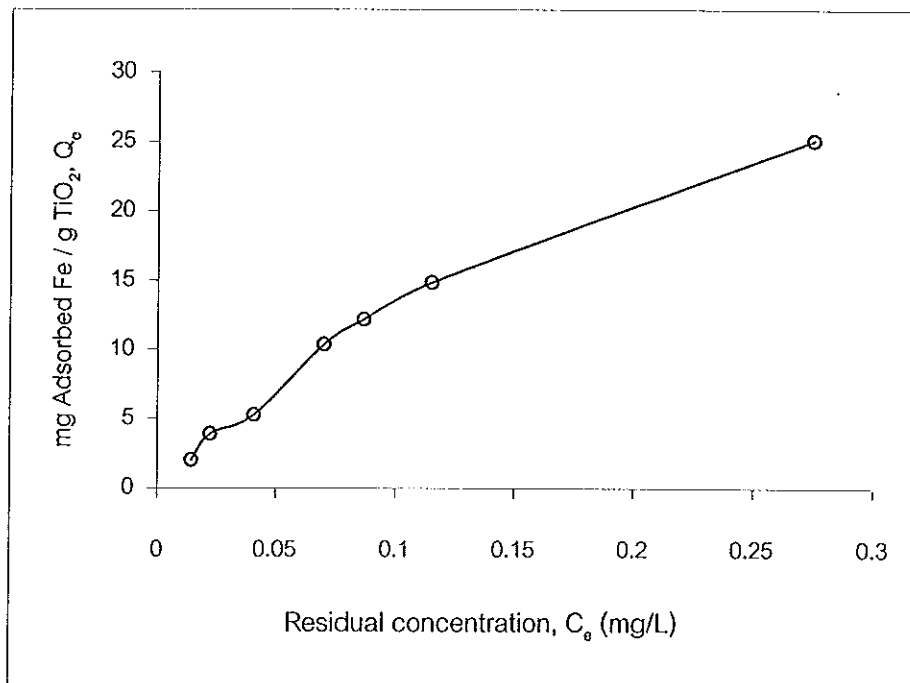
Figure 35 The relation between the adsorption capacity for the adsorption of Fe(III)

on TiO_2 (syn) and the residual concentration.

4.2.3 Comparison of the adsorption capacity between TiO_2 (syn) and

the commercial TiO_2 (anatase: Carlo Erba, P25, rutile: TOA Co.,)

The adsorption capacity is an important factor, because it determines how much TiO_2 can adsorb maximum of metal ions from solution. The results were presented in Table 31 (page 62), and the data of other types of TiO_2 were also given for comparison (Figure 36). It can be seen that the capacity of TiO_2(syn) is very high when compared (the adsorption capacity) with data from the literature as shown in Table 37. Because of the higher surface area of TiO_2(syn), 449 m^2/g , due to the present of –OH and NH_4^+ groups (from FT-IR data) on its surface.
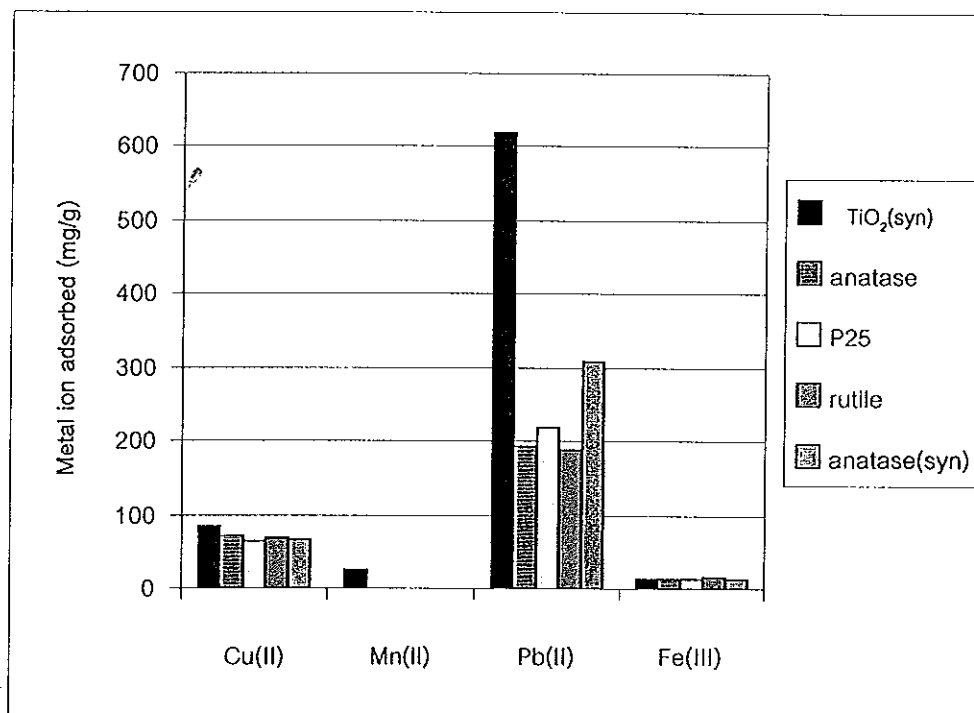
Figure 36 The adsorption capacity for the adsorption of metal ions on TiO_2 at pH 7 (room temperature) in this work. (Anatase(syn) was synthesized in this work according to Vassileva's method)

Table 37 The adsorption capacity (mg/g) of other TiO_2's (literatures).

Sample	Adsorption capacity (mg/g)			References
	Cu(II)	Mn(II)	Pb(II)	
T1(anatase, syn)	9.010	6.830	5.030	Vassileva, et al., 1996[b]
T2(anatase, Fluka)	0.270	-	0.220	Vassileva, et al., 1996[b]
SiO_2	17.400	-	3.200	Vassileva, et al., 1996[b]
Nanometer TiO_2	6.86	2.14	a	Liang, et al., 2001[c]
Amberlite XAD resin	3.37	9.33	a	Liang, et al., 2001[c]
Chelex-100 resin	6.99	7.69	a	Liang, et al., 2001[c]
Turkish coals	a	a	8.4952	Arpa, et al., 2000[d]

a not studied

b reported the adsorption capacity in unit of µg/g, at pH 8

c reported the adsorption capacity in unit of mmol/g, at pH 8

d at pH 5

Schemes for cation adsorption had reported in many researches. Malati and Smith (1979) and Malati, et al., (1982) proposed that the adsorption of cation is expected on the negative surface at pH values above the point of zero charge (PZC), shown in Table 38. Adsorption of cations at pH values equal to or less than the PZC is ascribed to specific adsorption. The charge of TiO_2 surface may be represented by

$$TiOH^+(surf) \quad \leftrightarrow \quad Ti(OH)(surf) + H^+(aq) \quad \leftrightarrow \quad TiO^-(surf) + 2H^+(aq)$$
H
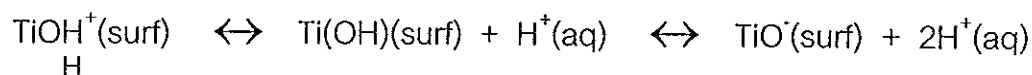
Positive surface   Point of zero charge   Negative surface

Table 38 Literature values for the point of zero charge (PZC) and isoelectric points (IEP) of TiO_2.

TiO_2	PZC	IEP	Reference
Anatase (Tioxide Ltd.)	6.2	-	Malati and Smith, 1979
Anatase	-	6.2	Vassileva, et al., 1996
Anatase (Sachtleben)	-	5.6	Winkler and Marmé, 2000
Rutile (Tioxide Ltd.)	5.3	-	Malati and Smith, 1979
Nanocrystlline microporous	5.7	-	Poznyak, et al., 1999
Hydrous TiO_2	5.0	5.0	Ottaviani, et al., 1985
Amorphous TiO_2	-	5.0	Tentorio and Canova, 1989

Whereas, Vassileva, et al., (1996) reported the scheme for cation adsorption that at pH values higher than the isoelectric point (IEP), shown in Table 38, the oxide surface is covered with OH groups and is negatively charged, as a result, it becomes active towards cation adsorption. The following simplified scheme may be proposed on the basis of their results:

$$\text{Ti}-\text{O} + \text{OH}^- \rightarrow \overset{\displaystyle \text{OH}^-}{\underset{\displaystyle |}{\text{Ti}-\text{O}}}$$

$$\overset{\displaystyle \text{OH}^-}{\underset{\displaystyle |}{\text{Ti}-\text{O}}} + M^{n+}(L)_{x+1} \rightarrow \overset{\displaystyle \text{OH}^- \quad M^{n+}(L)_x}{\underset{\displaystyle | \qquad |}{\text{Ti}-\text{O}}} + L$$
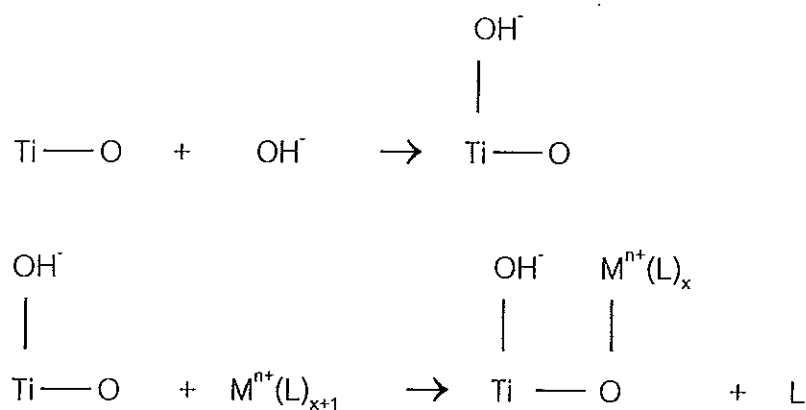
where   L   is a ligand.

M^{n+} is a heavy metal cation.

Anderson and Rubin (1981), proposed various possible reactions of a hydroxylated surface (Figure 37). The individual reactions are discussed in the subsequent paragraphs.

$$\text{a)}\quad \begin{array}{ccc} H \overset{(+)}{\diagdown} H & H & (-) \\ | & | & | \\ O & O & O \\ | & | & | \\ X & \rightleftharpoons \quad X & \rightleftharpoons \quad X \end{array}$$

$$\text{b)}\quad X-O-H + M^{Z+} \rightleftharpoons X-O-M^{(Z-1)+} + H^+$$

$$\begin{array}{c} X-O-H \\ \\ X-O-H \end{array} + M^{Z+} \rightleftharpoons \begin{array}{c} X-O \\ \diagdown \\ \diagup \\ X-O \end{array} M^{(Z-2)+} + 2H^+$$

$$\text{c)}\quad \begin{array}{c} X-O-H \\ \\ X-O-H \end{array} + HPO_4^{2-} \rightleftharpoons \begin{array}{c} X-O \quad OH \\ \diagdown \diagup \\ P \\ \diagup \diagdown \\ X-O \quad O \end{array} + 2\ OH^-$$

$$\text{d)}\quad X-O-H + M^{Z+} + L \rightleftharpoons X-O-M-L^{(Z-1)+} + H^+$$

$$\text{e)}\quad X-O-H + L + M^{Z+} \rightleftharpoons X-L-M^{(Z+1)+} + OH^-$$
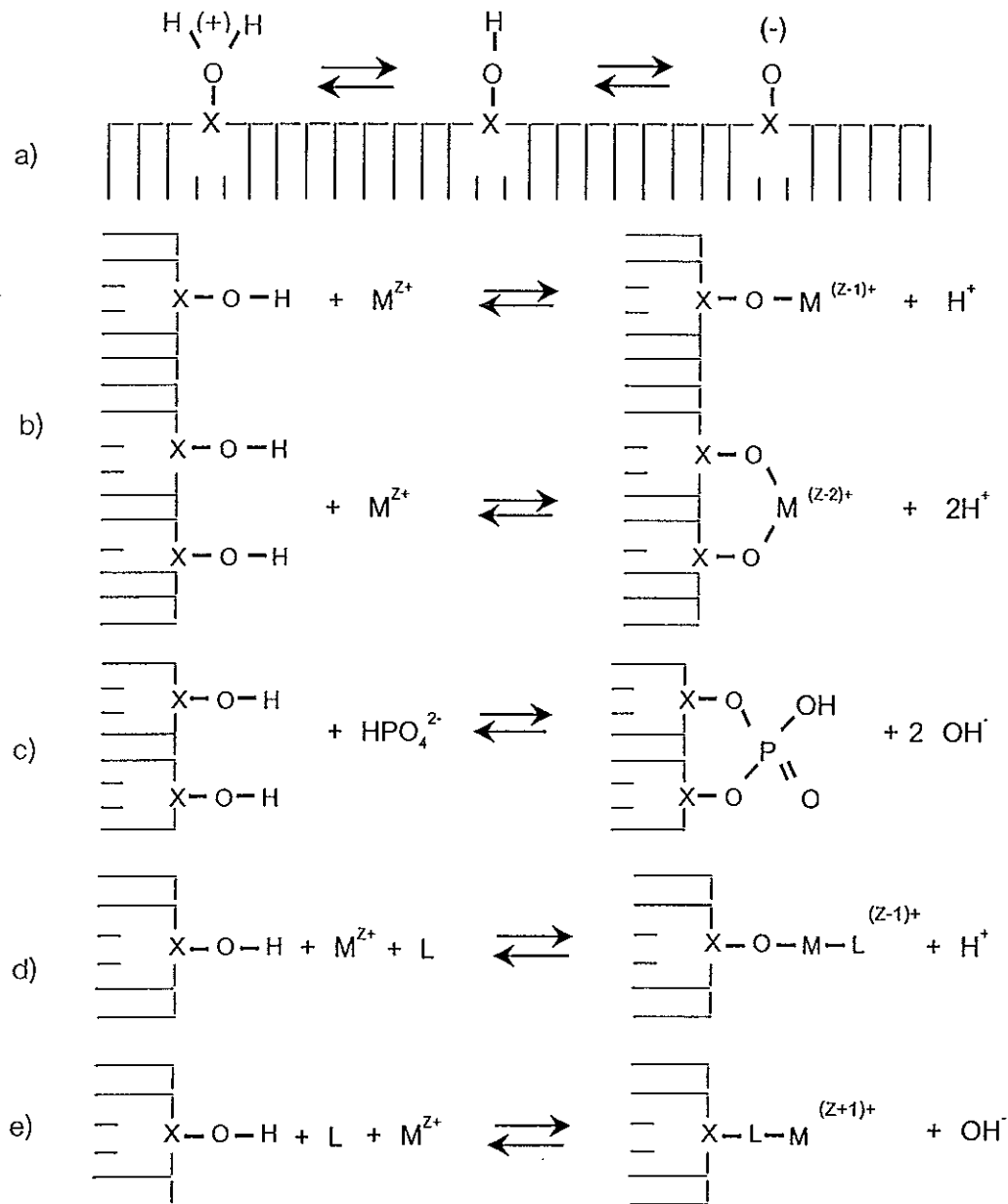
X : Si, Ti, Al, Fe, etc.

Figure 37 Coordination phenomena at oxide-water interfaces :

(Anderson and Rubin, 1981 : 6)

(a) Acid-base reactions of surface hydroxyls groups.

(b) Deprotonated surface hydroxyls coordinate with dissolved metal ions. Several species may be formed simultaneously.

(c) Surface hydroxyls are replaced by dissolved ligands.

(d) A dissolved metal ion coordinates with both deprotonated surface hydroxyls and dissolved ligands.

(e) A dissolved multidentate ligand coordinates with both X and the dissolved metal ion M.

In this work, scheme (a) can be used to describe the nature of TiO_2(syn) surface. At pH 7 which is higher than IEP or PZC of TiO_2 (Table 38) the surface can be described below.

(a)

Adsorption of cations (Cu^{2+}, Mn^{2+}, Pb^{2+} and Fe^{3+}) then can be is expected at the negative sites of TiO_2(syn) surface and scheme (b) can be applied as follows.

(b)

M : Cu, Mn, Pb and Fe.

Chapter 5

SUMMARY

Titanium dioxide (TiO_2) was prepared from the reaction between $TiCl_4$ and NH_3 solution by method A (concentrated NH_3 solution, room temperature) and method B (dilute NH_3 solution, at low temperature). The XRD spectrum of TiO_2(syn) from method A indicated that it is mainly the amorphous form of TiO_2 with small amount of anatase (~5%) mixed in (Chamnan Randorn, 2001, unpublished). While the XRD spectrum of TiO_2(syn) from method B indicated that the product is purely amorphous titanium dioxide. In this work, TiO_2(syn) from method B was used for studying their adsorption properties. The surface areas of TiO_2(syn) was 449 m^2/g which was higher than the commercial TiO_2. The EDXRF spectrum showed only peaks from K-lines of Ti indicating no contamination from other impurity (Cl^-). The FT-IR spectrum of TiO_2(syn) showed the presence of H_2O and NH_4^+ presumably on its surface. Elemental analysis showed that N was present in only small amount, 1.3 – 1.8%. This small amount rendered N(nitrogen) undetectable by SEM/EDX and WDXRF in subsequent measurements. The general formula of TiO_2(syn) thus can be written as $TiO_2 \cdot nH_2O$. Accordingly, a total weight loss of this product was 25.98% (measured by TGA) would pertain to the decomposition of the product $TiO_2 \cdot 1.6H_2O$ into TiO_2, putting n=1.6 in the general formula. Data from DSC pattern of TiO_2(syn) showed an endothermic peak $ca.$109 $^{\circ}C$ which could be attributable to liberation or decomposition of water (H_2O). A characteristic exothermic peak was also observed at $ca.$ 426 $^{\circ}C$ and was attributable to

crystallization of amorphous phase to anatase. The reaction to produce TiO_2(syn), therefore, can be expressed by :

$$TiCl_4 + 4NH_4OH \rightarrow TiO_2 \cdot 1.6H_2O + 4NH_4Cl + 0.4H_2O$$
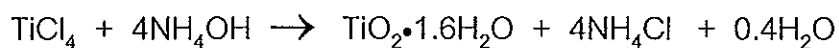
The adsorption of metal ions (Cu, Mn, Pb, and Fe) on TiO_2 (syn) were investigated by finding the optimum conditions and the adsorption isotherms. From the experiments, it was found that TiO_2(syn) adsorbed rapidly, for Cu(II) and Mn(II) ions and reached equilibrium in 10 minutes while it was 15 minutes for Pb(II) and Fe(III). From the results of the effect of sample volume the optimum ratio of the amount of TiO_2(syn) to one litre of metal ion solutions (g/L) can be obtained and were 2, 1.67, 0.5, and 1 for Cu(II), Mn(II), Pb(II), and Fe(III), respectively. In addition, the metal ions adsorbed depended on the concentrations of metal ions and the concentration which gave the maximum adsorption of Cu(II), Mn(II), Pb(II), and Fe(III) were 5, 4, 25, and 8 mg/L. The quantitative sorption of Cu(II) and Pb(II) occurred in the pH range 3-9, Mn(II) in the pH range 3-7, and Fe(III) in the pH range 5-9. In order to find the adsorption isotherm of all studied elements, a pH of 7 was selected. Based on the values of the correlation coefficient (R^2) for the different isotherm plots, the Langmuir isotherm gives the best fit for the adsorption of Cu, Mn, and Pb while the adsorption of Fe(III) fit both the Langmuir and Freundlich isotherms. When compared the adsorption capacity of TiO_2(syn) with other commercially available TiO_2's it was found that the adsorption capacity of TiO_2(syn), which were 84.78, 24.93, 618.79, and 14.85 mg/g for Cu(II), Mn(II), Pb(II), and Fe(III), respectively, was higher than those of other TiO_2's.

BIBLIOGRAPHY

Abe, M.; Wang, P.; Chitrakar, R. and Tsuji, M. 1989. "Synthesis Inorganic Ion-exchange Materials Part XLIX. *Adsorption and Desorption Behaviour of Heavy Metal Ions on Hydrated Titanium Dioxide", Analyst. 114(1989), 435-438.

Anderson, M. A. and Rubin, A. J. 1981. Adsorption of Inorganics at Solids-Liquid Interfaces. Michigan : Ann Arbor Science.

Arpa. Ç.; Başyilmaz, E.; Bektaş, S.; Genç, Ö. And Yürüm, Y. 2000. "Cation Exchange Properties of Low Rank Turkish Coals : Removal of Hg, Cd and Pb from Waste Water", Fuel Processing Technology. 68(2000), 111-120.

Bacsa, R. R.; Kiwi, J. 1998. "Effect of Rutile Phase on the Photocatalytic Properties of Nanocrystalline Titania During the Degradation of p-Coumaric Acid", Applied Catalysis B: Environmental. 16(24 June 1997), 19-29.

Bond, G. C. 1987. Heterogeneous Catalysis: Principles and Applications. 2nd ed. New York : Oxford University Press.

Büchner, W.; Schliebs, S.; Winter, G. and Büchel, K. H. 1989. Industrial Inorganic Chemistry. New York : VCH.

Castellan, G. W. 1983. Physical Chemistry. 3rd ed. California : Benjamin/Cummings.

Chamnan Randorn. 2001. "Study of the Chemical Properties of Titanium Dioxide", M.Sc. Inorganic Chemistry, Prince of Songkla University. (Unpublished)

Chen, D. and Ray, A. K. 2001. "Removal of Toxic Metal Ions from Wastewater by Semiconductor Photacatalysis", Chem. Eng. Sci. 56(2001), 1561-1570.

Clark, R. J. H. 1968. The Chemistry of Titanium and Vanadium. Amsterdam : Elsevier.

Dalai, A. K; Sethuraman, R.; Katikaneni, S. P. R. and Idem, R. O. 1998. "Synthesis and Characterization of Sulfated Titania Solid Acid Catalysts", Ind. Eng. Chem. Res. 37(1998), 3869-3878.

Devi, R. P. and Naidu, K. R. G. 1990. "Enrichment of Trace Metals in Water on Activated Carbon", Analyst. 115(1990), 1469-1471.

Esumi, K.; Hayashi, H.; Koide, Y.; Suhara, T. and Fukui, H. 1998. "Adsorption of Metal Ion and Aromatic Compounds by Anionic Surfactant-Coated Particles of Titanium Dioxide", Colloid and Surfaces. 144(10 June 1998), 201-206.

German, R. M.   1984.   Powder Metallurgy Science.   New Jersey : Metal Powder Industries Federation.

Gharaibeh, S. H.; ABU-EL-SHA'S, W. Y. and AL-KOFAHI, M. M.   1998. "Removal of Selected Heavy Metals from Aqueous Solutions using Processed Solid Residue of Olive Mill Products", Wat. Res. 32(1998), 498-502.

Ha, P. S.; Youn, H. –J.; Jung, H.S.; Hong, K.S.; Park, Y. H. and Ko, K. H. 2000. "Anatase-Rutile Transition of Precipitated Titanium Oxide with Alcohol Rinsing", J. Colliod Interface Sci. 223(2000), 16-20.

Hadjiivanov, K.; Klissurski, D.; Kantchev, M. and Davydov, A.   1991.   "State and Localization of Cobalt, Nickel and Copper Ions Adsorbed on Titania (Anatase)", J. Chem. Soc. Faraday Trans. 87(1991), 907-911.

Jalava, j. –P.; Heihkilä, L.; Hovi, O.; Laiho, R.; Hiltunen, E.; Hakanen, A. and Härmä, H.   1998.   "Structural Investigation of Hydrous TiO_2 Precipitates and Their Aging Products by X-Ray Diffraction Atomic Force Microscopy, and Transmission Electron Microscopy", Ind. Eng. Chem. Res.   37 (1998),1317-1323.

Khalil, K. M. S. and Zaki, I. Z.   1997.   "Synthesis of High Surface Area Titania Powders Via Basic Hydrolysis of Titanium(IV) Isopropoxide", Powder Technology. 92(15 April 1997), 233-239.

Kim, M-S. and Chung, J. G. 2001. "A Study on the Adsorption Characteristics of Orthophosphates on Rutile-Type Titanium Dioxide in Aqueous Solutions", J. Colliod Interface Sci. 233(2001), 31-37.

Lehmann, M.; Zouboulis, A. I.; Matis, K. A. 1999. "Removal of Metal Ions from Dilute Aqueous Solution: a Comparative Study of Inorganic Sorbent Materials", Chemosphere. 39(1999), 881-892.

Liang, P.; Qin, Y.; Hu, B.; Peng, T. and Jiang, Z. 2001. "Nanometer-Size Titanium Dioxide Microcolumn on-line Preconcentration of Trace Metals and their Determination by Inductively Coupled Plasma Atomic Emission Spectrometry in Water", Anal. Chim. Acta. 440(2001), 207-213.

Ludwig, C. and Schindler, P. W. 1995. "Surface Complexation on TiO_2 1. Adsorption of H^+ and Cu^{2+} Ions onto TiO_2(Anatase)", J. Colliod Interface Sci. 169(1995), 284-290.

Malati, M. A. and Smith, A. E. 1979. "The Adsorption of the Alkaline Earth Cations on Titanium Dioxide", Powder Technology. 22(1979), 279-282.

Malati, M. A.; McEvoy, M. and Hervey, C. R. 1982. "The Adsorption of Cadmium (II) and Silver (I) Ions on SiO_2 and TiO_2", Surface Technology. 17(1982), 165-174.

Manju, G. N.; Krishnan, A.; Vinod, V. P. and Anirudhan, T. S. 2002. "An Investigation into the Sorption of Heavy Metals from Wastewaters by Polyacrylamide-Grafted Iron (III) Oxide", J. Hazardous Materials. B91(2002), 221-238.

Masel, R. I. 1996. Principles of Adsorption and Reaction on Solid Surfaces. U.S.A. : John Wiley & Sons, Inc.

Mo, S. –D. and Ching, W. Y. 1995. "Electronic and Optical Properties of Three Phases of Titanium Dioxide: Rutile, Anatase, and Brookite", Physical Review B. 52(15 May 1995), 13023-13032.

Ohtani, B.; Ogawa, Y.; Nishimoto, S. -I. 1997. "Photocatalytic Activity of Amorphous-Anatase Mixture of Titanium(IV) Oxide Particles Suspended in Aqueous Solutions", J. Phys. Chem. B. 101(30 January 1997), 3746-3752.

Ottaviani, M. F.; Ceresa, E. M. and Visca, M. 1985. "Cation Adsorption at the TiO_2-Water Interface", J. Colliod Interface Sci. 108(November 1998), 114-122.

Park, N. –G.; Schlichthörl, G.; van de Lagemaat, J.; Cheong, H. M.; Mascarenhas, A. and Frank, A. I. 1999. "Dye-Sensitized TiO_2 Solar Cells: Srructural and Photoelectrochemical Characterization of Nanocrystalline Electrodes Fromed form the Hydrolysis of $TiCl_4$", J. Phys. Chem. B. 103(1999), 3308-3314.

Perkin-Elmer. 1996. <u>Atomic Absorption Spectroscopy, Analytical Methods</u>. U.S.A. : Perkin-Elmer Corporation.

Perkin-Elmer. 1997. Aanalyst 100/300 <u>Atomic Absorption Spectrometer, Hadware Guide</u>. U.S.A. : Perkin-Elmer Corporation.

Poznyak, S. K.; Pergushov, V. I.; Kokorin, A. I.; Kulak, A. I. And Scläpfer, C. W. 1999. "Structure and Electrochemical Properties of Species Formed as a Result of Cu(II) Ion Adsorption onto TiO_2 Nanoparticles", <u>J. Phys. Chem. B</u>. 103(1999), 1308-1315.

Skoog, D. A. and Leary J. J. 1992. <u>Principle of Instrumental Analysis</u>. 4th ed. Philadelphia : Saunders College Publishing.

Sclafani, A.; Palmisano, L. and Schiavello, M. 1990. "Influence of the Preparation Methods of TiO_2 on the Photocatalytic Degradation of Phenol in Aqueous Dispersion", <u>J. Phys. Chem</u>. 94(1990), 829-832.

Shao, L.; Zhang, L.; Chen, M.; Lu, H. and Zhou, M. 2001. "Reactions of Titanium Oxides with Water Molecules. A Matrix Isolation FTIR and Density Functional Study", <u>Chem. Phys. Latters</u>. 343(27 July 2001), 178-184.

Tentorio, A. and Canova, L. 1989. "Adsorption of α-Amino Acids on Spherical TiO_2 Particles", Colloids and Surfaces. 39(1989), 311-319.

Tony, A.; Akama, Y. and Tanaka, S. 1990. "Pre-concentration of Copper, Cobalt and Nickel with 3-Methyl-1-Phenyl-4-Stearoyl-5-Pyrazolone Loaded on Silica Gel", Analyst. 115(1990), 947-949.

Vanderborght, M. and Van Grieken, E. R. 1977. "Enrichment of Trace Metals in Water by Adsorption on Activated Carbon", Anal. Chem. 49(1977), 311-316.

Vassileva, E; Proinova, I. and Hadjiivanov, K. 1996. "Solid-Phase Extraction of Heavy Metal Ions on a High Surface Area Titanium Dioxide(Anatase)", Analyst. 121, 607-612.

Vohra, M. S. and Davis, A. P. 1997. "Adsorption of Pb(II), NTA, and Pb(II)-NTA onto TiO_2", J. Colliod Interface Sci. 194(9 July 1997), 59-67.

Wang, H. and Adesina, A. A. 1997. "Photocatalytic Causticization of Sodium Oxalate Using Commercial TiO_2 Particles", Appl. Catal. B. 14(1997), 241-247.

Weng, G. H.; Wang, J. H. and Huang, C. P. 1997. "Adsorption of Cr(VI) onto TiO_2 from Dilute Aqueous Solution", Wat. Sci. Tech. 35(1997), 55-62.

Whiston, C. 1991. X-ray Methods. Singapore : John Wiley & Sons.

Willard, H. H.; Merritt, L. L. and Dean, J. A. 1974. Instrumental Methods of Analysis. 4th ed. New York : D. Van Nostrand Co.

Winkler, J. and Marmé, S. 2000. "Titania as a Sorbent in Normal-Phase Liquid Chromatography", J. Chromatography A. 888(2000), 51-62.

Xu, N.; Shi, Z.; Fan, Y.; Dong, J.; Shi, J. and Hu, M. Z. –C. 1999. "Effect of Particles Size of TiO_2 on Photocatalytic Degradation of Methylene Blue in Aqueous Suspensions", Ind. Eng. Chem. Res. 38(1999), 373-379.

Yanagisawa, K. and Ovenstone, J. 1999. "Crystallization of Anatase from Amorphous Titania Using the Hydrothermal Technique: Effects of Starting Material and Temperature", J. Phys Chem. B. 103(12 May 1999), 7781-7787.

Youn, H. –J.; Ha, P. S.; Jung, H. S.; Hong, K. S.; Park, Y. H. and Ko, K. H. 1999. "Alcohol Rinsing and Crystallization Behaviour of Precipitated Titanium Dioxide", J. Colliod Interface Sci. 211(30 November 1998), 321-325.

Yu, J. C. and Chan, L. Y. L. 1998. "Photocatalytic of a Gaseous Organic Pollutant", J. Chem. Educ. 75(June 1998), 750-751.

Zhang, J-Y.; Boyn, J. W.; O'Sullivan, B. J.; Hurley, P. K.; Kelly, P. V. and Sénateur, J. –P. 2002. "Nanocrystalline TiO_2 Films Studies by Optical, XRD and FTIR Spectroscopy", J. Non-Crystalline Solids. 303(2002), 134-138.

Zhang, Q. –H.; Gao, L. and Guo, J. –K.   1999.   "Preparation and Characterization of Nanosized TiO$_2$ Powders from Aqueous TiCl$_4$ Solution", <u>Nanostructured Materials</u>. 11(5 November 1999), 1293-1300.

Zhang, Y.; Weidenkaff, A. and Reller, A.   2002.   "Mesoporous Structure and Phase Transition of Nanocrystalline TiO$_2$", <u>Materials Letters</u>. 54(June 2002), 375-381.

APPENDIX

Appendix A

A.1 Scanning electron microscope with energy dispersive x-ray spectrometer (SEM/EDX)

The SEM/EDX spectrum was acquired through the Scientific Equipment Center, Prince of Songkla University, Hat Yai, Songkla, using a scanning electron microscope, JSM-5800LV, JEOL, Japan, with energy dispersive x-ray spectrometer, ISIS300, Oxford Instruments, UK. In Figure A1 shows the SEM/EDX spectrum of TiO_2(syn) (form method B).

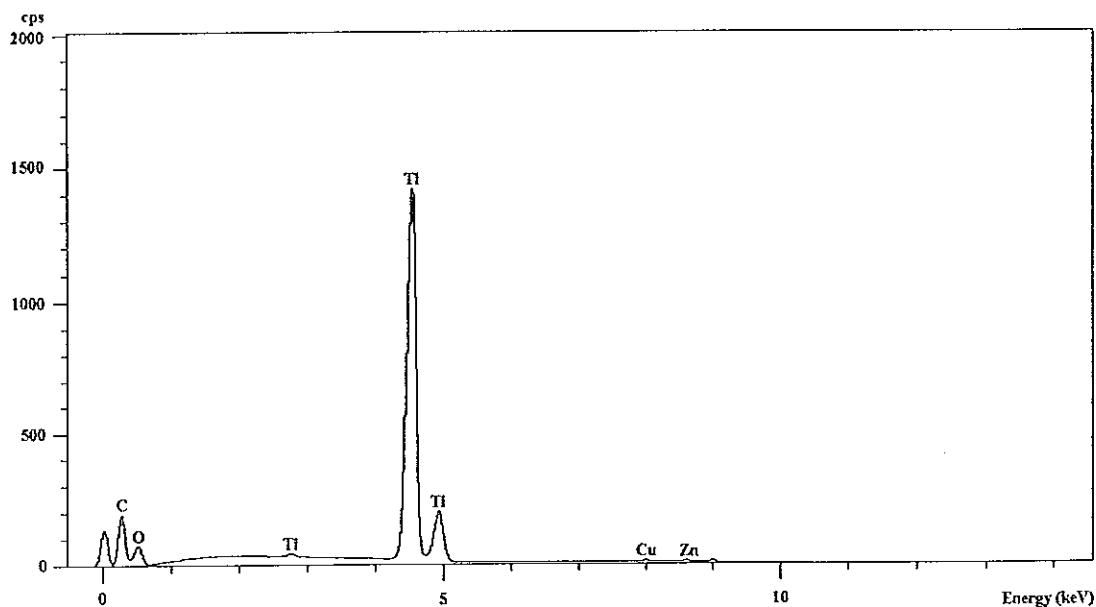Figure A1 SEM/EDX spectrum of TiO_2(syn).

A.2 Wavelength dispersive x-ray fluorescence spectrometer (WDXRF)

The WDXRF spectrum was acquired through the Scientific Equipment Center, Prince of Songkla University, Hat Yai, Songkla, using a wavelength dispersive x-ray fluorescence (WDXRF) spectrometer, PW2400, Philips Analytical x-ray B.V., Netherland. The x-ray tube uses Rh as target. In Figure A2 shows the WDXRF spectrum of O $K\alpha$ from TiO_2(syn) (from method B). WDXRF was used mainly to detect N (from NH_4^+) at the surface of TiO_2(syn) but was unable to detect it. This was interpreted as due to its presence in very small amount.
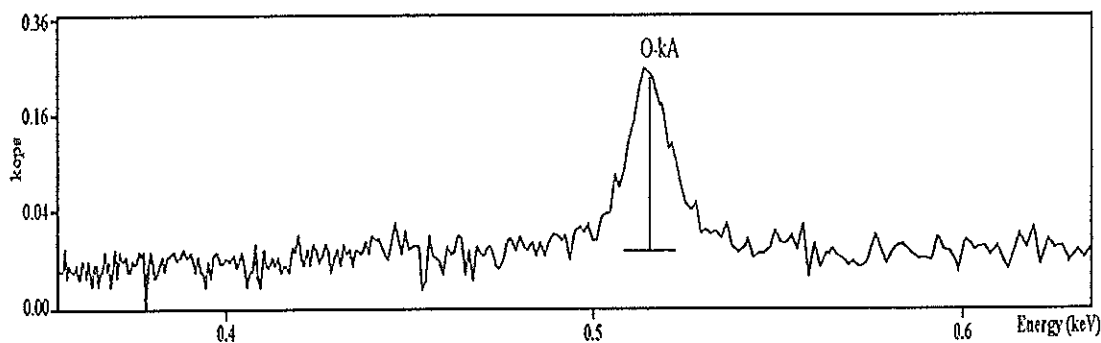

Figure A2 WDXRF spectrum of TiO_2(syn).

Appendix B

B.1 Atomic absorption spectrometer

Every element has a specific number of electrons associated with its nucleus. The normal and most stable orbital configuration of an atom is known as the "ground state." If energy is applied to an atom, the energy will be absorbed and an outer electron will be promoted to a less stable configuration known as the "excited state." Since this state is unstable, the atom will immediately return to the "ground state." Releasing light energy.

Atomic absorption process

The process of atomic absorption is illustrated in Figure B1.

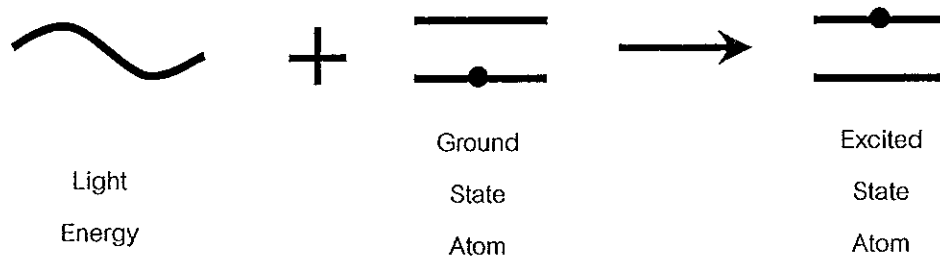| | Ground | Excited |
| Light | State | State |
| Energy | Atom | Atom |

Figure B1 Atomic absorption process.

The "ground state" atom absorbs light energy of a specific wavelength as it enters the "excited state." As the number of atoms in the light path increases, the amount of light absorbed also increases. By measuring the amount of light absorbed, a quantitative determination of the amount of analyte can be made. The use of special light sources and careful selection of wavelengths allow the specific determination of individual elements.

Atomic absorption instrumentation

There are five basic components of an atomic absorption instrument:

1. the light source that emits the spectrum of the element of interest

2. an "absorption cell" in which atoms of the sample are produced (flame, graphite furnace, MHS cell, FIAS cell, FIMS cell)

3. a monochromator for light dispersion

4. a detector which measures the light intensity and amplifies the signal

5. a display that shows the reading after it has been processed by the instrument electronics

There are two basic types of atomic absorption instruments: single-beam and double-beam.

Single-beam

A schematic diagram of a single-beam atomic absorption instrument is shown in Figure B2.
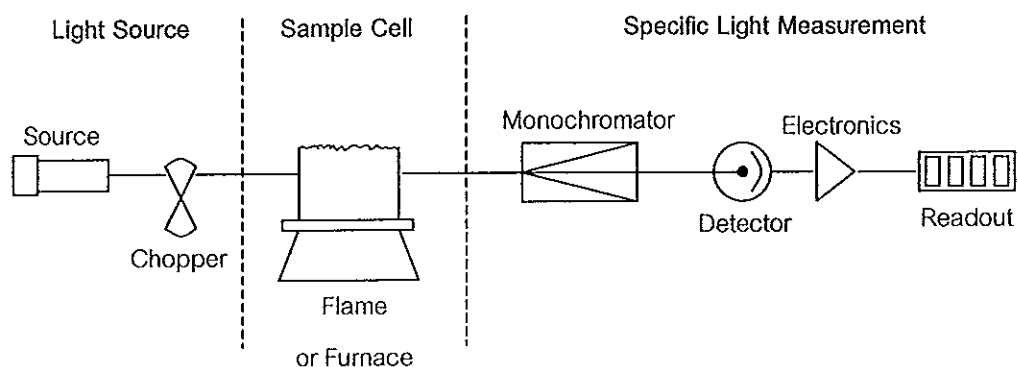

Figure B2 Single-beam atomic absorption spectrometer.

The light source (hollow cathode lamp or electrodeless discharge lamp) emits a spectrum specific to the element of which it is made, which is focused through the sample cell into the monochromator.

The light source must be electronically modulated or mechanically chopped to differentiate between the light from the source and the emission from the sample cell. The monochromator disperses the light, and the specific wavelength of light isolated passes the detector, which is usually a photomultiplier tube. An electrical current is produced depending on the light intensity and processed by the instrument electronics. The electronics will measure the amount of light attenuation in the sample cell and convert those readings to the actual sample concentration. With single-beam systems, a short warm-up period is required to allow the source lamp to stabilize.

Double-beam

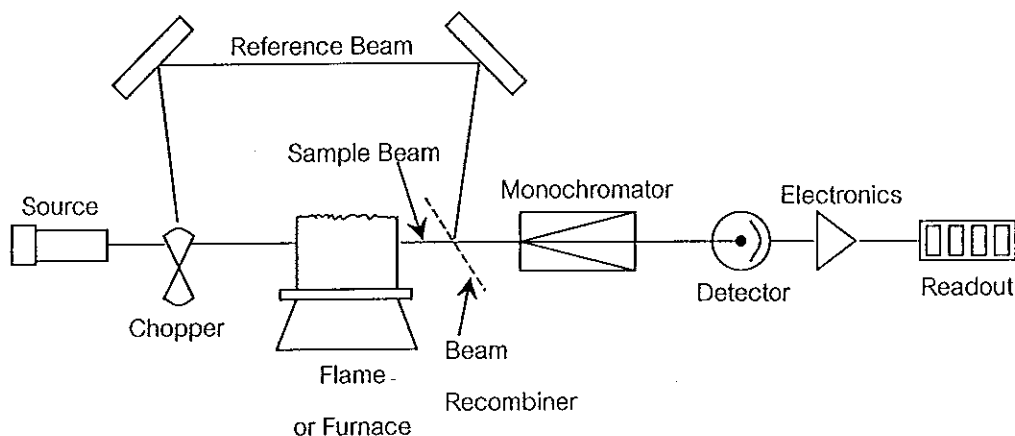A schematic diagram of a double-beam system is shown in Figure B3.

Figure B3 Double-beam atomic absorption spectrometer.

The light from the source lamp is divided into a sample beam, which is focused through the sample cell, and a reference beam, which is directed around the sample cell. In a double-beam system, the readout represents the ratio of the sample and reference beams. Therefore, fluctuations in source intensity do not become fluctuations in instrument readout, and stability is enhanced. Generally, analyses can be performed immediately with no lamp warm-up required.

The AAnalyst 300 atomic absorption spectrometer is a double-beam atomic absorption system capable of performing flame, furnace, and mercury/hydride sampling. It is a sophisticated analytical system capable of performing automated sequential multi-element analysis.

The AAnalyst 300 is designed for optimized, cost-effective, automatic flame, graphite furnace, FIAS, and mercury/hydride analysed. Standard features include complete system control from a computer keyboard and mouse, a motor-driven six- lamp turret for fully automatic multielement analyses, built-in deuterium arc background corrector and the Perkin Elmer burner with automatic, computer-programmed flame gas control.

Features of the AAnalyst 300 spectrometer include:

- automatic lamp selection with an automatic six-lamp turret

- high energy, double-beam optical system providing optimum precision and detection limits

- automatic monochromator setup for wavelength and slit width

- control of atomization systems and accessories by a central computer

- continuum source background correction.

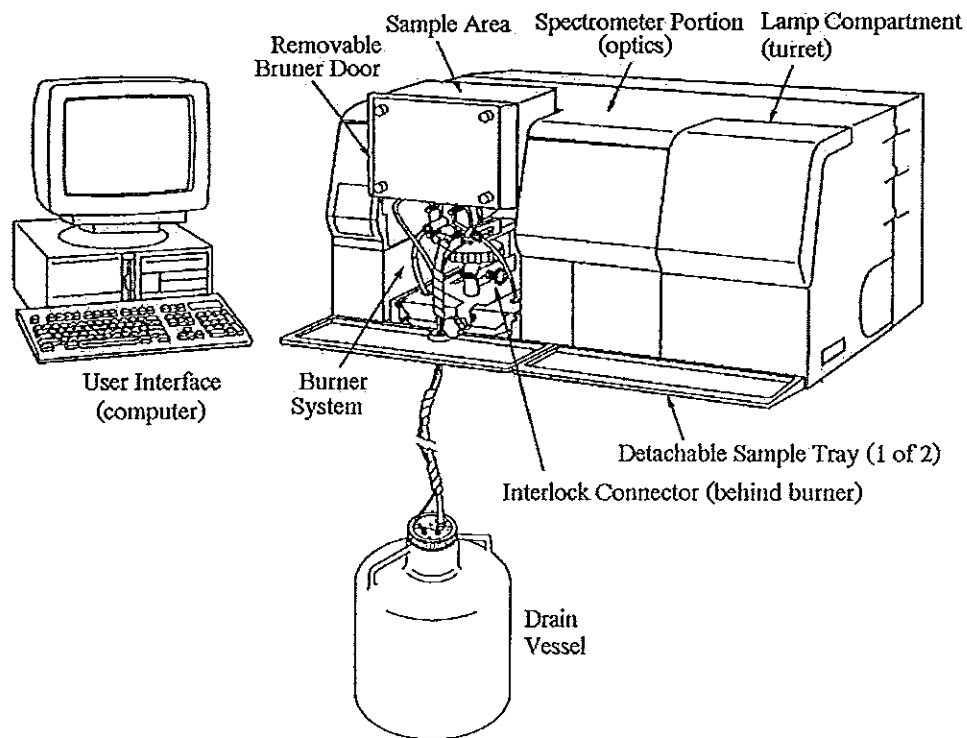Figure B4 General location of subassemblies in the AAnalyst 300.

B.2 Calculations

B.2.1 Standard solution

The equation below describes the determination of quantities required for the preparation of standard solutions.

From higher concentration stock solutions :

$$\text{mL of stock solution required} = \frac{(\text{conc. of dilute standard})(\text{vol. of dilute standard})}{(\text{conc. of stock solution})}$$

B.2.2 Sample solution

Element (mg/L) = (c) (d.f.)

where   c is the concentration of the element in the sample solution in mg/L

d.f. is the dilution factor as described below :

$$d.f. = \frac{(\text{volume of diluted sample solution in mL})}{(\text{volume of aliquot taken for dilution in mL})}$$

B.2.3 The characteristic concentration (sensitivity)

Characteristic concentration in atomic absorption (sometimes called "sensitivity") is defined as the concentration of an element (expressed in mg/L) required to produce a signal of 1% (0.0044 absorbance units). As long as measurements are made in the linear working range, characteristic concentration can be determined by reading the absorbance produced by a known concentration of the element, and solving the following equation:

$$\text{sensitivity} = \frac{\text{Conc. of Std} \times 0.0044}{\text{Measured Abs of Std}}$$

The characteristic concentration values and wavelength for each element (used in this work) are shown in Table 1.

Table 1 The characteristic concentration check for each element.

Metal	Wavelength (nm)	Characteristic concentration check (mg/L) (Conc. of Std)
Cu	324.8	4.0
Mn	247.7	3.0
Pb	279.8	6.0
Fe	283.3	20.0

B.2.4 Detection limit

Detection limit is defined as the concentration of the element which will produce a signal/noise ratio of 3. Thus, the detection limit considers both the signal amplitude and the baseline noise and is the lowest concentration which can be clearly differentiated from zero.

In this work, the detection limits for each elements (Cu, Mn, Pb and Fe) were calculated from 3σ, which σ is the standard deviation of blank (measured ten times). The ultra pure water (18.2 MΩ) was used for blank.

B.2.5 Precision and accuracy

Precision describes the reproducibility of measurements, that is, the closeness of the results that have been obtained in exactly the same way. Generally, the precision of a measurement is readily determined by simple repeating the measurement. Whereas, accuracy indicated closeness of the measurement to its true of accepted value and is expressed in terms of either absolute of relative error. Note the basic difference between accuracy and precision. Accuracy measures agreement between a result and its true value. Precision describes the agreement among several results that have been

measured in the same way. Precision is determined by simply replicating a measurement. On the other hand, accuracy can never be determined exactly because the true value of a quantity can never be known exactly. An accepted value must be used instead (Skoog, et al.,1996).

Accuracy was calculated in form of % recovery as shown in the following equation:

$$\% \text{ Recovery} = \frac{C_{sp} - C_s}{C_a} \times 100$$

where C_{sp} is the concentration of sample solution which added the known concentration of standard solution, (mg/L)

C_s is the concentration of sample solution, (mg/L)

C_a is the concentration of standard solution that added in the sample solution, (mg/L)

Appendix C

Calculation of data from TGA

The result from TGA indicated that $TiO_2(syn)$ lost 25.98% by weight upon heating to the final stage.

Let $TiO_2 \cdot nH_2O$ be the general formula of $TiO_2(syn)$. Therefore,

$$\left(\frac{18n}{79.9 + 18n} \right) \times 100 = 25.98$$

Solving this equation for the value of n yields n = 1.55 or ~1.6. Hence, the true formula of $TiO_2(syn)$ can be written as $TiO_2 \cdot 1.6H_2O$.

VITAE

Name   Miss Miki Kanna

Birth Date   2 October 1977

Educational Attainment

Degree	Name of Institution	Year of Graduate
Bachelor of Science (Chemistry)	Prince of Songkla University	1999

Scholarship Awards during Enrollment

Postgraduate Education and Research Program in Chemistry. (PERCH)

Teaching Assistant, Department of Chemistry, Prince of Songkla University.